

DISSERTATION FOR THE DEGREE OF DOCTOR OF PHILOSOPHY (PHD)

MORPHOLOGICAL AND NEUROCHEMICAL CHARACTERISTICS, AND SYNAPTIC
TARGETS OF GLYCINERGIC NEURONS IN LAMINAE I-IV OF THE SPINAL
DORSAL HORN

by CAMILA DE OLIVEIRA MIRANDA

UNIVERSITY OF DEBRECEN
DOCTORAL SCHOOL OF NEUROSCIENCE

DEBRECEN, 2023

DISSERTATION FOR THE DEGREE OF DOCTOR OF PHILOSOPHY (PHD)

MORPHOLOGICAL AND NEUROCHEMICAL CHARACTERISTICS, AND SYNAPTIC
TARGETS OF GLYCINERGIC NEURONS IN LAMINAE I-IV OF THE SPINAL
DORSAL HORN

by CAMILA DE OLIVEIRA MIRANDA

Supervisor: MIKLÓS ANTAL



UNIVERSITY OF DEBRECEN
DOCTORAL SCHOOL OF NEUROSCIENCE

DEBRECEN, 2023

Morphological and neurochemical characteristics, and synaptic targets of glycinergic neurons in laminae I-IV of the spinal dorsal horn

Dissertation submitted in partial fulfilment of the requirements for the doctoral (PhD) degree in Neurosciences

Written by Camila de Oliveira Miranda certified MSc

Prepared in the framework of the Doctoral School of Neurosciences of the University of Debrecen

Dissertation supervisor: Dr. Miklos Antal, MD, PhD, DSc.

The official opponents of the dissertation:

Prof. Dr. Nándor Nagy, PhD, DSc

Dr. Éva Szőke, PhD

The evaluation board:

Chairperson: Prof. Dr. Béla Fülesdi, PhD, DSc

members: Dr. Éva Rácz, PhD

Dr. Ádám Deák, PhD

The date and venue of the dissertation defence:

lecture hall of Institute of Pediatrics, Faculty of Medicine, University of Debrecen, at 11 a.m., on 29th of November, 2023

Contents

Abbreviations.....	7
1. Introduction.....	10
2. Theoretical Background.....	12
2.1. The somatosensory system.....	12
2.1.1. Primary sensory neurons.....	12
2.1.1.1. Peripheral axons of DGR neurons.....	12
2.1.1.1.1. Encapsulated nerve endings.....	13
2.1.1.1.2. Free nerve terminals.....	14
2.1.1.1.3. Sensory transduction. Conversion of stimuli to nerve signals.....	14
2.1.2. Course and site of termination of the central processes of DRG neurons in the spinal cord	15
2.1.3. Ascending pathways.....	16
2.2. The pain processing system.....	17
2.2.1. Peripheral mechanisms of nociception.....	17
2.2.2. Spinal processing.....	19
2.2.3. Multiple ascending systems conducting nociceptive signals to higher brain centers ...	20
2.2.4. Pain perception in the cerebral cortex.....	21
2.3. Neuroanatomical substrates of spinal nociceptive/pain processing.....	22
2.3.1. The spinal dorsal horn.....	22
2.3.2. Primary afferents terminating in laminae I-IV.....	23
2.3.3. Spinal interneurons in laminae I-IV.....	25
2.3.3.1. Morphological classification.....	25
2.3.3.2. Neurochemical classification.....	26
2.3.3.3. Inhibitory and excitatory interneurons.....	27
2.3.4. Descending fibres.....	28
2.3.5. Projection neurons.....	29
2.3.6. Neuronal circuits.....	30
2.4. Complexity and plasticity of spinal nociceptive/pain processing.....	32
2.4.1. Complexity of spinal nociceptive/pain processing.....	32
2.4.2. Plasticity of spinal nociceptive/pain processing neural circuits.....	32
2.5. Fast inhibitory neurotransmission in the spinal dorsal horn.....	32
2.5.1. GABAergic versus glycinergic inhibition in the spinal dorsal horn.....	33
3. Aims.....	35
4. Material and Methods.....	36

4.1.	Animals	36
4.2.	Hemisection	37
4.3.	Preparation of tissue sections	38
4.3.1.	For immunohistochemistry	38
4.3.2.	For <i>in situ</i> hybridization	38
4.4.	Immunohistochemistry for light microscopy	39
4.4.1.	Single immunostaining of sections obtained from wild type animals	40
4.4.2.	Single immunostaining of sections obtained from GlyT2::CreERT2-tdTomato animals	40
4.4.3.	Double immunostaining on sections obtained from GlyT2::CreERT2-tdTomato animals to reveal colocalization between GlyT2 and GAD65/67	41
4.4.4.	Double immunostaining on sections obtained from wild type animals to reveal close appositions between GlyT2-IR and other axon terminals identified by various axonal markers .	41
4.4.5.	Double immunostaining on sections obtained from PAX2::Cre-tdTomato animals	42
4.4.6.	Triple immunostaining on sections obtained from PKC γ ::CreERT2-tdTomato animals	43
4.5.	Immunohistochemistry for electron microscopy	43
4.6.	Multiplex <i>in situ</i> hybridization.....	44
4.7.	Confocal microscopy	45
4.8.	NeuroLucida reconstruction	45
4.9.	Statistical analysis	45
4.9.1.	Expression of markers within the cell bodies of GlyT2::CreERT2-tdTomato labelled neurons	45
4.9.2.	Expression of GlyT2 and GAD65/67 within the axon terminals of GlyT2::CreERT2-tdTomato labelled neurons.....	46
4.9.3.	Changes in the numbers of GlyT2 immunostained boutons following hemisection of the spinal cord	47
4.9.4.	Colocalization of td-Tomato, GAD1/2 (GAD65/67), and GlyT2 mRNAs.....	47
4.9.5.	Expression of PAX2 in the cell bodies of neurons immunostained for various neuronal markers	48
5.	Results.....	49
5.1.	Specificity of tdTomato labelling in the GlyT2::CreERT2-tdTomato transgenic mice.....	49
5.2.	Distribution of glycinergic neurons in laminae I-IV	50
5.3.	Morphology of glycinergic neurons.....	52
5.3.1.	Laminae I-II	53
5.3.2.	Laminae III-IV	55
5.4.	Neurochemical markers of glycinergic neurons	59
5.4.1.	Galanin and Calretinin	60

5.4.2.	Neuropeptide Y	60
5.4.3.	Neuronal nitric oxide synthase.....	60
5.4.4.	Parvalbumin	61
5.4.5.	Tyrosine kinase RET.....	62
5.4.6.	Nuclear orphan beta receptor ROR β	62
5.5.	Colocalization of GlyT2 and GAD65/67 mRNA in neurons within laminae I-III and IV ...	63
5.6.	Colocalization of GlyT2 and GAD65/67 in axon terminals within laminae I-II	65
5.7.	Spinal vs supraspinal glycinergic innervation of laminae I-III of the spinal dorsal horn	68
5.8.	Synapses made by GlyT2-IR axon terminals in laminae I-III of the spinal dorsal horn.....	69
5.9.	Neurons receiving axo-somatic inputs from glycinergic axon terminals in laminae I-III	72
5.10.	Axon terminals receiving axo-axonic inputs from glycinergic axon terminals in laminae I-III	76
5.11.	Distribution of glycinergic axon terminals in post- and presynaptic positions along the dendrites of PKC γ - containing neurons	79
6.	Discussion.....	82
6.1.	Specificity of GlyT2::CreERT2-tdTomato construction for the labelling of glycinergic neurons in the spinal dorsal horn	82
6.2.	Morphological characteristics	82
6.3.	Neurochemical markers	83
6.4.	GABAergic vs glycinergic inhibition in the spinal dorsal horn.....	84
6.5.	Synaptic targets of glycinergic inhibition in laminae I-III.....	86
6.5.1.	Postsynaptic <i>versus</i> presynaptic inhibition	87
6.5.2.	Targets of postsynaptic glycinergic inhibition.....	87
6.5.3.	Targets of presynaptic glycinergic inhibition	88
7.	Summary	90
8.	References.....	92
9.	Keywords	104
10.	Acknowledgement	106
11.	List of publications	107
12.	Appendix.....	107

Abbreviations

5-HT	Serotonin
ABC	Avidin biotinylated horseradish peroxidase solution
ACC	Anterior cingulate cortex
ACD	Advanced Cell Diagnostics
ALS	Anterolateral
AMYG	Amygdala
ASIC	Acid-sensing ion channels
BAC	Bacterial artificial chromosome
BK	Bradykinin receptor
Ca ⁺⁺	Calcium
CaB	Calbindin
Cat#	Catalog number
CCK	Cholecystokinin
CGRP	Calcitonin gene related peptide
CO ₂	Carbon dioxide
CR	Calretinin
DAPI	4',6-diamidino-2-phenylindole
DRG	Dorsal root ganglia
DYN	Dynorphin
ER	Estrogen receptor
FISH	Fluorescence <i>in situ</i> hybridization
GABA	Gamma butyric acid
GAD65	Glutamic acid decarboxylase 65
GAD67	Glutamic acid decarboxylase 67
GAL	Galanin
GDNF	Glial cell line-derived neurotrophic factors
GLY	Glycine
GlyT2	Glycine transporter 2
H ₂ O ₂	Hydrogen peroxide
H	Hypothalamus
IB4	Isolectin B
IgG	Immunoglobulin G
iPVINs	Inhibitory parvalbumin interneurons
IR	Immunoreactive
kD	Kilodalton
L4	Lumbar 4
L5	Lumbar 5
L6	Lumbar 6
M	Molar
MDcv	Ventrocaudal part of the medial dorsal nucleus

mIPSCs	Miniature inhibitory postsynaptic currents
mRNA	Messenger RNA
Na ⁺	Sodium
NA	Noradrenaline
nAChR	Nicotinic acetylcholine receptor
NADPH	Nicotinamide adenine dinucleotide phosphate
NGF	Nerve growth factor
NiDAB	Nickel-intensified diaminobenzidine
NK	Neurokinin receptor
NK1R	Neurokinin 1 receptor
NMDA	N-methyl-D-aspartate
nNOS	Neural nitric oxide synthase
NPY	Neuropeptide Y
O ₂	Oxygen
OsO ₄	Osmium tetroxide
PA	Pennsylvania
PAG	Periaqueductal grey
PAX2	Paired box gene 2 transcription factor
PB	Parabrachial nucleus of the dorsolateral pons
PB	Phosphate buffer
PBS	Phosphate-buffered saline
PCC	Posterior cingulate cortex
PF	Prefrontal cortex
PKCg	Gamma isoform of protein kinase
PPC	Posterior parietal complex
PV	Parvalbumin
RET	Tyrosine kinase
RNA	Ribonucleic acid
RRID	Research Resource Identifiers
S-1	First somatosensory cortical area
S-2	Second somatosensory cortical area
sIPSCs	Spontaneous inhibitory postsynaptic currents
SMA	Supplementary motor area
SP	Substance P
T	Thalamus
Th11	Thoracic 11
Th12	Thoracic 12
TrkA	Tyrosine kinase A
TRP	Transient receptor potential
TRPA1	Transient receptor potential ankyrin 1
TRPV1	Transient receptor potential vanilloid 1
USA	United States of America

RORb	Beta isoform of nuclear orphan receptor
RMV	Rostral ventromedial medulla
VGLUT	Vesicular glutamate transporter
VGLUT 1	Vesicular glutamate transporter 1
VGLUT 2	Vesicular glutamate transporter 2
VGLUT 3	Vesicular glutamate transporter 3
VIAAT	Vesicular Inhibitory Amino Acid Transporter
VMpo	Ventromedial part of the posterior nuclear complex
VPL	Ventroposterior lateral nucleus
VT	Vermont

1. Introduction

According to the definition of the International Association for the Study of Pain, nociceptive pain arises from actual or threatened damage to non-neural tissue and is due to the activation of nociceptors. The term is used to describe pain occurring with a normally functioning somatosensory nervous system to contrast with the abnormal function seen in neuropathic pain. The term pain is going to be used in this thesis according to this definition.

As the definition defines, damages to non-neuronal tissue as a set of stimuli act on membrane receptors of axon terminals of nociceptors, representing peripheral axon terminals of C and A δ primary sensory fibres with cell bodies in the dorsal root ganglia. The activation of the membrane receptors results in membrane depolarization which is converted into action potentials at the first node of Ranvier along the axons. The action potentials will be conducted to the nociceptive zone of the spinal dorsal horn. In the dorsal horn, spinal neurons will be activated, the nerve impulses will be processed by neuronal circuits, then the nerve signals will be transmitted to various brainstem and diencephalic nuclei by projection neurons. The brainstem and diencephalic nuclei forward the nerve activities to several cortical areas where a complex sensation called pain will be generated.

As described in the previous paragraph, the first relay station of pain processing is the spinal dorsal horn, which presents a complex neural apparatus that can attenuate, or even block, the incoming nociceptive signals, or enhance and forward them to higher brain centers. Thus, although spinal cord neural circuits cannot generate pain sensation, they play essential roles in pain modulation. For this reason, the investigation of spinal neural circuits underlying nociceptive/pain processing is in the forefront of pain research.

Fast inhibitory neurotransmission mediated by GABA and/or glycine plays essential roles in shaping up all functional states of nociceptive/pain processing neural circuits of the spinal dorsal horn. The relative contribution of GABA and glycine to the inhibitory events is, however, under continuous debate. Recent physiological and pharmacological observations indicate that although GABAergic transmission is very important, glycine seems to be the neurotransmitter which mediates most of the fast inhibitory neurotransmission in the spinal nociceptive/pain processing neuronal circuits. Results of morphological studies, however, strongly emphasize the primary importance of GABA-mediated inhibition over glycine-mediated inhibition. One of the main reasons of this contradiction is that our knowledge about the morphology of glycinergic neurons, and about the way how they contribute to the formation

of nociceptive/pain processing neuronal circuits in the spinal dorsal horn is very limited. To fill up this gap in our knowledge, we intended to explore the morphology, neurochemical characteristics, and synaptic relations of glycinergic neurons in Rexed laminae I-IV of the spinal dorsal horn.

2. Theoretical Background

2.1. The somatosensory system

Sensory information processed by the nervous system arises from stimulation of receptors located on the external surface of or within the body. Concerning the specific types of stimuli and specific types of receptors detecting the stimuli with high sensitivity, different sensory modalities can be clearly distinguished (Pleger and Villringer, 2013). One of them is the somatosensory system which serves three major functions: proprioception, exteroception and interoception. All of them are essential for the maintenance of the homeostasis of the body, enabling us to have conscious awareness of posture and movements (proprioception); to have the sense of touch, temperature and pain evoked by external stimuli (exteroception); to monitor body functions by the activation of internal chemo-, thermal- and mechanoreceptors (interoception) (Di Lernia *et al.*, 2016).

2.1.1. Primary sensory neurons

The somatosensory information is conducted from the peripheral receptors to the spinal cord and brainstem by primary sensory neurons the cell bodies of which are in the spinal dorsal root ganglia (DRG) and sensory ganglia of cranial nerves (Matthews and Cuello, 1982; Krames, 2015). Because our work described in this thesis is focused exclusively on spinal cord mechanisms, in the following sections we are going to limit our overview to somatosensory signals conducted to the spinal cord.

DRG neurons present a pseudo-unipolar morphology, with a peripheral axon terminating in various parts of the body (e.g., skin, muscles, internal organs) and a central axon terminating in the spinal cord or brainstem (Abraira and Ginty, 2013). In addition to this common feature, DRG neurons show also distinct features. For example, according to size, they are divided into small and large categories. The size of the cell bodies is also reflected into the myelination, diameter, and conduction velocities of their axons (Todd and Koerber, 2013).

2.1.1.1. Peripheral axons of DGR neurons

The peripheral axons of DRG neurons can be unmyelinated (C fibres; peripheral axons of the small DRG neurons, Figure 1C) and myelinated (A fibres, peripheral axons of the large DRG neurons, Figure 1A, C). The thickness of the myelin sheath around the A fibres also vary from very thin ($A\delta$, Figure 1A), to very thick ($A\alpha$) through an intermediate category ($A\beta$, Figure 1C) (Djoughri and Lawson, 2004).

The degree of myelination, more exactly the distances between adjacent nodes of Ranvier, defines the conduction velocity of the axons. The unmyelinated C-fibres conduct nerve signals slowly (0.4-2.0 m/s), whereas the conduction velocity of A α -fibres with the thickest myelin sheath goes up to 120 m/s (Todd and Koerber, 2013). This is a remarkable difference among the axons of DRG neurons, and it becomes even more important when we note that the terminals of the different categories of axons detect different types of stimuli.

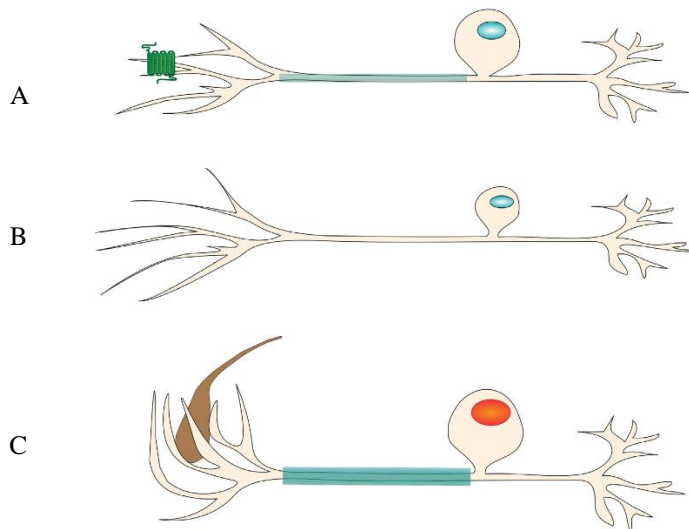


Figure 1: Illustration of (A) A δ thinly myelinated DRG axons (myelin in light green), (B) C unmyelinated DRG axons, and (C) thick myelinated A β DRG axons (modified from Hill and Bautista, 2020).

Sensory receptors are expressed in the terminals of the peripheral axons of DRG neurons. Apart from the unique structure of muscle spindles, the peripheral axon terminals can be classified into two main categories according to their morphology: encapsulated nerve endings and free nerve terminals (Willis, 2007).

2.1.1.1.1. Encapsulated nerve endings

In encapsulated nerve endings the peripheral axons of DRG neurons terminate in a non-neuronal capsule the morphology of which is highly variable. They are sensitive to low intensity stimulation and represent terminals of A α and A β fibres (Johnson, 2001). Most of them are out of the focus of this thesis. There is only one group of these endings that we would like to mention here, namely the mechanosensitive nerve endings of A β fibres (Figure 2B). These nerve endings are in the skin and skeletal muscles, most of them are classified as Meissner and Merkel corpuscles, Pacinian bodies, or hair-guard receptors and sensitive to light touch or stretch (Lewin and Moshourab, 2004; Roudaut *et al.*, 2012).

2.1.1.1.2. Free nerve terminals

Terminals of C and A δ peripheral axons are not surrounded by non-neuronal capsules, they freely arborise in peripheral tissues (Figure 2A). They are activated only by high intensity, tissue damaging, noxious stimuli, for this reason, they are also regarded as nociceptors that detect intense mechanical, thermal (cold or heat) and chemical stimuli (Comitato and Bardoni, 2021).

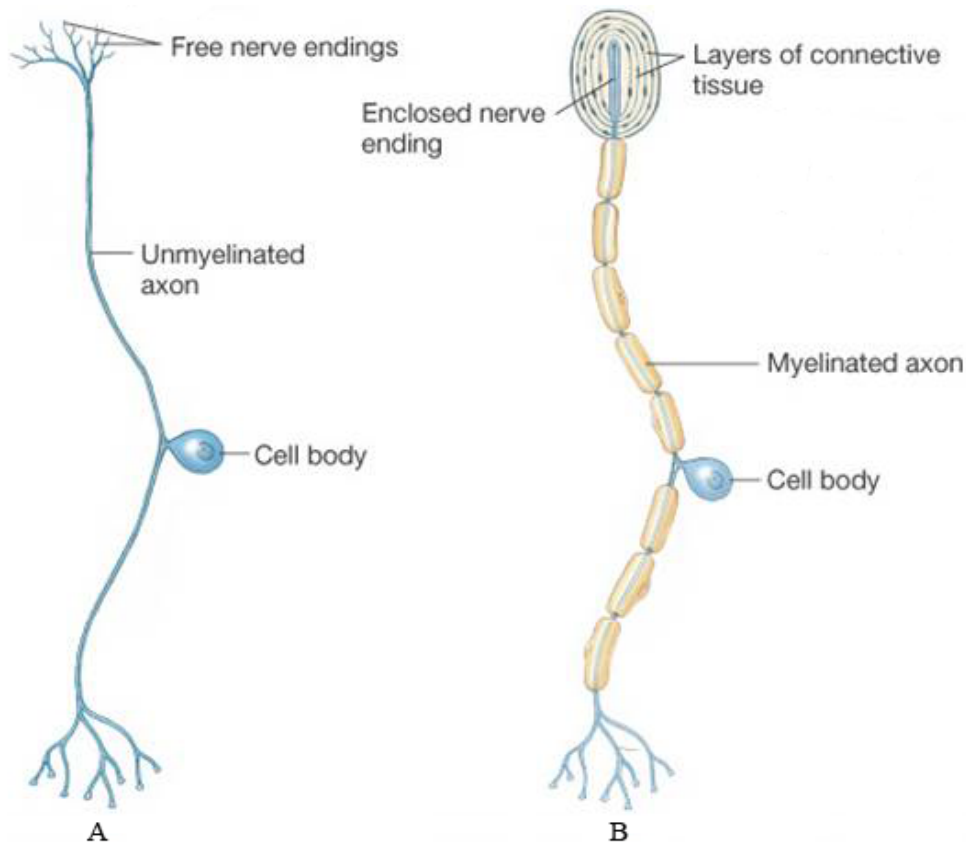


Figure 2: Illustration of (A) unmyelinated DRG axon with free nerve endings, and (B) myelinated DRG axon with encapsulated nerve endings (modified from Austin Community College District, accessed on June 5th 2023 <https://www.austincc.edu/apreview/PhysText/PNSafferentpt1.html>).

2.1.1.1.3. Sensory transduction. Conversion of stimuli to nerve signals

When mechanical, thermal, or chemical stimuli with an appropriate intensity hit the membrane of the peripheral axon terminals of DRG neurons the stimulus will be converted into a membrane depolarization (McHugh and McHugh, 2000). The molecular mechanism of this conversion process depends on the nature of the stimulus.

Mechanical stimuli, like pressure or stretch cause deformation of specific membrane associated proteins that result in the opening of stretch-sensitive Na⁺ and Ca⁺⁺ ion channels (Ellis and

Bennett, 2013). The increased Na^+ and Ca^{++} conductance then depolarizes the membrane of the axon terminal.

Thermal stimuli, like cold or warm activate transient receptor potential (TRP) ion channels. There are several subtypes of TRP receptors that are different in chemical structure and can be activated by different temperatures; some of them are sensitive for cold, others can detect only extreme heat (Willis, 2007).

Chemical stimuli usually activate proton-gated ion channels. They are known as acid-sensing ion channels (ASIC). There are at least five types of ASICs that are sensitive for different pH, and like TRP channels they are also modulating the conductance of Na^+ and Ca^{++} ion channels (Wemmie *et al.*, 2013). In case of peripheral inflammation, other chemical agents (molecules of the so called “inflammatory soup”) also act at other chemoreceptors (Ellis and Bennett, 2013), but these additional mechanisms are out of the focus of the present dissertation.

Although the different stimuli can activate a wide range of membrane receptors, the activation of all the receptors results in Na^+ and Ca^{++} influx and the depolarization of the axon terminals (Gu and Lee, 2010). If the depolarization is strong enough it can be conducted to the first node of Ranvier along the axon, where it can generate action potential. Then the action potential will be conducted along the peripheral and central processes of DRG neurons into the spinal dorsal horn.

2.1.2. Course and site of termination of the central processes of DRG neurons in the spinal cord

The course and termination fields of the central axons of DRG neurons in the spinal cord show a unique segregated pattern.

$\text{A}\alpha$ and $\text{A}\beta$ fibres enter the dorsal funiculus and divide into ascending and descending branches. The ascending branch convey impulses directly into the gracile and cuneate nuclei in the caudal part of the medulla oblongata, whereas the descending branch run one-two spinal segment caudally. Both the ascending and descending branches give rise to local collaterals that terminate in the spinal grey matter at the level of the spinal entrance of the axon and one-two segment rostrally and caudally to that (Basbaum *et al.*, 2009). The local collaterals of $\text{A}\alpha$ axons terminate primarily in the deep dorsal horn (laminae V-VI) and in the intermediate grey matter (lamina VII). $\text{A}\alpha$ fibres innervating muscle spindles run even more ventral and make synaptic

contacts with homonymous motoneurons. Collaterals of $A\beta$ fibres terminate primarily in laminae III and IV of the dorsal horn (Figure 3).

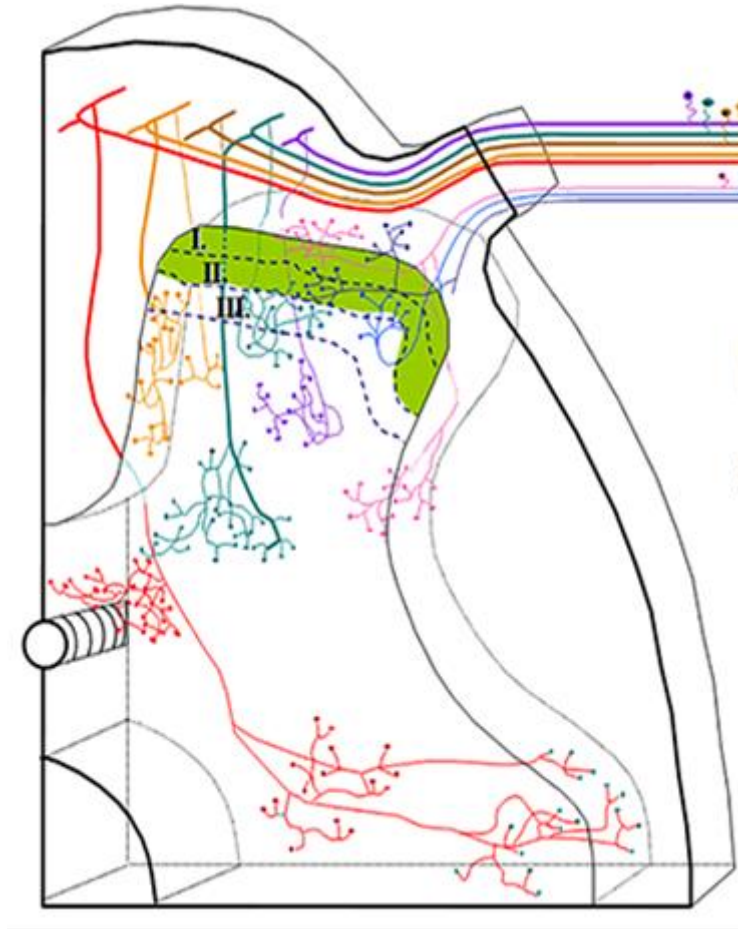


Figure 3: Illustration of course and termination patterns of the central axons of DGR neurons in the spinal cord. Please find the detailed description of the scheme in the text. (Fyffe, 1984)

C and $A\delta$ fibres do not enter the dorsal funiculus but reach the dorsal margin of the dorsal horn, where they divide into ascending and descending branches, forming the tract of Lissauer (Lingford-Hughes and Kalk, 2012). Both branches cover one-two spinal segments while they give rise two collaterals terminating primarily in laminae I-II (Figure 3).

2.1.3. Ascending pathways

After local information processing, sensory information conveyed from the spinal cord to higher brain centers by multiple parallel ascending pathways.

Proprioceptive and tactile information conducted by $A\alpha$ and $A\beta$ fibres conveyed by the dorsal column-medial lemniscus pathway to the thalamus, from where this information will be transmitted to the cerebral cortex by thalamo-cortical pathways, where the sensory inputs

generate sensory perception of position sense, vibration, touch, pressure, etc (Giesler *et al.*, 1984). Along this pathway sensory information from the periphery is transmitted to the cortex without any sensory processing in the spinal dorsal horn. Collaterals of A α and A β fibres, however, terminate also in laminae V-VII of the spinal grey matter. After some spinal information processing, these sensory signals are conveyed to the cerebellum by spino-cerebellar pathways ascending in the lateral part of the lateral funiculus (Wercberger and Basbaum, 2019). This sensory information is inevitable in motor coordination. These pathways are out of the focus of the present thesis; for further details see Brooks and Tracey (2005), and Wang *et al.* (2022).

As mentioned earlier noxious mechanical, thermal, and chemical signals carried by C and A δ fibres to laminae I-II of the spinal dorsal horn. After complex information processing these signals are conveyed further by the contralateral anterolateral ascending system. Ascending fibres in the anterolateral system terminate in various regions and nuclei of the brainstem and thalamus, where they generate further information processing (Chandar and Freeman, 2014). From here the signals are conveyed further to multiple regions of the cerebral cortex, where perception of pain and thermal sensation are generated (Iggo, *et al.*, 1985; Spike, *et al.*, 2003; Wercberger and Basbaum, 2019). Further details of this pathway are given in the next sections of the thesis.

2.2. The pain processing system

As defined earlier nociceptive pain arises from actual or threatened damage to non-neural tissue and is due to the activation of nociceptors. At the cortical level, these nerve signals generate a complex unpleasant sensation serving a vital protective function. It is a warning signal telling us that something happened in our body that needs attention and proper response or treatment. Without the acute form of pain sensation, one may call it as nociception, we would not be able to protect our body against tissue damaging stimuli, and properly maintain the homeostasis of our body. On the other hand, however, the long lasting, chronic pain experience may make our life almost unbearable. Thus, pain processing can be regarded as one of the most important functions of the nervous system. In this thesis, we are going to deal only with the acute pain / nociceptive mechanisms.

2.2.1. Peripheral mechanisms of nociception

Peripheral axon terminals presenting receptors that can detect high intensity, tissue damaging, noxious stimuli form free nerve endings. They represent terminals of C and A δ type primary

afferents, and according to their specific stimuli they can be classified into three categories: thermo-, mechano-, and polymodal nociceptors (Gardner and Johnson, 2013). Thermal nociceptors can detect extreme temperatures, higher than $+45^{\circ}\text{C}$ and lower than $+5^{\circ}\text{C}$ with various TRP receptors like TRPV1 or TRPA1 (Basbaum *et al.*, 2009). Mechanical nociceptors are sensitive to intense pressure. Polymodal nociceptors can be activated by a much wider range of stimuli, they can detect intense thermal, mechanical, and chemical stimuli. In addition to thermosensitive and mechanosensitive channels they also express a wide range of chemoreceptors sensitive to biologically active mediators that can be released in case of tissue injury or inflammation (McHugh and McHugh, 2000; Ellis and Bennett, 2013) (Figure 4).

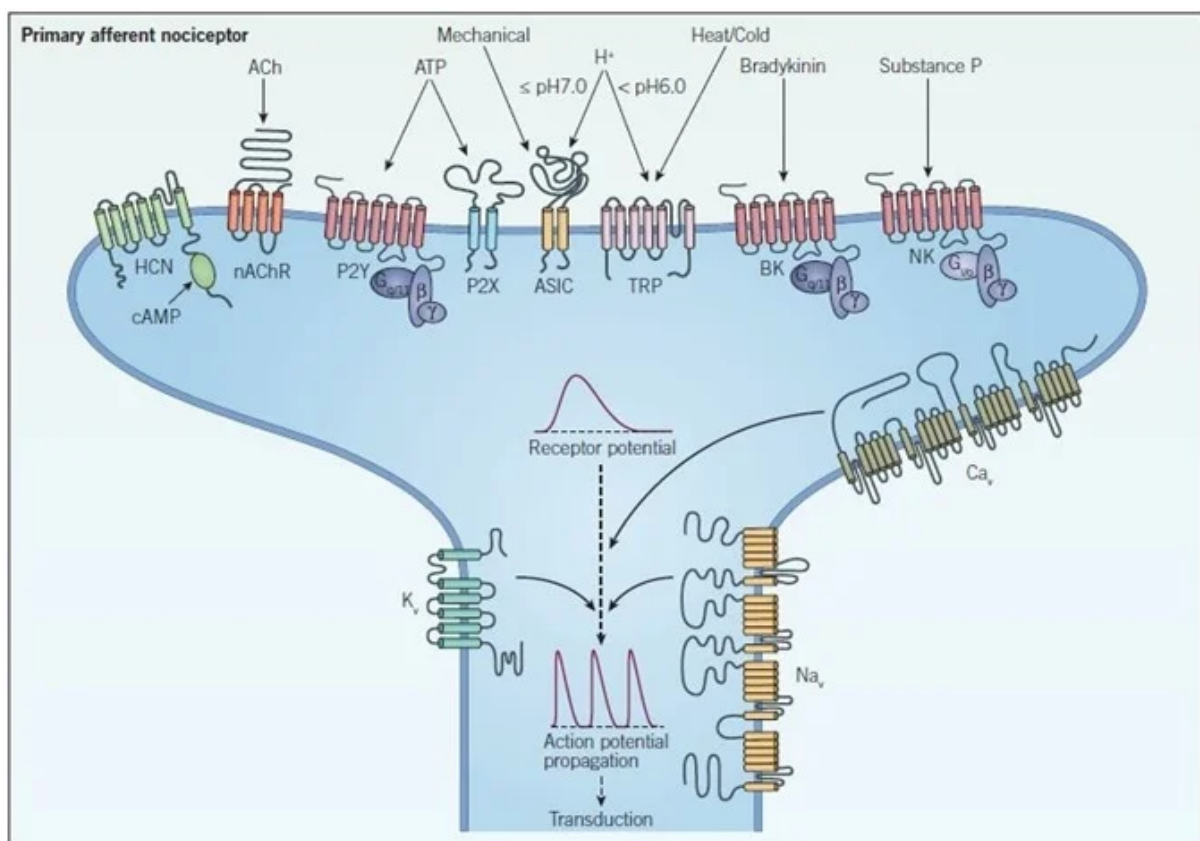


Figure 4: Illustration of a primary afferent nociceptor and some thermo, mechano, and polymodal receptors, as nAChR, P2Y, ASIC, TRP, BK, NK (2019, Peripheral sensitization and signal propagation in nociception, Sponsored Content by Tocris Bioscience, accessed on 5th June 2023 <https://www.news-medical.net/whitepaper/20190817/Ion-Channels-Involved-in-Pain.aspx>).

The specific stimuli and functional properties of these receptors are quite heterogeneous, but in case of activation all of them open, directly or indirectly, Na^+ and/or Ca^{++} channels and thus depolarize the membrane of the primary afferent axon terminals (Basbaum *et al.*, 2009). The initial depolarization can be converted into action potential at the first node of Ranvier along

the axon, then the action potential shall be conducted by the activated C and A δ primary afferents to the spinal cord where they terminate in the dorsal horn.

2.2.2. Spinal processing

The incoming C and A δ fibres activate excitatory and inhibitory interneurons as well as projection neurons in the spinal dorsal horn (Yasaka *et al.*, 2007; Neumann *et al.*, 2008). If the incoming nociceptive signals are strong enough projection neurons can be directly activated. In most of the cases, however, the nociceptive impulses first activate interneurons, and after some spinal processing, the interneurons will make the projection neurons fire (Todd, 2010). Based on behavioural observations, Melzack and Wall (1965) pointed out first, that the spinal processing of nociceptive signals can be substantially influenced by nerve impulses generated by low threshold mechanoreceptors and conducted to the spinal cord by A β fibres (Figure 5). A β -inputs can activate inhibitory neurons in the spinal cord that can attenuate the primary nociceptive signals and can even block the activation of projection neurons. Thus, if one wants to understand spinal nociceptive/pain processing in the spinal cord, in addition to nerve impulses conducted by C and A δ nociceptive primary afferents, non-nociceptive inputs conducted by A β fibres, and possible integration mechanisms of these nociceptive and non-nociceptive signals should also be seriously taken into consideration.

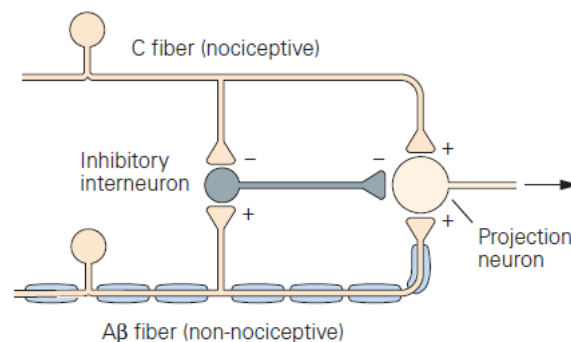


Figure 5: Illustration of the gate control theory, published by Melzack and Wall in 1965. Nociceptive and non-nociceptive fibres can activate the projection neuron, which can be inhibited by an inhibitory interneuron. The C fibre input “opens the gate” by inhibiting the inhibitory interneuron, with consequent activation of the projection neuron, while A β fibre activates the inhibitory interneuron “closing the gate” for the activation of the projection neuron. (Basbaum and Jessel, 2013)

2.2.3. Multiple ascending systems conducting nociceptive signals to higher brain centers

If the spinal processing and integration of nociceptive and non-nociceptive signals results in the activation of projection neurons, nociceptive/pain signals will be forwarded to higher brain centers by the axons of projection neurons (Figure 6). Axons of most projection neurons cross the midline and collect within the contralateral anterolateral white matter forming the anterolateral ascending system (Figure 6). This is a complex ascending system constructed by axonal bundles/pathways that terminate in multiple regions of the brainstem and diencephalon (Brooks and Tracey, 2005). The spinobulbar pathway end in the medulla oblongata and activate the ventrolateral reticular formation, the rostral ventromedial medulla, and the nucleus of the solitary tract. The spinopontine pathway terminate primarily in the parabrachial nucleus. The spinomesencephalic pathway end primarily in the periaqueductal grey matter. The spinodiencephalic pathway is the most rostral component of the anterolateral ascending system. Some of these fibres terminate in the lateral thalamus including the ventral posterolateral nucleus; this component is usually referred to as the spinothalamic pathway. In addition to this, however, spinodiencephalic fibres end also in the medial thalamus and hypothalamus. Thus, nociceptive signals generate a complex and widespread activation in the brainstem and diencephalon (Suzuki and Dickenson, 2005; Basbaum and Jessel, 2013).

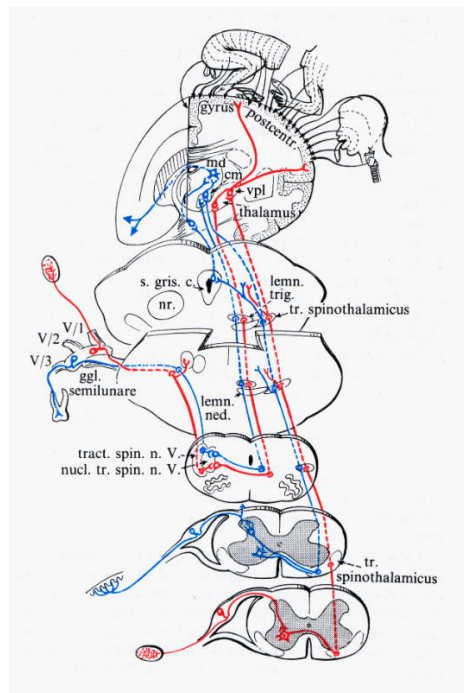


Figure 6: Illustration of the ascending tracts from the dorsal horn to higher brain centers (Szentágothai and Réthelyi, 1989).

2.2.4. Pain perception in the cerebral cortex

Many brainstem and diencephalic nuclei activated by different constituents of the anterolateral ascending system project to various regions of the cerebral cortex (Tracey and Mantyh, 2007). In addition to the primary somatosensory cortex, various parts of the limbic cortical areas including the anterior cingulate cortex, the insular cortex and frontal cortical territories will be activated (Willis and Westlund, 1997; Garland, 2012) (Figure 7). Thus, the nociceptive/pain signals evoke a complex network activity at the level of the cerebral cortex. This is the reason why pain sensation is much more complex than any other sensory modality. In addition to the sensory-discriminative component, which is characteristic to all sensory modalities, pain also has motivational-affective (emotional-cognitive) and autonomic (e.g., raise of blood pressure and pulse rate, sweating etc.) components (Basbaum *et al.*, 2009). This complex nature of pain sensation creates serious problems in the clinical evaluation and treatment strategies of chronic pain.

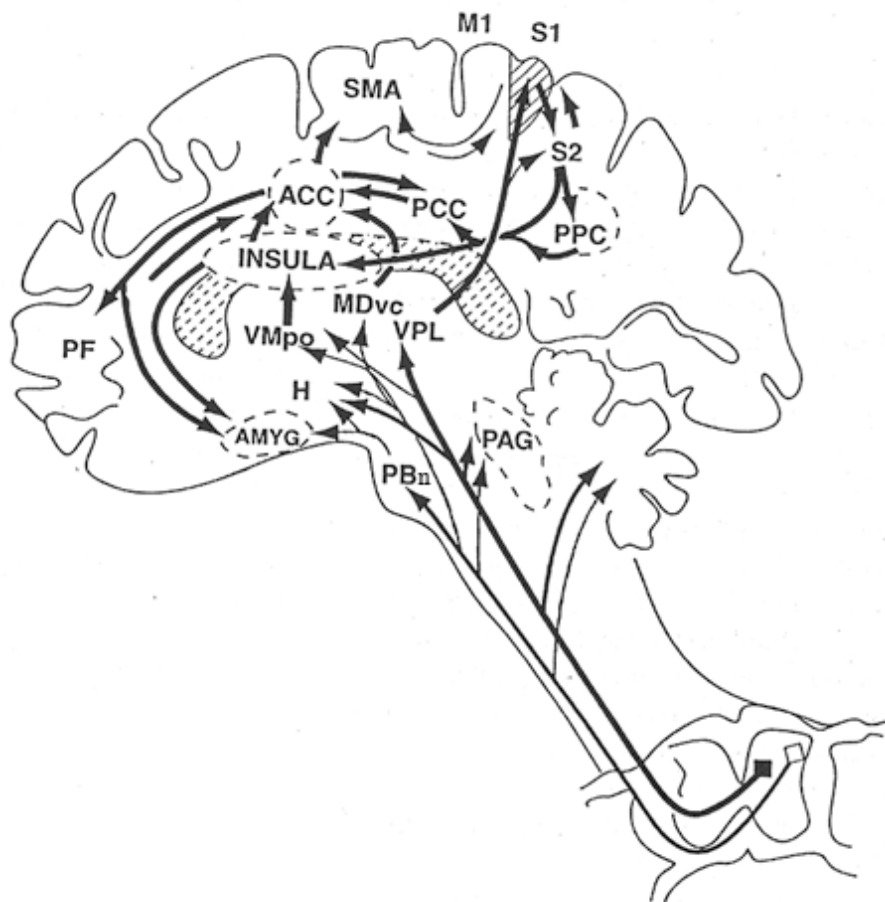


Figure 7: Illustration of areas of the cerebral cortex that may be activated through nociceptive sensation (Price, 2000). PAG: periaqueductal grey; PBn: parabrachial nucleus of the dorsolateral pons; VMpo: ventromedial part

of the posterior nuclear complex; MDvc: ventrocaudal part of the medial dorsal nucleus; VPL: ventroposterior lateral nucleus; ACC: anterior cingulate cortex; PCC: posterior cingulate cortex; H: hypothalamus; S-1 and S-2: first and second somatosensory cortical areas; PPC: posterior parietal complex; SMA: supplementary motor area; AMYG: amygdala; PF: prefrontal cortex.

2.3. Neuroanatomical substrates of spinal nociceptive/pain processing

2.3.1. The spinal dorsal horn

Based on its cytoarchitectonic organization, the spinal dorsal horn can be divided into 6 layers (Rexed, 1952 and 1954), and numbered from dorsal to ventral direction (Figure 8). Lamina I, the most dorsal lamina, known also as marginal layer, contain large projection neurons together with a limited number of interneurons; lamina II presents a high density of small interneurons and referred to as substantia gelatinosa; laminae I-II together are also named as the superficial spinal dorsal horn; laminae III and IV are like each other in cytoarchitectonic organization and named together as nucleus proprius; the deep dorsal horn, laminae V-VI contain large neurons and receives inputs primarily from A α primary afferents (McClung and Castro, 1978; Molander *et al.*, 1984; Peirs *et al.*, 2020). Because neural signals conducted by A α fibres do not participate in pain processing, later we are going to limit our overview to laminae I-IV of the spinal dorsal horn.

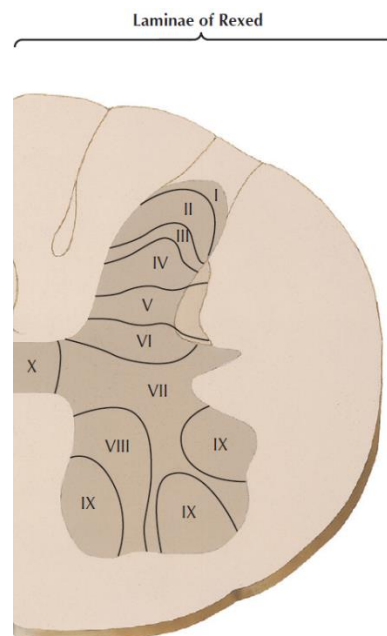


Figure 8: Illustration of the Rexed laminae of the spinal cord. The dorsal horn is divided into 6 laminae in a dorso-ventral arrangement. Lamina VII represents the intermediate gray matter. Laminae VIII and IX label the medial and lateral parts of the ventral horn, respectively. Lamina X surrounds the central canal. (Netter, 2011).

2.3.2. Primary afferents terminating in laminae I-IV

It is generally accepted that, with some overlap, laminae I-II receive terminals of C and A δ nociceptive primary afferents, whereas laminae III-IV are innervated by A β non-nociceptive fibres (Figure 9). For this reason, laminae I-II are usually interpreted as the nociceptive zone of the spinal cord. This is, however, an oversimplified view and in this thesis, I would like to give a more elaborated description about these primary afferents.

The non-myelinated nociceptive C fibres usually divided into two groups based on their neurochemical characteristics. One of them consists of afferents sensitive to nerve growth factor (NGF), express tyrosine kinase A (TrkA) receptors, and contain neuropeptides like calcitonin gene related peptide (CGRP) or substance P (SP); while the other population of C fibres are sensitive to glial cell line-derived neurotrophic factors (GDNFs), express the receptor tyrosine kinase (RET), binds the isolectin B4 (IB4), and do not contain neuropeptides (Alvarez and Fyffe, 2000; Hunt and Mantyh, 2001). Based on the presence or absence of neuropeptides in them, the two subgroups are distinguished from each other as peptidergic and non-peptidergic. The peptidergic C fibres terminate mainly in lamina I and the outer layer of lamina II (IIo), whereas the non-peptidergic ones arborize mainly in the inner part lamina II (IIi) (Todd and Koerber, 2013) (Figure 9). Concerning its neuropeptide content and termination areas peptidergic and non-peptidergic nociceptive C-fibres are quite segregated from each other, but it is not clear that they represent different functional types of nociceptive primary afferents.

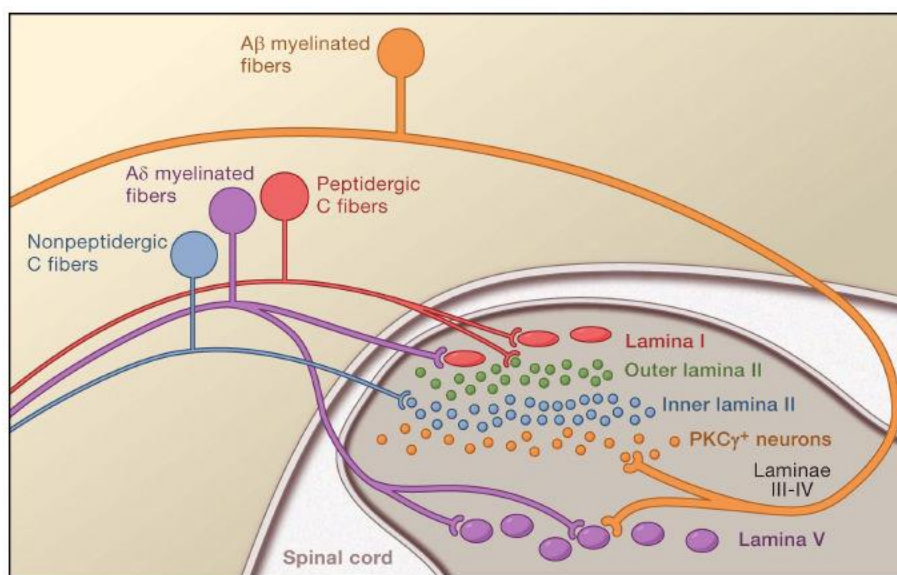


Figure 9: Illustration of the non-nociceptive and nociceptive fibres termination sites in the spinal dorsal horn. Myelinated A δ and A β fibres terminate in laminae I and V, and III-IV, respectively; while peptidergic C fibres terminate in laminae I and outer lamina II, and non-peptidergic C fibres in inner lamina II. (Basbaum *et al.*, 2009).

The myelinated nociceptive A δ primary afferents are also heterogeneous in their neurochemical properties, e.g., some of them contain neuropeptides such as CGRP and SP, but they cannot be divided into clearly distinguishable subgroups (Zeitz *et al.*, 2002; Shin *et al.*, 2003). After leaving the tract of Lissauer, they arborize and terminate in laminae I and II. They also give rise to branches that run into the ventral direction and terminate in the deep dorsal horn (Figure 9), but these deep collaterals are out of the focus of the present thesis.

The non-nociceptive myelinated low threshold mechanoreceptive A β primary afferents enter the dorsal column, where they bifurcate. Both the ascending and descending branches give rise to collaterals that terminate mainly in laminae III-IV (Figure 9), but some of their terminals project also into lamina III (Todd *et al.*, 2003).

All primary afferents are excitatory and use glutamate as their main neurotransmitter. For some reason, however, they use different vesicular glutamate transporters (VGLUTs) for pumping glutamate into the synaptic vesicles. Neuropeptide containing afferents can also release neuropeptides such as SP, galanin, somatostatin that can act together with glutamate on the postsynaptic neurons and modify the postsynaptic effect of glutamate (Todd and Koerber, 2013).

Primary afferents transmit their neural activities to spinal interneurons by making synaptic contacts with them. They establish mostly simple synaptic contacts with dendrites (axo-dendritic) and in a lesser extent with somata (axo-somatic) of spinal neurons (Todd and Koerber, 2013). In addition to this, a substantial proportion of primary afferent terminals make axo-axonic synapses, a significant number of which were found in complex, so called glomerular synaptic arrangements. In the synaptic glomeruli, the primary afferent terminals appear as large central boutons, which is surrounded with dendrites and axon terminals. Within these synaptic arrangements the central primary afferent boutons establish axo-dendritic contacts with usually more than one dendrite, and form axo-axonic synapses in which it may appear as pre- and also as postsynaptic elements (Ribeiro-da-Silva, 2004). Two main types of synaptic glomeruli have been described. Type 1 synaptic glomeruli have a central bouton with electro dense matrix, densely packed synaptic vesicles, and low number of mitochondria; the central axon terminals in type 2 synaptic glomeruli have a lighter matrix, less synaptic vesicles, and more mitochondria (Ribeiro-da-Silva, A., 2004). The different types of primary afferents form different types of synaptic glomeruli with different probability. In rodents, peptidergic nociceptive primary afferents can be found in synaptic glomeruli very rarely. Type 1 synaptic

glomeruli are established by nonpeptidergic C fibres, whereas A δ primary afferents and presumably A β fibres also form type 2 glomeruli (Zeilhofer *et al.*, 2012).

2.3.3. Spinal interneurons in laminae I-IV

Interneurons represent the largest neuronal population in the spinal dorsal horn, including laminae I-IV. Most of these neurons have their dendrites and axons in the same lamina where their cell bodies are, while others have dendrites and axons extending to other laminae. Until recently it was a general idea, that the dendritic and axonal trees of interneurons do not leave the confines of laminae I-III. Thus, the nociceptive processing area of the spinal cord have been regarded as a “closed system”. Although this idea still has many supporters, more and more experimental data show that the axons and dendrites of many of these neurons are not confined to an area around the cell bodies, but they have abundant intersegmental connections, whereas others project deeper into the spinal grey matter (Todd, 2010; Peirs and Seal, 2016).

Interneurons can be classified based on several attributes including the location of their cell bodies, axonal and dendritic morphologies, neurochemical characteristics, and functional properties. Because the location of the cell bodies does not tell much about the contribution of the neurons to the formation of nociceptive/pain processing neuronal circuits, I am going to describe these interneurons based on their axonal and dendritic morphology, and neurochemical characteristics. Concerning the functional properties, I shall take a simple approach and divide the interneurons into excitatory and inhibitory categories.

2.3.3.1. Morphological classification

From old Golgi impregnation studies to recent genetic analysis, interneurons in laminae I-IV had been classified into several subgroups. In the last two decades, it turned out that the most reliable classification of these interneurons had been made by Grudt and Perl (2002). They studied interneurons in lamina II, but most of the interneurons in the other laminae can also be classified according to their scheme. According to Grudt and Perl (2002), taking the dendritic arborization patterns into account, interneurons in lamina II can be grouped into four morphological groups: islet, central, radial, and vertical. Islet and central cells have rostro-caudally oriented dendritic trees, but the extension of the dendrites of islet cells is much wider than that of central cells. As the name indicates, radial cells give rise to short but widely arborizing dendrites that form a stellate like dendritic arbor. While the dendritic arbors of islet, central and radial cells are confined to the laminar location of the cell bodies, the dorso-ventral extension of the dendrites of vertical cells is much wider, they cross laminar boundaries.

Although interneurons in lamina I were classified differently (Lima and Coimbra, 1986), later it turned out that they are not different from the morphologies described by Grudt and Perl (2002). Many interneurons in laminae III-IV also show the morphologies of islet, central and radial cells, however, in these layers the cell morphologies are more diverse. In these laminae, there are also inverted vertical cells (inverted stalked cells, as they were described by Gobel (1975) in his classical Golgi studies), and pyramidal cells described first by Réthelyi and Szentágothai (1969). In addition, there are other interneurons with dendritic morphologies which cannot be classified so easily.

2.3.3.2. Neurochemical classification

Interneurons in the spinal dorsal horn show many distinct neurochemical features. They express various neuropeptides, calcium binding proteins, enzymes, receptors and other markers in different quantities and combinations, providing a basis for neurochemical classification of the interneurons (Todd and Koerber, 2013; Peirs *et al.*, 2014). In this thesis, I would like to deal with only those molecules which are frequently used for the identification of specific populations of interneurons in morphological studies.

Calbindin (CaB) is a calcium-binding protein with a molecular weight of 28 kD. CaB positive neurons form an abundant cell population in lamina II, but some of them can be found also in adjacent laminae (Antal *et al.*, 1990).

Parvalbumin (PV) is a calcium-binding protein of 9-11 kD located primarily, if not exclusively, in laminae II-III of the spinal dorsal horn; most of them regulate the effect of non-nociceptive inputs on pain processing neural circuits (Antal *et al.*, 1990; Hughes *et al.*, 2012).

Calretinin (CR) is a 29 kD calcium binding protein showing a 58% homology to mammalian 28kD calbindin. CR interneurons represent a significant proportion of neurons in laminae I-II, they receive substantial monosynaptic inputs from C and A δ primary afferents and produce sustained activation following stimulation and are regarded as pain amplifiers (Ren *et al.*, 1993; Smith *et al.*, 2015; Gutierrez-Mecinas *et al.*, 2019).

Gamma isoform of protein kinase C (PKC γ) positive neurons are mostly distributed in laminae II-III, they are present only occasionally in lamina I or lamina IV; they receive strong innervation from A β fibres and play a major role in the development of mechanical allodynia (Miraucourt *et al.*, 2007; Alba-Delgado *et al.*, 2015; Artola *et al.*, 2020).

Cholecystokinin (CCK) containing neurons are distributed in laminae I-IV and contribute to the development of both punctate and dynamic allodynia (Gutierrez-Mecinas *et al.*, 2019; Peirs *et al.*, 2020).

Neural nitric oxide synthase (nNOS) is the neuronal NADPH diaphorase. nNOS positive neurons are present in moderate numbers and widely distributed in laminae I-IV; it synthesises nitric oxide, a gas that has diverse effects on nociceptive/pain signalling in the dorsal horn (Huang *et al.*, 2018; Peirs *et al.*, 2020).

Dynorphins (DYN) are opioid peptides derived from the precursor protein prodynorphin. DYNs are expressed in relatively low numbers of interneurons in the superficial layers of the spinal dorsal horn, but they were shown to play important roles in the processing of certain pain modalities (Duan *et al.*, 2014; Peirs *et al.*, 2020).

Galanin (GAL) is a neuropeptide of 29 amino acids. GAL interneurons form a small but distinct population of interneurons in the superficial spinal dorsal horn (Simmons *et al.*, 1995; Tiong *et al.*, 2011).

Neuropeptide Y (NPY) is a neuropeptide of 36 amino acid. NPY-containing cells represent a low proportion of interneurons but reported to play an important role in the attenuation of nociceptive activities in the dorsal horn (Polgár *et al.*, 1999; Iwagaki *et al.*, 2016).

Receptor tyrosine kinase (RET) positive neurons are located mostly in deeper laminae of the spinal dorsal horn, but some of them can be found also in laminae I-IV (Cui *et al.*, 2016).

Beta isoform of nuclear orphan receptor (ROR β) containing cells are sparsely distributed in laminae I-IV and represent a functionally diverse population of neurons (Koch *et al.*, 2017).

2.3.3.3. Inhibitory and excitatory interneurons

Interneurons in the central nervous system including the spinal dorsal horn can be divided into two main functional categories: excitatory and inhibitory neurons. Excitatory spinal interneurons are glutamatergic which is released alone or together with neuropeptides like SP modulating the effect of glutamate on the postsynaptic neuron (Todd and Koerber, 2013). Inhibitory spinal interneurons release gamma amino butyric acid (GABA) and/or glycine that may evoke inhibitory postsynaptic potentials together or alone on the postsynaptic cells. The proper and reliable identification of the cell bodies of excitatory and inhibitory interneurons with morphological methods is difficult, because the very low concentrations of GABA,

glycine and glutamate, the synthesizing enzymes of GABA, glutamic acid decarboxylase (GAD65 and GAD67), or the neuron specific glycine transporter (GlyT2) make the direct and reliable immunohistochemical detection of these transmitters and enzymes in the cell bodies almost impossible (Zeilhofer *et al.*, 2012). On the other hand, the concentrations of GABA, GlyT2 and GAD65/67 is sufficiently high in axon terminals for a trustworthy identification of the inhibitory axon terminals. However, the identification of excitatory axon terminals based only on their glutamate content is not so trivial. For this reason, the morphological identification of inhibitory and excitatory interneurons requires a complex methodological approach in which immunocytochemistry is combined with physiological, pharmacological, genetic, and transgenic technologies. These complex methodological approaches revealed that GABAergic inhibitory interneurons in laminae I-II can be grouped into five, neurochemically definable populations: neurons expressing 1) GAL, 2) NPY, 3) nNOS, 4) PV, and 5) CR (Boyle *et al.*, 2017). This classification cannot be applied to laminae III-IV, because in these laminae large populations of inhibitory interneurons express RET, and some others contain ROR β (Peirs *et al.*, 2020). The classification of excitatory interneurons based on neurochemical markers is more difficult. Among the several markers that have been identified, CaB, CCK and PKC γ seem to be the most useful markers for the identification of excitatory interneurons when studying the construction of neural circuits underlying nociceptive/pain processing in the spinal dorsal horn (Todd, 2010; Benarroch, 2016; Comitato, and Bardoni, 2021). It is also important to note that no neurochemical markers have been identified till now that would label exclusively excitatory or inhibitory interneurons. There is general agreement, that in a neuronal population expressing a given neurochemical marker there are always excitatory and inhibitory neurons in highly variable proportions.

2.3.4. Descending fibres

The central nervous system has an internal pain attenuation mechanism which is driven by centers of the limbic system like the anterior cingulate cortex or amygdala (Figure 10). The activities of these areas are forwarded by mesencephalic structures like the periaqueductal grey to serotonergic and noradrenergic nuclei of the brainstem that project to the spinal dorsal horn (Hossaini *et al.*, 2012). Most of these descending serotonergic and noradrenergic fibres arise from the rostral ventromedial medulla and locus coeruleus and evoke a strong inhibition on spinal dorsal horn neurons processing nociceptive/pain signals; it was also shown that descending fibres arising from the rostral ventromedial medulla, in addition to serotonin, release also GABA and glycine in the spinal dorsal horn (Antal *et al.*, 1996) (Figure 10). Thus,

descending fibres arising from brainstem nuclei can evoke a strong inhibition on spinal nociceptive/pain processing by releasing a mix of serotonin, noradrenalin, GABA, and glycine.

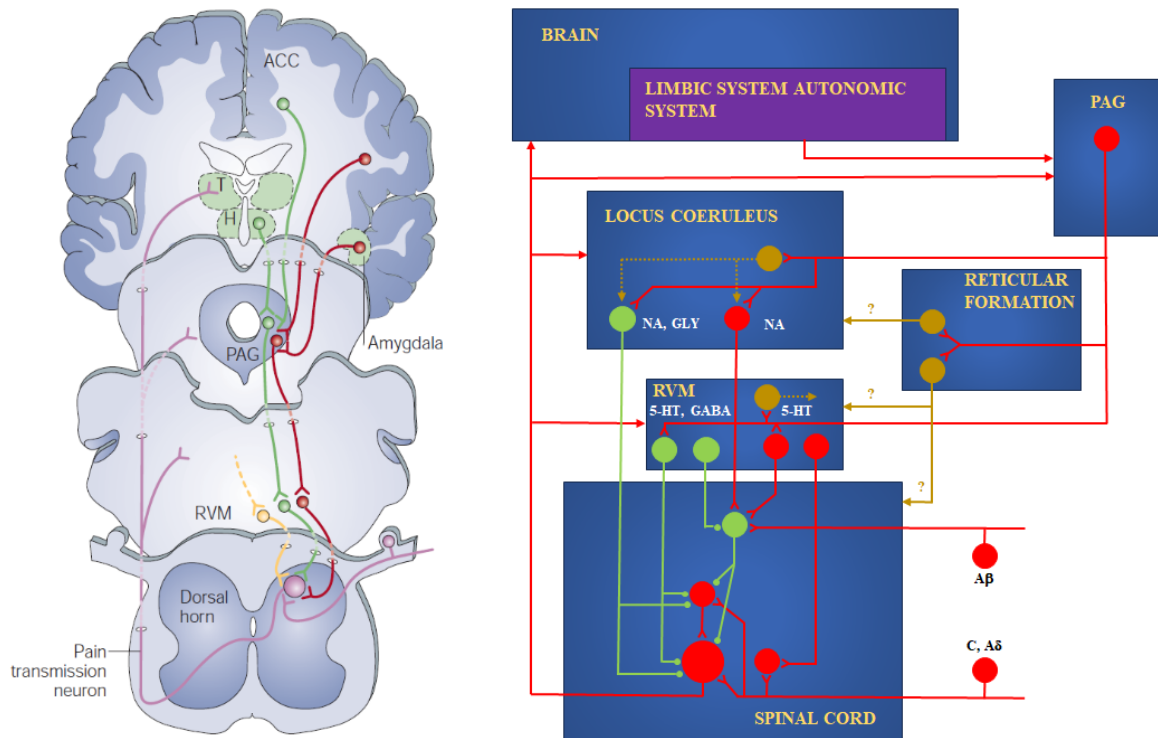


Figure 10: Illustration and schematic diagram of the descending fibres from the cerebral cortex to the spinal dorsal horn (image on the left from Fields, 2004). RVM: rostral ventromedial medulla; PAG: periaqueductal grey; H: hypothalamus; T: thalamus; ACC: anterior cingulate cortex; NA: noradrenaline; GLY: glycine; 5-HT: serotonin.

2.3.5. Projection neurons

Nociceptive/pain information is relayed to higher brain centers by two sets of projection neurons. One of them is within lamina I, and the other is in laminae III-IV. Axons arising from both sets of neurons cross the midline and ascend in the contralateral anterolateral white matter (ALS) (Werceberger and Basbaum, 2019). As discussed earlier, axons ascending in the ALS terminate in several parts of the brainstem and diencephalon. Recent studies, however, showed that axons of lamina I and laminae III-IV projection neurons terminate in different areas. Lamina I neurons project primarily to the brainstem including the parabrachial nucleus, whereas the axons of laminae III-IV terminate mostly in the lateral thalamus (Todd, 2010). Thus, the target territories of lamina I projection neurons primarily activate cortical territories which generate the motivational-affective component of pain, whereas neural signals

conducted by the axons of laminae III-IV projection neurons seem to be used mostly for the generation of the sensory-discriminative component of pain (Al-Khater and Todd, 2009).

2.3.6. Neuronal circuits

As I tried to demonstrate in the previous sections, the neuronal apparatus of laminae I-IV is very complex. The major constituents are the following: C, A δ and A β primary afferents, spinal excitatory and inhibitory interneurons that show highly variable neurochemical and functional properties, superficial and deep projection neurons, and descending fibres releasing various neurotransmitters evoking different forms of inhibitions on spinal neurons. On top of these, these elements are interacting with each other in a way which is poorly understood. Thus, because of the high level of complexity of this neural apparatus, the construction of neuronal circuits that may explain the major morphological and functional properties of spinal nociceptive/pain processing is not an easy task. Despite this, different authors have created hypothetical neuronal circuits summarising some elements of the possible constituents and explaining some functional properties of the network, but nobody has had the ambition to build up a neural network that may include all elements of this complex neural apparatus. For this reason, I would like to present only one hypothetical neural circuit here, which is one of the most complex ones and created by Peirs and Seal (2016). See the description of the model in the legend of Figure 11.

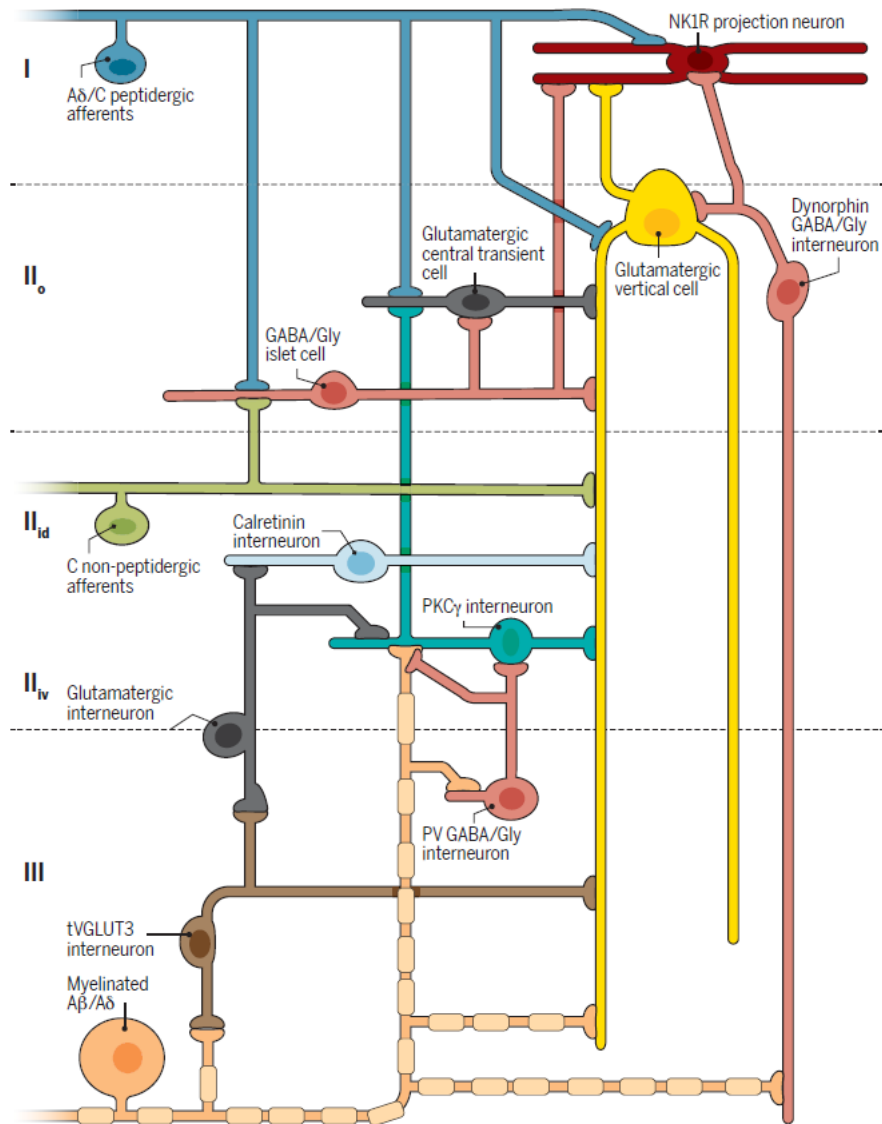


Figure 11: Illustration of a dorsal horn neural circuit of pain. A δ and peptidergic C primary afferents (blue) project onto excitatory interneurons in lamina II_o (central cells (dark grey); vertical cells (yellow)) and onto NK1R projection neurons (red) in lamina I. Non-peptidergic C primary afferents (green) project to lamina II_{id}, including to excitatory vertical cells with ventrally directed elongated dendrites. Both primary A δ , peptidergic and non-peptidergic afferents also contact inhibitory islet cells (horizontally elongated (pink)). Stimulation of nociceptive afferents activates excitatory central cells, vertical cells, and NK1R projection neurons to mediate noxious pain. Inhibitory islet cells modulate this activity. A β and A δ primary afferents (orange) project onto excitatory interneurons expressing tVGLUT3 in lamina III (brown), PKC γ in lamina II_{iv} (teal), and vertical cells in lamina II_o. These myelinated afferents also contact PV inhibitory interneurons in lamina III (radial (light red)) and dynorphin inhibitory vertical cells in lamina II_o (vertical (light red)). tVGLUT3 interneurons project onto excitatory vertical cell dendrites and intermediate excitatory interneurons in lamina III. Intermediate interneurons project onto PKC γ and calretinin excitatory interneurons in lamina II_{iv}. Inhibitory interneurons prevent myelinated A-fibres-mediated activation of the nociceptive network through feed-forward circuits that act on

PKC γ interneurons, vertical cells, and NK1R projection neurons. (Peirs and Seal, 2016) Despite this, different authors have created hypothetical neuronal circuits summarizing some elements of the possible constituents and explaining some functional properties of the network (Todd, 2010; Benarroch, 2016), but nobody has had the ambition to build up a neural network that may include all elements of this complex neural apparatus.

2.4. Complexity and plasticity of spinal nociceptive/pain processing

2.4.1. Complexity of spinal nociceptive/pain processing

As discussed earlier, spinal nociceptive/pain processing is a complex information processing in which several neuronal elements play vital roles. This information processing machinery, however, is even more complex, because in addition to neuronal players and glutamatergic, GABAergic and glycinergic mechanisms, the contribution of glial cells (microglia and astrocytes), other signaling mechanisms (e.g. various peptides or cannabinoid mediated events), ion channels and membrane transporters regulating the resting membrane potentials of neurons (e.g. hyperpolarization-activated and cyclic nucleotide-gated cation channels) are also inevitable for the proper propagation and modification of nociceptive/pain signals in the spinal dorsal horn (Zeilhofer *et al.*, 2012, 2018, 2021).

2.4.2. Plasticity of spinal nociceptive/pain processing neural circuits

Usually evoked by inflammatory or neuropathic peripheral events, nociceptive primary afferents may become overexcited, and they carry these increased activities to the spinal dorsal horn. In addition to glutamate, the overexcited primary afferents can release other substances like neuropeptides (e.g., SP), neurotrophic factors (e.g., brain derived neurotrophic factor), the release of which induces a complex chemical tuning of dorsal horn neurons and glial cells that appears in changes in biophysical membrane properties, synaptic plasticity, and network plasticity (Colangelo *et al.*, 2008; West *et al.*, 2015). Finally, all these events result in an enhanced excitatory state of neural circuits in the superficial spinal dorsal horn leading to hyperalgesia and allodynia, and pain sensation at the level of the cerebral cortex. The role of inhibitory neurons, and plasticity of inhibitory neurotransmission cannot be overestimated in these processes.

2.5. Fast inhibitory neurotransmission in the spinal dorsal horn

Inhibition plays essential roles in all different functional states of nociceptive/pain processing neural circuits of the spinal dorsal horn. i) The GABAergic and glycinergic cells are tonically active even in situations when the dorsal horn does not receive any specific activation from primary afferents (Zeilhofer *et al.*, 2012). In these cases, a resting level of GABA and glycine

release is needed to prevent spontaneous activities of spinal neurons, which may lead to spontaneous pain. ii) During stimulation of nociceptive afferents, feedback and feedforward ways of inhibition are needed to maintain appropriate levels of neural excitation, to avoid hyperalgesia (Zhang *et al.*, 2018). iii) Inhibition in the dorsal horn is also required to restrict evoked neural activities to the locally activated areas of the dorsal horn. In the lack of this collateral type of inhibition the local excitation may spread to non-stimulated areas of the spinal cord causing radiating and/or mirror-image pain (Kopach *et al.*, 2017). iv) Inhibition is vital in the separation of spinal neural circuits processing nociceptive and non-nociceptive peripheral signals (Todd, 2010). This is very important because these circuits are interconnected by pre-existing pathways. The reduced level or lack of this type of inhibition allows crosstalk between the two systems and non-nociceptive inputs may activate nociceptive neurons leading to the phenomenon of allodynia (Peirs *et al.*, 2021). v) In case of enhanced excitatory states of spinal pain processing neural circuits, presynaptic inhibition reduces the release of glutamate and other substances from primary afferents, whereas postsynaptic inhibition dampens Ca^{++} transients in spinal neurons evoked by NMDA receptors activated by the incoming nociceptive inputs (Zeilhofer *et al.*, 2012; Chen *et al.*, 2014; Gradwell *et al.*, 2020). If for some reason, the pre- and postsynaptic inhibition is reduced, the enhanced excitatory state of the superficial spinal dorsal horn may lead to chronic pain conditions (Foster *et al.*, 2015; Lu *et al.*, 2013).

2.5.1. GABAergic versus glycinergic inhibition in the spinal dorsal horn

As presented in the previous section, fast inhibitory neurotransmission mediated by GABA and glycine plays a vital role in shaping up neural activities in the nociceptive/pain processing neuronal circuits. The relative contribution of GABA and glycine to the inhibitory events is, however, under continuous and vivid debate.

Early immunohistochemical studies revealed strong colocalization between GABA and glycine in laminae I-III of the spinal dorsal horn in a way that glycine was detected exclusively in GABA-containing neurons (Todd and Sullivan, 1990; Todd, 1996; Todd *et al.*, 1995, 1996), whereas glycine was found in only less than half of the GABAergic cells (Todd and Sullivan, 1990; Mitchell *et al.*, 1993). Thus, one may expect that cells displaying glycine-mediated miniature inhibitory postsynaptic currents (mIPSCs) would also show GABA-mediated mIPSCs. However, in addition to mixed GABA-glycine and GABA-only mIPSCs, glycine-only mIPSCs have been also recorded from neurons in the superficial spinal dorsal horn (Chéry and De Korninck, 1999; Keller *et al.*, 2001). Following these early observations, experimental

data substantiating the fundamental role of glycine-only inhibition in the nociceptive/pain processing neuronal circuits are continuously piling up (Foster *et al.*, 2015; Takazawa and McDermott, 2010; Lu *et al.*, 2013; Punnakkal *et al.*, 2014; Takazawa *et al.*, 2017; Aubrey and Supplisson, 2018; El Khoueiry *et al.*, 2022). These data clearly indicate that a substantial proportion of the inhibitory input onto neurons in the superficial spinal dorsal horn is glycinergic (Takazawa and McDermott, 2010; Punnakkal *et al.*, 2014; Foster *et al.*, 2015; Lu *et al.*, 2015; Takazawa *et al.*, 2017). Convincing experimental evidence accumulates showing that the suppression of glycinergic synaptic transmission induces spontaneous pain, hyperalgesia, allodynia, and chronic pain conditions (Zeilhofer, 2005; Torsney and MacDermott, 2006, Miraucourt *et al.*, 2007, 2009; Zeilhofer *et al.*, 2012; Lu *et al.*, 2013; Foster *et al.*, 2015; Peirs and Seal, 2016). Strongly reinforcing the importance of glycinergic inhibition, Foster *et al.* (2015) found that more than 70% of the total inhibitory postsynaptic current amplitude recorded in excitatory neurons was blocked by the application of the glycine receptor antagonist strychnine and only the rest could be blocked by the GABA_A receptor antagonist bicuculline. In addition, by recording mIPSCs in spinal dorsal horn neurons it was demonstrated that postsynaptic currents mediated by either glycine or GABA_A receptors were common, but the occurrence of mixed postsynaptic currents was remarkably low (Inquimbert *et al.*, 2007; Mitchell *et al.*, 2007; Anderson *et al.*, 2009; El Khoueiry *et al.*, 2022).

These observations indicate that although GABAergic transmission is very important, glycine seems to be the neurotransmitter which mediates most of the fast inhibitory neurotransmission in the nociceptive/pain processing neuronal circuits in the spinal dorsal horn. Thus, further studies are needed to investigate the cellular and molecular features, synaptic relations of glycinergic neurons and the way how they contribute to the formation of neuronal circuits in the spinal dorsal horn.

3. Aims

As exposed in the Theoretical Background, a great deal of experimental evidence shows that glycinergic neurons play an essential role in spinal pain processing (Lu *et al.*, 2013; Foster *et al.*, 2015). However, apart from some early studies (Todd and Sullivan, 1990; Powell and Todd, 1992), there is no report about the morphological and neurochemical properties, and the synaptic relations of glycinergic neurons in the spinal dorsal horn. Without this fundamental knowledge, however, the contribution of glycinergic inhibition to spinal pain processing cannot be accurately evaluated. Thus, we intended to explore:

- the distribution,
- the morphology,
- the neurochemical properties,
- the synaptic relations

of glycinergic neurons in laminae I-IV of the spinal dorsal horn to advance our understanding about the contribution of glycinergic inhibition to spinal pain processing.

4. Material and Methods

4.1. Animals

The experiments were performed on adult male mice. The Animal Care and Protection Committee at the University of Debrecen approved all animal experimental protocols (2/2017/DEMÁB) which were conducted by following the European Community Council Directives.

Four types of mice were used:

- 1) Wild-type B6
- 2) Transgenic mice
 - a. GlyT2::CreERT2- mice

The GlyT2::CreERT2 mice, expressing CreERT2 recombinase under the transcriptional control of the GlyT2 gene were a gift from Professor Hans Ulrich Zeilhofer. A bacterial artificial chromosome (BAC) was used to carry a Cre that expresses a target gene (Zeilhofer *et al.*, 2005; Xu and Anderson, 2010).

- b. Tg(PAX2-Cre)1Akg/Mmnc- mice

The Tg(Pax2-cre)1Akg/Mmnc mice, expressing Cre recombinase under the transcriptional control of the Pax2 gene were obtained from Mutant Mouse Regional Resource Centers, Stock Number: 010569-UNC.

- c. Prkcg^{tm2}/Cre/ERT2/Ddg/J- mice

The B6; 129S6-Prkcg^{tm2}/cre/ERT2)Ddg/J mice, expressing CreERT2 recombinase under the transcriptional control of the PKC γ gene were obtained from The Jackson Laboratory, Bar Harbor, ME, USA, Stock number: 030289. In case of Cre-ERT2, Cre is combined with human estrogen receptor (ER) (Indra *et al.*, 1999).

- d. 007914-B6.Cg-Gt(ROSA)26Sortm14(CAG-tdTomato)Hze/J

The 007914-B6.Cg-Gt(ROSA)26Sortm14(CAG-tdTomato)Hze/J reporter mice were obtained from The Jackson Laboratories, Bar Harbor, ME, USA.

Table 1: List of transgenic animals.

Name	Strain aim	Expression
GlyT2::CreERT2	CreERT2-Driver	GlyT2
Tg(PAX2-Cre)1Akg/Mmnc	Cre-Driver	PAX2
Prkcg ^{tm2} /Cre/ERT2/Ddg/J	CreERT2-Driver	PKC γ
007914-B6.Cg-Gt(ROSA)26Sortm14(CAG-tdTomato)Hze/J	Reporter	tdTomato

The Cre or CreERT2 lines were crossed with the tdTomato reporter mice, and a postnatal (at 8th to 10th days) intraperitoneal tamoxifen injection (2 mg/pup, Sigma, Cat# T5648) was given to the offspring of the CreERT2 lines (a, c) to induce the tdTomato expression (Figure 12). The tamoxifen was prepared as described by Zheng *et al.* (2019), it was dissolved in 20mg/mL concentration in ethanol, combined with double volume of sunflower seed oil (Sigma) and vortexed for 5–10 minutes. Next, the mixture was centrifuged under vacuum for 20–30 minutes to remove the ethanol. The final solution was maintained at -20°C.

All the offspring were genotyped for the tdTomato transgene, and for GlyT2::CreERT2, Tg(PAX2-Cre)1Akg/Mmnc, and Prkcgtm2/Cre/ERT2/Ddg/J transgenes at the 18th to 20th postnatal days. The animals that expressed both genes were used for the experiments at the age of 3 to 5 months.

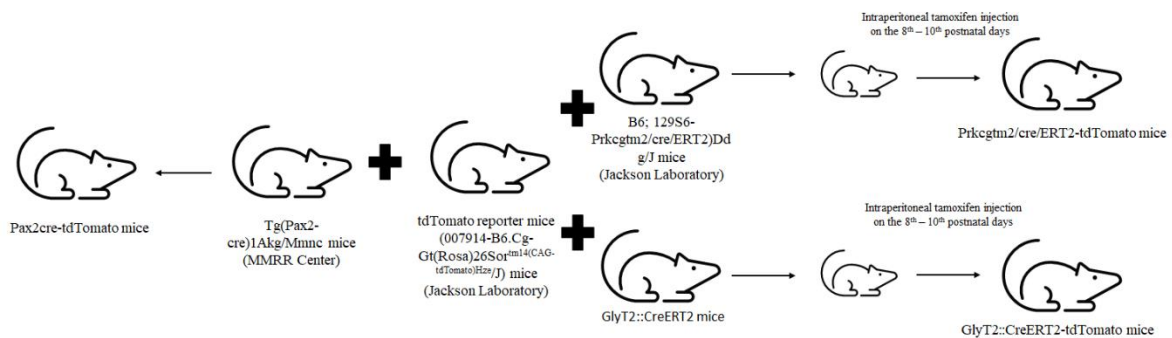


Figure 12: Schematic illustration of the crossing used to obtain the 3 transgenic mice line used in this project.

4.2. Hemisection

Animals used for the investigation of the synaptic targets of GlyT2 positive axon terminals underwent a laminectomy at the level of the 9th and 10th thoracic vertebrae under deep sodium pentobarbital anaesthesia (50 mg/kg, intraperitoneal). One side of the spinal cord at the level of the 11th and 12th thoracic spinal segment was transected whereas the other side remained intact. The back muscles and skin were sutured. The animals recovered from the surgery and further experiments were performed on them after 3 to 4 weeks. For the confirmation of the accuracy of the hemisection, sections from the site of hemisection were stained with cresyl violet (Figure 13). The experiments were performed on the hemisected side at the level of the L4 and L5 segments of the spinal cord.

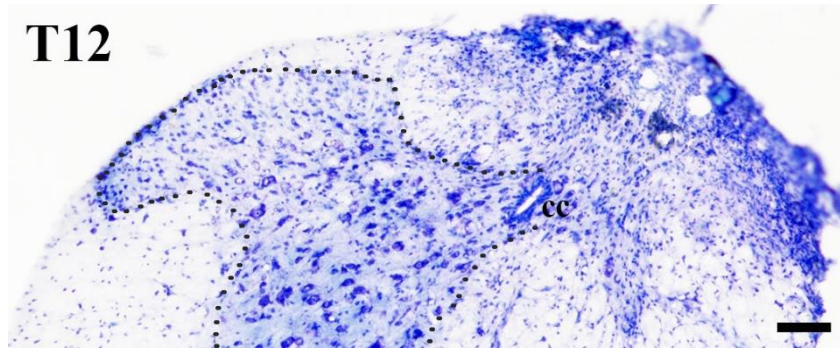


Figure 13: Light microscope image of cresyl violet-stained section of the spinal cord, at the level of hemisection. One side of the spinal cord (left to the central canal) exhibits the typical cytoarchitectonic pattern of the spinal cord, whereas the other side (the hemisected side, right to the central canal) does not. The border between the grey and white matter is marked by dotted line on the intact side. Central canal (cc). Bar: 100 μ m.

4.3. Preparation of tissue sections

4.3.1. For immunohistochemistry

The animals were anesthetized with sodium pentobarbital (50 mg/kg, intraperitoneal), and perfused transcardially with Tyrode's solution (oxygenated with a mixture of 95% O₂, 5% CO₂), followed by a fixative containing 4.0% paraformaldehyde (in 0.1 M phosphate buffer (PB; pH7.4) for light microscopy, or 2.5% paraformaldehyde and 0.5% glutaraldehyde (in 0.15 M cacodylate buffer (pH7.4) for electron microscopy. The lumbar segments of the spinal cord were removed and postfixed in the same fixative for 4 hours. Then, they were placed into 10 and 20% sucrose solutions (in 0.1 M PB) until they sink. Liquid nitrogen was used to freeze-thaw the spinal cord, which was then sectioned at 50 or 100 μ m (only from the GlyT2::Cre ERT2-tdTomato animals) on a vibratome and washed several times in 0.1 M PB or in 0.15 M cacodylate buffer. The 100 μ m sections were cut in sagittal orientation and affixed on glass slides, while 50 μ m sections were cut in sagittal, transverse, and horizontal orientations. Sections which were fixed for electron microscopy were treated with 0.1% H₂O₂ and 1% sodium borohydride for 15 and 30 minutes, respectively.

4.3.2. For *in situ* hybridization

Animals were deeply anesthetized with sodium pentobarbital (50 mg/kg, intraperitoneal). The lumbar segments of the spinal cord were removed and frozen on liquid nitrogen. The frozen spinal cord was embedded in a cryo-embedding medium. Sections (16 μ m thick) were cut at a cryostat, affixed on Superfrost Plus glass slides (Thermo Fischer Scientific, Cat# J1800AMNZ), and placed under -20°C until antibodies treatments.

4.4. Immunohistochemistry for light microscopy

In general, the free-floating sections were incubated with 10% normal goat or rabbit serum (Vector Laboratories., Burlingame, CA, USA) for 50 minutes, followed by the primary antibodies listed in Table 2, diluted in 10 mM PBS pH 7.4 with 1% normal goat or rabbit serum, for 2 days at 4°C. Then, the sections were transferred into a solution containing the respective secondary antibodies diluted in 10 mM PBS pH 7.4 with 1% normal goat or rabbit serum for 5 to 6 hours at room temperature. Finally, the sections were affixed on glass slides and covered with Vectashield mounting medium (Vector Laboratories., Burlingame, CA, USA).

Table 2: List of primary antibodies used in immunohistochemistry for light and electron microscopy.

Primary antibody					
Target	Host species	Dilution	Company	Catalog number (Cat#)	Research Resource Identifier (RRID)
biotinylated IB4 (b-IB4)		1:2000	Thermo Fisher Scientific	I21414	
paired box gene 2 transcription factor (PAX2)	rabbit	1:1000		71-6000	AB_2533990
CGRP		1:3000	Peninsula Laboratories	T-4239	AB_518150
GAL		1:12000		T-4334.0050	AB_518348
GAD 65/67 (65kD and 67 kD enzyme isoform)		1:2000	Abcam	AB183999	EPR19366
NPY		1:400		AB30914	AB_2807030
PKC γ		1:2000		AB71558	AB_1281066
VGLUT2		1:1000		AB216463	AB_2893024
VGLUT1		1:2000		AB227805	AB_2868428
CaB		1:10,000	Swant	CB38	AB_10000340
PV		1:60,000		PV27	AB_2631173
CR	goat	1:30,000		CG1	AB_10000342

nNOS		1:8000	Abcam	ab1376	AB_1566510
PV	mouse	1:20,000	Swant	PV235	AB_10000393
GlyT2	guinea pig	1:40,000	Synaptic Systems	272004	AB_2619998

4.4.1. Single immunostaining of sections obtained from wild type animals

Free-floating section from hemisected and non-operated wild type mice were incubated with guinea pig anti glycine transporter 2 (GlyT2) (diluted 1:40,000, Synaptic Systems, Göttingen, Germany, Cat# 272 004, RRID: AB_2619998) primary antibody and with goat anti-guinea pig IgG secondary antibody conjugated with Alexa Fluor 488 (diluted 1:1000, Thermo Fisher Scientific, Cat#A-11073, RRID: AB_2537117), following the protocol described in section 4.4.

4.4.2. Single immunostaining of sections obtained from GlyT2::CreERT2-tdTomato animals

Free-floating sections from GlyT2::CreERT2-tdTomato mice were incubated with one of the subsequent primary antibodies:

(1) rabbit anti-paired box gene 2 transcription factor (PAX2) (diluted 1:1000, Thermo Fisher Scientific Cat# 71-6000, RRID: AB_2533990),

(2) goat anti-neuronal nitric oxide synthase (nNOS) (diluted 1:8000, Abcam Cat# ab1376, RRID: AB_1566510),

(3) rabbit anti-neuropeptide Y (NPY) (diluted 1:400, ABCAM Cat# AB30914, RRID: AB_2807030),

(4) rabbit anti-parvalbumin (PV) (diluted 1:60,000, Swant Cat# PV27, RRID: AB_2631173) or mouse anti-PV (diluted 1:20,000, Swant Cat# PV235, RRID: AB_10000393),

(5) rabbit anti-galanin (diluted 1:12000, Peninsula Laboratories Cat# T-4334.0050, RRID: AB_518348), and

(6) goat anti-calretinin (diluted 1:30,000, Swant Cat# CG1, RRID: AB_10000342).

And with the respective secondary antibody conjugated with Alexa Fluor 488:

(7) goat anti-rabbit IgG (diluted 1:1000, Thermo Fisher Scientific Cat# A-11008, RRID: AB_143165),

(8) goat antimouse IgG (diluted 1:1000, Thermo Fisher Scientific Cat# A-11001, RRID: AB_2534069), or

(9) rabbit anti-goat IgG (diluted 1:1000, Thermo Fisher Scientific Cat# A-11078, RRID: AB_2534122).

Following the protocol described in section 4.4.

4.4.3. Double immunostaining on sections obtained from GlyT2::CreERT2-tdTomato animals to reveal colocalization between GlyT2 and GAD65/67

Free-floating sections from hemisected and non-operated GlyT2::CreERT2-tdTomato mice were incubated with a mixture of guinea pig anti-GlyT2 (diluted 1:1000, Synaptic Systems Cat# 272004, RRID: AB_2619998) and rabbit anti-GAD recognizing both 65kD and 67 kD isoforms of the enzyme (GAD65/67) (diluted 1:2000, Abcam, Cat# AB183999, EPR19366) primary antibodies. Then, they were treated with a mixture of goat anti-guinea pig IgG conjugated with Alexa Fluor 488 (diluted 1:1000, Thermo Fisher Scientific Cat# A-11073, RRID: AB_2534117) and goat anti-rabbit IgG conjugated with Alexa Fluor 647 (diluted 1:1000, Thermo Fisher Scientific Cat# A-21244, RRID: AB_2535812) secondary antibodies, following the protocol described in section 4.4.

4.4.4. Double immunostaining on sections obtained from wild type animals to reveal close appositions between GlyT2-IR and other axon terminals identified by various axonal markers

Following hemisection, free-floating section from wild type mice were incubated with a mixture of guinea pig anti-glycine transporter 2 (GlyT2) (diluted 1:40,000, Synaptic Systems Cat# 272 004, RRID: AB_2619998) and one of the following primary antibodies:

(1) rabbit anti-calcitonin gene-related peptide (CGRP, diluted 1:3000, Peninsula Laboratories, Augst, Switzerland, Cat# T-4239; RRID: AB_518150),

(2) biotinylated isolectin B4 (b-IB4, diluted 1:2000, Thermo Fisher Scientific, Cat# I21414),

(3) rabbit anti-vesicular glutamate transporter 2 (VGLUT2, diluted 1:1000, ABCAM, Cambridge, UK, Cat# AB216463; RRID: AB_2893024), or

(4) rabbit anti-vesicular glutamate transporter 1 (VGLUT1, diluted 1:2000, ABCAM, Cat#, AB227805; RRID: AB_2868428).

Sections were then incubated with a mixture of goat anti guinea pig IgG conjugated with Alexa Fluor 555 (diluted 1:1000, Thermo Fisher Scientific, Cat# A-21435, RRID:AB_2535856) and goat anti-rabbit IgG conjugated with Alexa Fluor 488 (diluted 1:1000, Thermo Fisher Scientific Cat# A11034, RRID:AB_2576217) or streptavidin conjugated with Alexa Fluor 488 (1:1000, Thermo Fisher Scientific, Cat# S11223) secondary antibodies, following the protocol described in section 4.4.

4.4.5. Double immunostaining on sections obtained from PAX2::Cre-tdTomato animals

Free-floating section from PAX2::Cre-tdTomato mice were incubated with a mixture of guinea pig anti-GlyT2 (diluted 1:40,000, Synaptic Systems Cat# 272 004, RRID:AB_2619998) and one of the following primary antibodies:

(1) rabbit anti-neuronal nitric oxide synthase (nNOS) (diluted 1:4000, Abcam Cat# AB76067, RRID: AB_2152469),

(2) rabbit anti-parvalbumin (PV) (diluted 1:60,000, Swant AG, Burgdorf, Switzerland, Cat# PV27, RRID: AB_2631173),

(3) rabbit anti-galanin (GAL) (diluted 1:10,000, Peninsula Laboratories Cat# T-4334, RRID: AB_518348),

(4) rabbit anti-calretinin (CR) (diluted 1:5000, Swant Cat# 7697, RRID: AB_2721226),

(5) rabbit anti-calbindin (CaB) (diluted 1:10,000, Swant, Cat# CB38, RRID: AB_10000340,

(6) rabbit anti-gamma isoform of protein kinase C (PKC γ) (diluted 1:2000, Abcam, Cat# AB71558, RRID: AB_1281066).

Sections were transferred into a mixture of goat anti-guinea pig conjugated with Alexa Fluor 647 (diluted 1:1000, Thermo Fisher Scientific, Cat# A21450, RRID: AB_2735091) and goat anti-rabbit IgG conjugated with Alexa Fluor 488 (diluted 1:1000, Thermo Fisher Scientific, Cat# A11034, RRID: AB_2535849) secondary antibodies, following the protocol described in section 4.4.

4.4.6. Triple immunostaining on sections obtained from PKC γ ::CreERT2-tdTomato animals

Free-floating section from PKC γ ::CreERT2-tdTomato mice were incubated with a mixture of guinea pig anti-GlyT2 (diluted 1:40,000, Synaptic Systems Cat# 272 004, RRID: AB_2619998), rabbit anti-PAX2 (diluted 1:200, Thermo Fisher Scientific, Cat# 71-6000, RRID: AB_2533990) and either biotinylated IB4 (b-IB4, diluted 1:2000, Thermo Fisher Scientific, Cat# I21414), or goat anti-vesicular glutamate transporter 1 (VGLUT1, diluted 1:5000, Synaptic System, Cat# 135 307; RRID: AB_2619821). Sections were then incubated with a mixture of donkey anti-guinea pig IgG conjugated with Alexa Fluor 647 (diluted 1:1000, Jackson ImmunoResearch, West Grove, PA, USA, Cat# 706-605-148, RRID: AB_2340476), donkey anti-rabbit conjugated with 405 (diluted 1:1000, Thermo Fisher Scientific, Cat# A48258, RRID: AB_2890547) and donkey anti-goat IgG conjugated with Alexa Fluor 488 (diluted 1:1000, Thermo Fisher Scientific Cat# A11055, RRID: AB_2534102) or streptavidin conjugated with Alexa Fluor 488 (diluted 1:1000, Thermo Fisher Scientific, Cat# S11223) secondary antibodies, following the protocol described in section 4.4.

4.5. Immunohistochemistry for electron microscopy

Sections were placed into 10% normal goat serum for 50 minutes, followed by 1% normal goat serum for 10 minutes and incubated with guinea pig anti-GlyT2 (diluted 1:40,000, Synaptic Systems Cat# 272 004, RRID: AB_2619998) for 2 days at 4°C. Then, the sections were transferred into biotinylated goat anti-guinea pig IgG (diluted 1:200, Vector Laboratories Cat# BA-7000, RRID: AB_2336132) for 5-6 hours, followed by avidin biotinylated horseradish peroxidase solution (ABC) for overnight. The immunostaining was visualized with nickel-intensified diaminobenzidine (NiDAB) chromogen solution. The NiDAB end-product was intensified with silver precipitation, which was stabilized with gold toning according to Kalló *et al.* (2001) and Bardóczy *et al.* (2017). After this, the sections were treated with a mixture of 0.5% OsO₄ and 1.5% ferricyanide dissolved in 0.15 M cacodylate buffer for 15 minutes, followed by dehydration. Finally, the sections were embedded in Durcupan. Ultrathin sections were cut at 50-60 nm thickness, collected onto Formvar-coated single-slot grids, and counterstained with 2% lead citrate. They were analysed with a JEOL1010 transmission electron microscope, and images were taken with an Olympus Veleta slow scan cooled digital camera.

4.6. Multiplex *in situ* hybridization

- a. To reveal colocalization between tdTomato and RET as well as ROR β mRNAs

The hybridization was performed following the RNAScope® Multiplex Fluorescent Assay (ACD, Biotechne, Cat# 320850, Minneapolis, USA), the manufacturer's pre-treatment protocol for fresh frozen tissue (document number 320513, revision date: November 5, 2015) and detection protocol (document number 320293-USM, revision date: March 14, 2017). The probes used were Slc6a5 (GlyT2) (ACD, Biotechne, Cat# 409741-C3), tdTomato (ACD, Biotechne, Cat# 317041 and 317041-C2), retinoic acid-related orphan nuclear receptor β (ROR β) (ACD, Biotechne, Cat# 444271-C3), and receptor tyrosine kinase RET (ACD, Biotechne, Cat# 431791) (Table 3). The sections were covered with Vectashield mounting medium with DAPI (Vector Laboratories, Burlingame, CA, USA).

- b. To reveal colocalization between GlyT2 and GAD65/67 mRNAs in tdTomato mRNA expressing neurons

The hybridization was performed on PAX2::Cre-tdTomato mice spinal cord sections, following the same Assay, pre-treatment protocol, and detection protocol described in the previous section. The probes used were Mm-GAD1 (GAD67, ACD, Bio-technne, Cat# 400951), Mm-GAD2 (GAD65, ACD, Bio-technne, Cat# 439371), Mm-Slc6a5-C2 (GlyT2, ACD, Bio-technne, Cat# 409741-C2), and tdTomato-C3 (ACD, Biotechne, Cat# 317041-C3). Sections were covered with Vectashield mounting medium containing DAPI.

Table 3: List of probes used in the *in situ* hybridization experiments.

<i>In situ</i> hybridization probes			
Target	Probe design	Company	Catalog number (Cat#)
Mm-GAD1 (GAD67)	ACD	Biotechne	400951
Mm-GAD2 (GAD65)			439371
Mm-Slc6a5-C2 (GlyT2)			409741-C2
receptor tyrosine kinase RET			431791
retinoic acid-related orphan nuclear receptor β (ROR β)			444271-C3
Slc6a5 (GlyT2)			409741-C3
tdTomato			317041 and 317041-C2
tdTomato-C3			317041-C3

4.7. Confocal microscopy

Serial optical sections with 1 μm thickness and 0.5 μm overlap were obtained in an Olympus FV3000 confocal microscope using a 40x oil-immersion lens (numerical aperture: 1.3). For all images, the confocal aperture and gain, and laser power were the same, and no saturated images were taken. The images were evaluated at Adobe Photoshop CS5 software. Immunohistochemical stainings were evaluated in 1 μm thick optical sections. In case of FISH, we created 3 μm thick compressed images by merging five consecutive optical sections.

4.8. Neurolucida reconstruction

Neurolucida system (v.11.07, MicroBrightfield Bioscience, Williston, VT, USA) was used for the reconstruction of the neurons. In the first set of reconstruction, sections from GlyT2::CreERT2-tdTomato mice were used, in which tdTomato-labelled cell bodies and dendrites were reconstructed in 3D, from serial image stack.. In the second set of reconstruction, sections from PKC::Cre/ERT2-TtdTomato mice triple immunostained for GlyT2, PAX2, and VGLUT1 or IB4- binding were used, in which tdTomato-labelled PKC γ -containing cell bodies and dendrites, together with GlyT2 and VGLUT1 immunostained or IB4-binding axon terminals making contact with tdTomato-labelled cell bodies and dendrites were reconstructed in 3D, from serial image stack.

4.9. Statistical analysis

4.9.1. Expression of markers within the cell bodies of GlyT2::CreERT2-tdTomato labelled neurons

To investigate the colocalization of GlyT2::CreERT2-tdTomato labelling with the expression of PAX2, nNOS, NPY, GAL, PV, CR, GlyT2, ROR β , and RET, the numbers of cell bodies labelled with tdTomato and/or immunostained for PAX2, nNOS, NPY, GAL, PV, CR, and/or giving positive hybridization signal for GlyT2, ROR β , and RET were counted in laminae of the dorsal horn where the immunostaining for the marker was present. It was calculated what percentage of the tdTomato-labelled neurons were also positive for the markers. Three animals were used to evaluate all the investigated markers' colocalization. The quantitative measurements were carried out in three animals, and five sections were selected from each animal. Thus, the final calculations were based on the investigation of 15 independent sections.

4.9.2. Expression of GlyT2 and GAD65/67 within the axon terminals of GlyT2::CreERT2-tdTomato labelled neurons

Considering the limited penetration of both antibodies into the sections, the colocalization of the GlyT2::CreERT2-tdTomato labelling with immunostaining for GlyT2 and GAD65/67, and the colocalization between GlyT2 and GAD65/67 immunostaining were investigated in the superficial layers of the tissue sections (2 to 3 μm from the surface) in which immunostaining for both GlyT2 and GAD65/67 were strong. The quantification of the immunostained profiles were done manually. A 10x10 standard square grid in which the edge-length of the unit square was 5 μm was placed onto the regions of confocal images corresponding to laminae I–II and lamina III of the superficial spinal dorsal horn.

The grids were placed onto the sections according to the subsequent standards:

- (1) the border between the dorsal column and the dorsal horn was distinguished on the premise of the density of immunostaining;
- (2) the border between lamina II and lamina III was estimated based on earlier findings. Ultrastructural studies showed that myelinated axons are abundant in lamina III, while they are essentially non-existent in lamina II. Thus, the border between lamina II and III can be precisely defined and the thickness of laminae I-II can be exactly measured in ultrastructural studies (McClung and Castro, 1978; Molander *et al.*, 1984; McNeill *et al.*, 1988);
- (3) cytoarchitectural studies showed that at the level of L4 and L5 segments of the mouse spinal cord lamina III is as thick as laminae I and II together (Sengul *et al.*, 2013).

Based on these earlier observations, immunolabeling was examined a) in the most superficial 60 μm zone of the dorsal horn, corresponding to laminae I-II, and b) in a zone from 60 to 120 μm from the dorsal border of the dorsal horn corresponding to lamina III at the L4 and L5 level of the mouse spinal dorsal horn.

The profiles showing tdTomato labelling or immunoreactivity for GlyT2 or GAD65/67 and located over the edges of the 5 μm grids were counted. Data were evaluated according to the following approaches:

- (a) how many of the tdTomato-labelled profiles were also immunoreactive for GlyT2,
- (b) how many of the profiles double labelled for tdTomato and GlyT2 were also immunoreactive for GAD65/67,

- (c) how many of the GlyT2-positive axon terminals, regardless of whether they were positive or negative for tdTomato, were also immunostained for GAD65/67.

Considering that the GlyT2 antibody used in this investigation was produced against the transporter's intracellular domain, the GlyT2 immunolabelling was expected to be located within the confines of the axon terminals. The colocalizations were investigated in 3 animals. Three sections from each animal were arbitrarily selected, thus 9 independent sections were used to acquire the quantitative data.

4.9.3. Changes in the numbers of GlyT2 immunostained boutons following hemisection of the spinal cord

The numbers of GlyT2 immunostained boutons in laminae I-II, and lamina III of L4-L5 spinal cord were compared in sections collected from non-operated animals and animals subjected to hemisection of the Th11–Th12 spinal cord. For animals that underwent hemisection, immunostained boutons were quantified ipsilateral to the hemisection. Considering the limitation in the penetration of the antibodies into the sections, the quantification was performed on confocal optical images recorded from the superficial layer of the sections (2 to 3 μm from the surface). Data were collected according to the procedure described in section 4.9.2.

The evaluation was carried out on 3 non-operated animals, and 3 mice that underwent hemisection. Five sections from each animal were arbitrarily selected; therefore, 15 independent sections were used to acquire the quantitative data.

4.9.4. Colocalization of td-Tomato, GAD1/2 (GAD65/67), and GlyT2 mRNAs

Multiplex FISH was used to analyse the colocalization of tdTomato, GAD1/2 (GAD67/65), and GlyT2 mRNAs in 3 μm thick optical sections were taken from PAX2:Cre-tdTomato transgenic animals. Neurons stained for the mRNAs were counted in laminae I-II, and lamina III. The borders of the laminae were defined following the procedure described in section 4.9.2.

Neurons stained for tdTomato, GAD1/2, and GlyT2 mRNAs were quantified in 3 animals. Five sections from each animal were arbitrarily selected; therefore, 15 independent sections were used to acquire the quantitative data.

4.9.5. Expression of PAX2 in the cell bodies of neurons immunostained for various neuronal markers

The cell bodies of neurons immunostained for nNOS, GAL, PV, CaB, CR, and PKC γ and positive or negative for PAX2::Cre-tdTomato were counted in laminae I-III, for the assessment of the colocalization. The quantification of immunostained neurons were made in 3 animals. Five sections from each animal were chosen arbitrarily; therefore, 15 independent sections were used to acquire the quantitative data.

5. Results

5.1. Specificity of tdTomato labelling in the GlyT2::CreERT2-tdTomato transgenic mice

The GlyT2::CreERT2 mice was generated by Zeilhofer (University of Zurich, Switzerland) using the same strategy as GlyT2:Cre (Foster *et al.*, 2015) and GlyT2:eGFP (Zeilhofer *et al.*, 2005) were generated . After crossing these mice with tdTomato reporter animals, as described in the Materials and Methods, first we tested the specificity of tdTomato expression in the GlyT2::CreERT2-tdTomato mice for glycinergic neurons.

We first analysed the expression of PAX2, a transcription factor that is commonly employed as an accurate marker of inhibitory neurons in the spinal cord (Alaynick *et al.*, 2011; Balázs *et al.*, 2017), in the cell bodies of neurons that had been labelled with tdTomato (Figure 14 a-c). A total of 183 tdTomato labelled cell bodies were observed in laminae I to IV of the 9 analysed sections, in which $97.35 \pm 2.38\%$ of them were also stained for PAX2. Therefore, the tdTomato-labelled neurons in the spinal dorsal horn can be classified as inhibitory neurons. To confirm if these inhibitory neurons were glycinergic, we detected GlyT2 and tdTomato mRNAs using multiplex FISH (Figure 14 d-f). We counted 152 cells positive for tdTomato mRNA and all of them showed positive signal also for GlyT2 mRNA in laminae I-IV, indicating that the tdTomato labelling in the GlyT2::CreERT2-tdTomato transgenic mice is selective for glycinergic neurons.

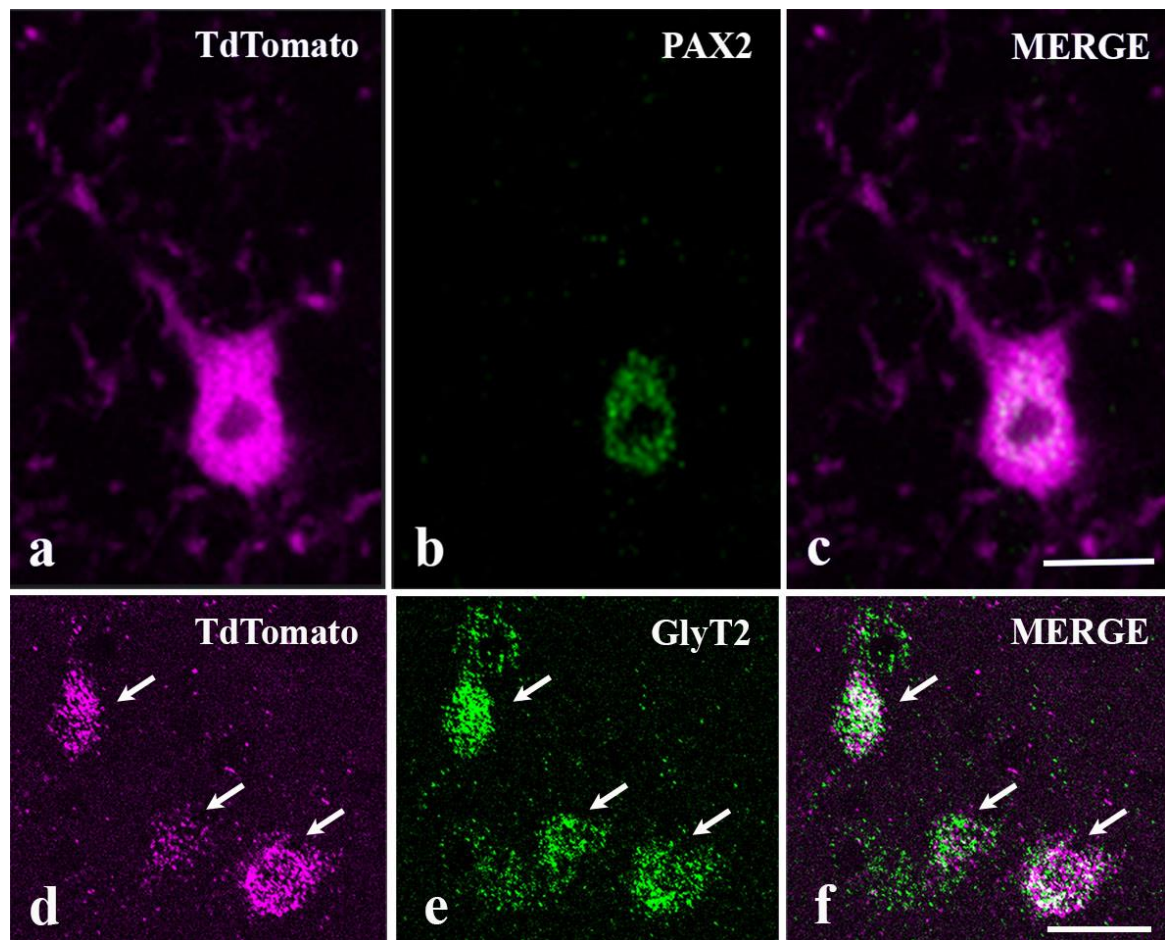


Figure 14: Pax2 and GlyT2 expressed in GlyT2::CreERT2-tdTomato-labelled neurons. (a–c) Micrograph of a single Pax2 immunostained 1 μ m thick confocal section from a GlyT2::CreERT2-tdTomato animal. The mixed colour in the combined image (c) depicts the colocalization of Pax2 immunostaining (b; green) and tdTomato labelling (a; magenta). (d–f) Micrograph of a 3 μ m thick confocal section from a GlyT2::CreERT2-tdTomato animal in which tdTomato and GlyT2 mRNAs were detected using multiplex in situ hybridization. The mixed colour in the combined image (f) depicts the colocalization of the GlyT2 (e; green) and tdTomato (d; magenta) mRNAs. Neurons within which tdTomato and GlyT2 mRNAs colocalize are indicated by arrows. Bars: 10 μ m (a–c) and 20 μ m (d–f)

5.2. Distribution of glycinergic neurons in laminae I-IV

Studying tdTomato labelling in the lumbar spinal dorsal horn of GlyT2::CreERT2-tdTomato animals, strong labelling was observed in laminae I to IV; tdTomato labelled both cell bodies and punctate profiles (Figure 15a). Elongated labelled profiles, resembling dendrites or interbouton segments of axons, were also frequently observed (Figure 15a). The punctate labelling was the most dominant and showed a relatively homogeneous labelling throughout laminae I to IV. Although labelled cell bodies were rare in lamina II and only a slightly more numerous in lamina I (Figure 15b, c), the punctate labelling was remarkably strong in these

superficial laminae, indicating that glycinergic neurons in the deeper layers of the dorsal horn send their dendrites and/or axons into the superficial dorsal horn. The number of labelled neurons was higher in lamina III, but the highest density was observed in lamina IV (Figure 15b, c).

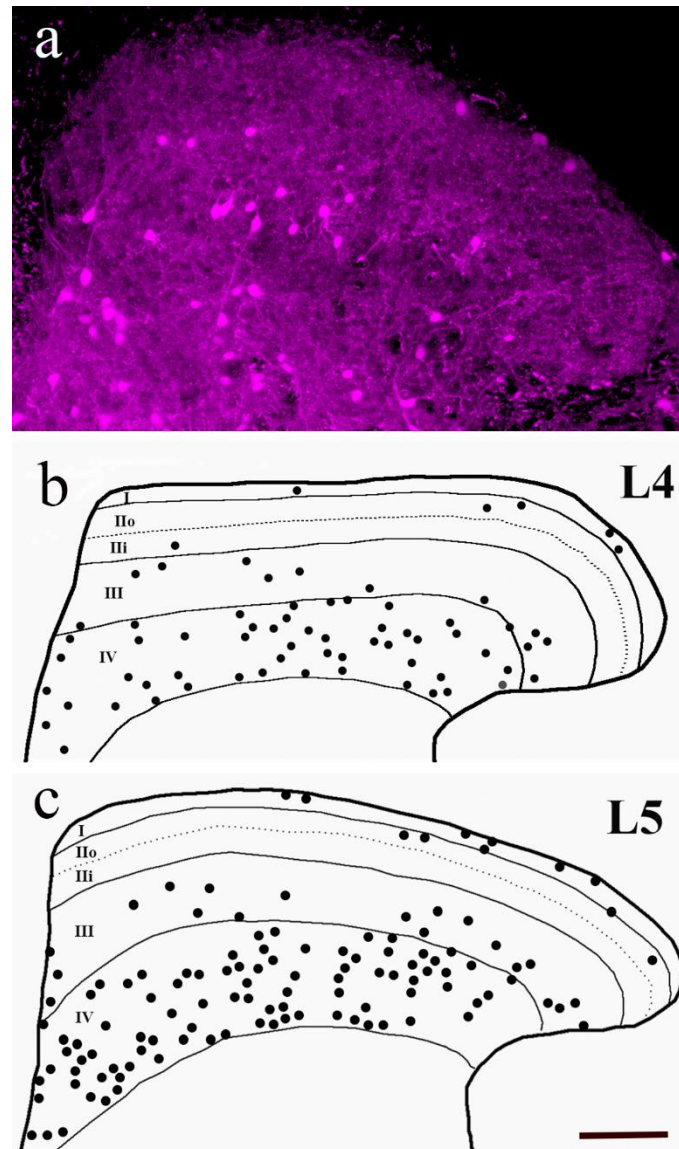


Figure 15: Distribution of GlyT2::CreERT2-tdTomato labelling in the spinal dorsal horn. (a) A micrograph of a single confocal section illustrating the dorsal horn of the L6 lumbar segment with extensive tdTomato staining of cell bodies, dendrites, and axonal profiles. (b, c) The distribution of labelled cell bodies at the level of the L4 and L5 segments in laminae I to IV of the spinal grey matter is shown schematically. Approximately 500 μm long pieces of the L4 and L5 spinal segments were used to collect labelled neurons. The shape of the spinal grey matter and the boundaries between the adjacent laminae are depicted according to Sengul *et al.* (2013), Bar: 100 μm.

5.3. Morphology of glycinergic neurons

After the description of the distribution of tdTomato-labelled glycinergic neurons, we studied the dendritic morphology of these cells in laminae I to IV of the L4-L5 spinal segments. Transverse, horizontal, and sagittal sections of the lumbar spinal cord were cut to reveal the major orientations of the dendritic trees of the labelled neurons (Figure 16). In transverse sections, it was not possible to identify longer segments of the dendritic trees (Figure 16a). In horizontal sections, it was observed that the dendrites of many tdTomato-labelled neurons showed a prominent rostro-caudal orientation (Figure 16c), whereas the mediolateral extension of these dendritic trees was narrow, not more than 50-100 μm (Figure 16c). The dendritic trees could be seen in their greatest extent in sagittal sections. In this orientation, the dendritic trees' rostro-caudal extension was just as clearly visible as in the horizontal sections (Figure 16b). However, it was also observed that, although the dendrites were extending in the rostro-caudal directions, most of them took oblique courses and extended also into the dorsal or ventral directions (Figure 16b, d).

Considering that the dendrites of the tdTomato-labelled glycinergic neurons extend primarily into rostro-caudal and dorsoventral direction, and their medio-lateral extent is less than 100 μm , we cut 100 μm thick sagittal sections and studied the dendritic morphology of the tdTomato-labelled neurons in stacks of long series of confocal section.

In most cases, it was possible to image and investigate the labelled neurons over the whole 100 μm thickness of the sections. However, along the dendrites the strength of the tdTomato labelling continuously declined, making it difficult or impossible to follow the dendrites in their full extent. As a result, we could only see the proximal part of the dendritic trees and were unable to analyse dendrites that extended further away from the cell body. Moreover, even though tdTomato-labelling appeared as punctate staining in laminae I-IV, and most of these puncta could be axonal swellings, we were unable to track the arborization of axons. To overcome this problem and enhance axonal as well as dendritic staining, we applied an anti-tdTomato immunostaining to the sections. Even though anti-tdTomato immunostaining revealed axonal and dendritic segments within which the original tdTomato labelling was barely apparent and increased the intensity of the tdTomato signal, the antibody only penetrated no further than 10 μm into the sections. Therefore, deeper than this penetration limit, representing 80- μm -thick layer of our 100- μm -thick sections, where most of our labelled

neurons were found, we were unable to benefit from the immunohistochemical amplification of the tdTomato signal.

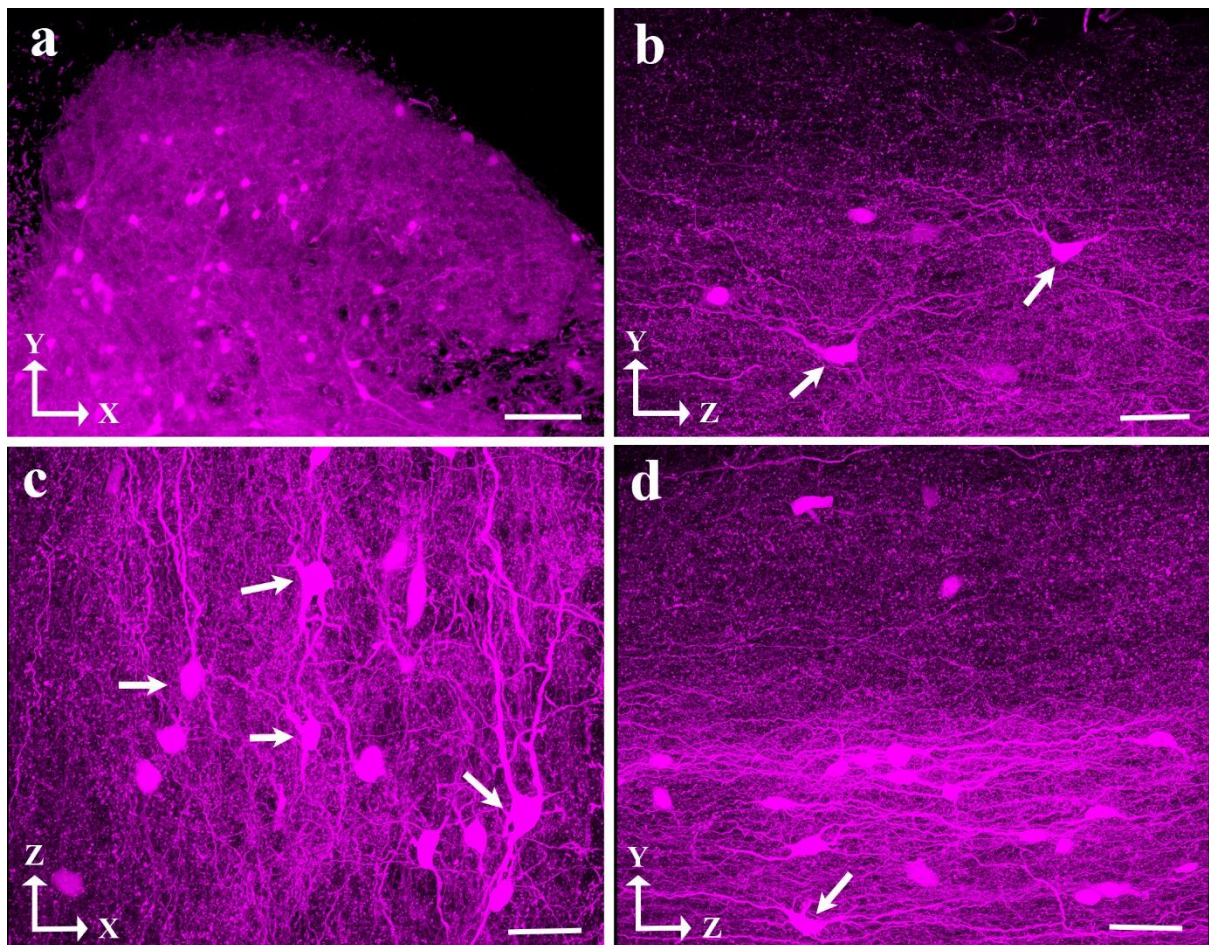


Figure 16: Dendritic orientation of GlyT2::CreERT2-tdTomato-labelled neurons. Micrographs of the spinal dorsal horn in transverse (a), horizontal (c), and sagittal (b, d) sections, displaying the cell bodies, dendrites, and axons of GlyT2::CreERT2-labelled neurons. The horizontal section (c) illustrates labelled neurons at the border of laminae III and IV. The border between the white (dorsal funiculus) and grey (dorsal horn) matters is at the upper edge of the images in (b) and (d). The dendrites (b-d) have an obvious rostro-caudal direction, but a dorso-ventral orientation can also be observed in case of many labelled neurons (b, d). Arrows point to neurons with dorsally extending dendrites (b, d) as well as neurons with rostro-caudally orientated dendrites (c). Bars: 100 μm (a); 50 μm (b-d).

5.3.1. Laminae I-II

Considering the shape and size of the cell bodies and dendritic morphology, tdTomato-labelled neurons in laminae I and II were classified into 3 groups.

- (1) Type 1. These neurons had small rostro-caudally oriented fusiform cell bodies with a short and long axis of about 10 μm and 20 μm , respectively. The cell bodies' two ends

gave rise to dendrites, which spread out in opposing rostro-caudal directions to form a short, weakly arborizing dendritic tree. Into the rostro-caudal direction, the dendrites extended 40 to 50 μm , while into dorso-ventral direction they extended only 20 to 30 μm (Figures 17a, b, 18a). In a few cases, we also noticed dendrites originating from the ventral side of the cell body (Figures 17a, 18a), but they also extended rostro-caudally, just like the dendrites originating from the extremities of the fusiform cell body.

- (2) Type 2. These neurons were also fusiform, but their cell bodies were twice as large as the cell bodies of type 1 neurons. The origin and orientation of their dendrites were similar to type 1 neurons. Their dendrites extended 40 to 50 μm both in the dorso-ventral and rostro-caudal directions (Figures 17c, 18b).
- (3) Type 3. The cell bodies of these neurons were multipolar with a diameter of about 20 μm . They had 3 or 4 stem dendrites, some of which extended rostro-caudally, others turned ventrally and run 30 to 40 μm in an oblique direction (Figures 17d, 18c).

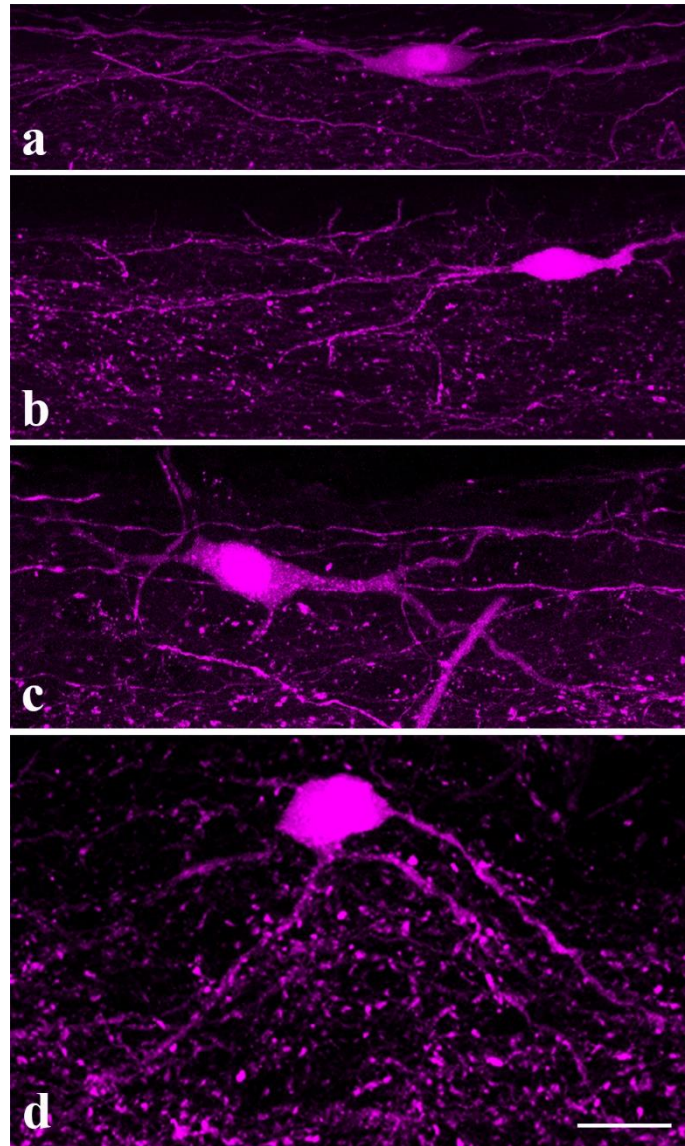


Figure 17: Types 1 to 3 of GlyT2::CreERT2-tdTomato-labelled neurons in laminae I–II of the spinal dorsal horn. The cells are illustrated in long stacks of confocal images (a: 55 optical sections, b: 25 optical sections, c: 95 optical sections, d: 30 optical sections) obtained from sagittal sections. Bar: 20 μm .

5.3.2. Laminae III-IV

Deeper, in laminae III and IV, the cell morphology was more diverse, and the tdTomato-labelled neurons were divided into 6 groups:

- (1) Type 1. Most of the neurons were classified into this group. These neurons had small fusiform cell bodies similar in shape and size to type 1 neurons in laminae I and II. The dendrites arising from the 2 ends of the cell body extended rostro-caudal for at least 150 μm in both directions. The dorso-ventral extension of the dendritic tree was much smaller, 15 to 20 μm (Figures 19a, b, c, d, 18d, f). Some neurons presented poorly

arborizing (Figures 19a, b, 18b), others richly arborizing dendritic tree (Figures 19c, d, 18f).

(2) Type 2. Their cell bodies were multipolar, with 15 to 20 μm diameter, and with 4 to 5 stem dendrites that extended rostro-caudally forming a rich arborization. The dendritic tree extended 200 to 250 μm into the rostro-caudal direction, and only 40 to 50 μm dorso-ventrally (Figures 19f, 18e).

(3) Type 3. The cell bodies were similar to type 2 multipolar neurons in shape and size, but the dendritic tree was different. Although some of the dendrites was running rostro-caudally, others extended ventrally for at least 50 to 70 μm (Figures 19e, 18g).

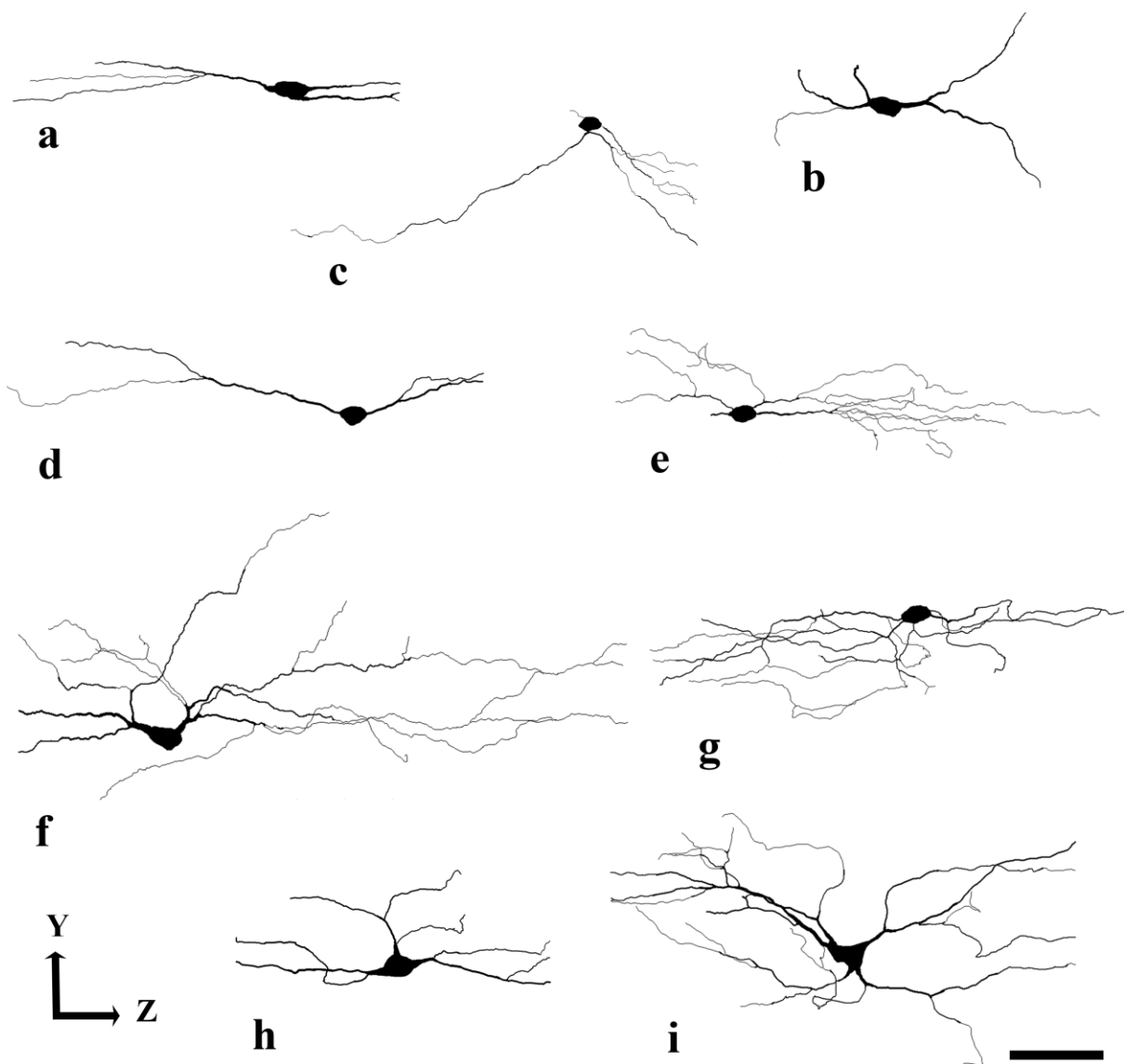


Figure 18: Types 1 to 3 and types 1 to 6 of GlyT2::CreERT2-tdTomato-labelled neurons in laminae I–II and III–IV, respectively, of the spinal dorsal horn. NeuroLucida reconstructions presenting dendritic morphologies of different types of glycinergic neurons reconstructed from sagittal sections. (a) Type 1 neuron from laminae I–II,

(b) Type 2 neuron from laminae I–II, (c) Type 3 neuron from laminae I–II, (d) Type 1 neuron from laminae III–IV, (e) Type 2 neuron from laminae III–IV, (f) Type 4 neuron from laminae III–IV, (g) Type 3 neuron from laminae III–IV, (h) Type 5 neuron from laminae III–IV, (i) Type 6 neuron from laminae III–IV. To estimate the laminar position of the reconstructed neurons, identify them in Figures 17, 19, and 20 in the following way: a—Figure 17a, b—Figure 17c, c—Figure 17d, d—Figure 19b, e—Figure 19f, f—Figure 19c; g—Figure 19e, h—Figure 20c; i—Figure 20f. Bar: 50 μ m.

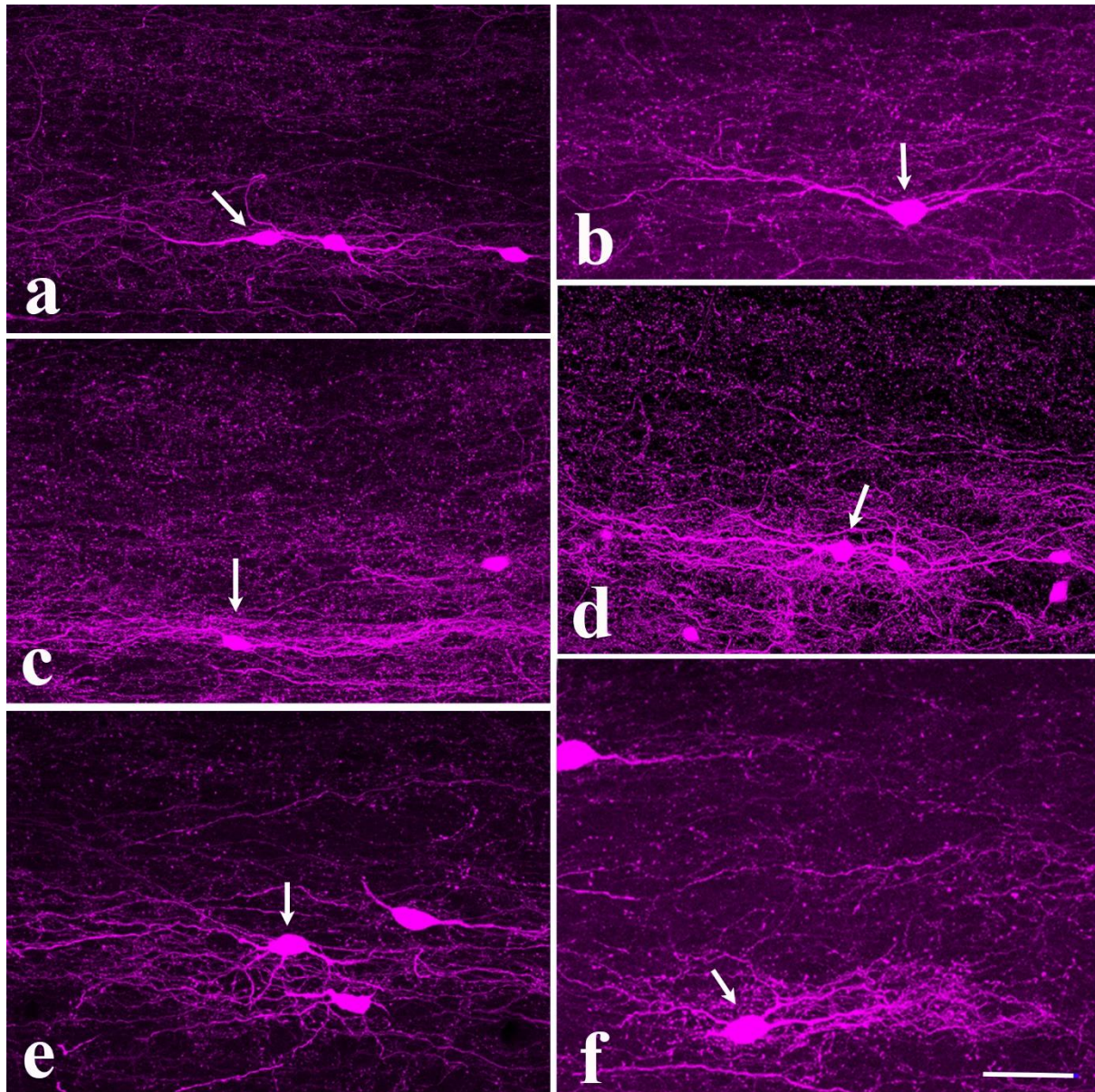


Figure 19: Types 1 to 3 of GlyT2::CreERT2-tdTomato-labelled neurons in laminae III–IV of the spinal dorsal horn. Neurons are illustrated in merged images of long series of confocal sections (a: 95 optical sections, b: 40 optical sections, c: 65 optical sections, d: 45 optical sections, e: 70 optical sections, f: 65 optical sections). Arrows point to cells of interest. Bar: 50 μ m.

- (4) Type 4. These neurons presented 15 to 20 μm large, elongated cell bodies. Some cells possessed 2 dendrites arising from the poles of the cell body (Figure 20b). In other cases, 1 dendrite arose from one end and 2 to 4 ones from the other end of the cell body (Figure 20a). The dendrites took oblique courses and extended 100 to 150 μm into the rostral-caudal, and 50 to 70 μm into the dorsal direction as well.
- (5) Type 5. They had pyramidal-shaped cell bodies with 3 stem dendrites: 2 arising from the base and 1 arising from the apex. The basal dendrites extended rostro-caudally and showed poor arborization. The 20 to 30 μm long apical dendrite run dorsally before splitting into 2 branches. The secondary dendritic branches adopted an oblique position and presented additional branching. By doing so, they approached grey matter regions that were more dorsal to the cell body and expanded the dendritic field rostro-caudally (Figures 20c, d, 18h).
- (6) Type 6. We grouped the neurons into this category that we could not classify into the other groups. They are considered as unclassified neurons (Figures 20e, f, 18i).

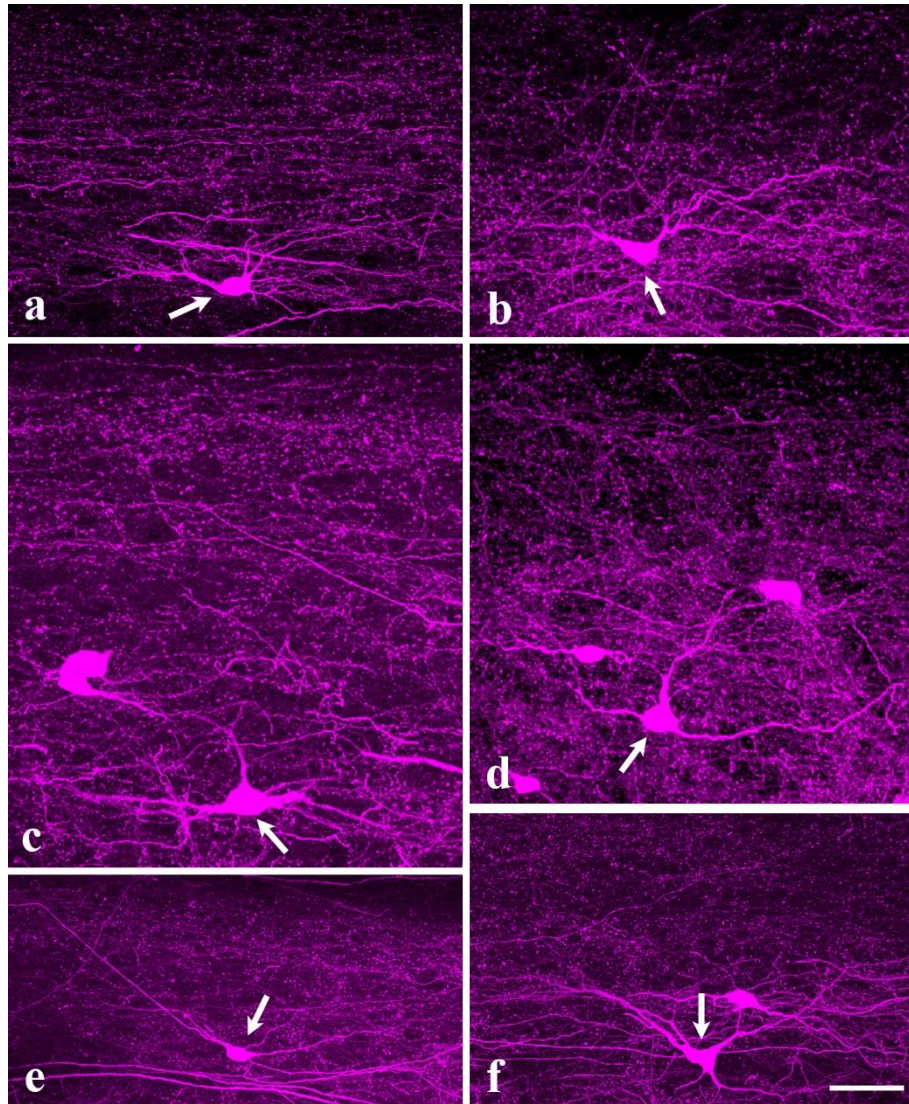


Figure 20: Types 4 to 6 of GlyT2::CreERT2-tdTomato-labeled neurons in laminae III–IV of the spinal dorsal horn. Neurons are illustrated in merged images of long stacks of confocal sections (a: 90 optical sections, b: 30 optical sections, c: 90 optical sections, d: 55 optical sections, e: 45 optical sections, f: 100 optical sections) s. Arrows point to cells of interest. Bar: 50 μ m.

5.4. Neurochemical markers of glycinergic neurons

In consideration of the premise that all inhibitory neurons were GABAergic in the superficial dorsal horn, they were divided in 5 more or less non-overlapping groups regarding their immunoreactivity for galanin, neuropeptide Y, neuronal nitric oxide synthase, parvalbumin and calretinin, described in previous reports (Boyle *et al.*, 2017; Peirs *et al.*, 2020). In deeper laminae, they were reported to also express the tyrosine kinase RET and the nuclear orphan beta receptor ROR β (Cui *et al.*, 2016; Del Barrio *et al.*, 2013).

To analyse the colocalization of GlyT2 with GAL, NPY, nNOS, PV, and CR, single-labelling immunohistochemistry was performed for these markers in GlyT2::CreERT2-tdTomato mice. For RET and ROR β , due to unavailability of specific and accurate antibodies against these markers, the co-expression of GlyT2 and the markers was detected using FISH for tdTomato and the markers mRNA. Both analyses took place on transverse sections since it was not our goal to combine the dendritic morphology with the neurochemical character of the glycinergic neurons. GlyT2::CreERT2-tdTomato-labelled neurons were collected in large numbers throughout the entire spinal dorsal horn's mediolateral extension.

5.4.1. Galanin and Calretinin

Cell bodies showed strong immunostaining for both GAL and CR in lamina II, and laminae I-IV, respectively, as reported previously (Zhang *et al.*, 1995; Ren *et al.*, 1993). In the regions where GAL and CR immunostained neurons were detected, we found 49 and 45 tdTomato-labelled cells, respectively, but none of them were positive for GAL or CR.

5.4.2. Neuropeptide Y

We evaluated a variety of anti-NPY antibodies from various suppliers. While almost all of them stained NPY-containing axonal boutons in laminae I–II, none of them showed immunostained cell bodies, in contrast to earlier reports (Sasek and Elde, 1985; Rowan *et al.*, 1993). Therefore, we were searching for NPY immunostaining in tdTomato-labelled axon terminals rather than examining the colocalization of NPY and tdTomato in cell bodies. Using this approach, we found double labelled axon terminals only occasionally and in very low numbers (Figure 21c, f, i). Our findings imply that NPY-containing cells may make up a very small percentage of glycinergic neurons.

5.4.3. Neuronal nitric oxide synthase

As previously reported, nNOS immunoreactive neurons can be found in both laminae I-II and III-IV (Saito *et al.*, 1994). In our investigation, we found 46 tdTomato-labelled neurons in laminae I-II from which 13 were also positive for nNOS (28,2%), and 231 tdTomato-labelled neurons in laminae III-IV from which 15 were also positive for nNOS (6.5%) (Figure 21a, d, g).

5.4.4. Parvalbumin

The immunostaining for PV was strong in the dorsal horn, mainly in laminae Iii-III, but also in lamina IV, supporting earlier findings (Antal *et al.*, 1990; Yoshida *et al.*, 1990; Hughes *et al.*, 2012). A total of 367 tdTomato-labelled neurons were counted in laminae Iii-III-IV, from which 150 were also positive for PV (40.8%) (Figure 21b, e, h).

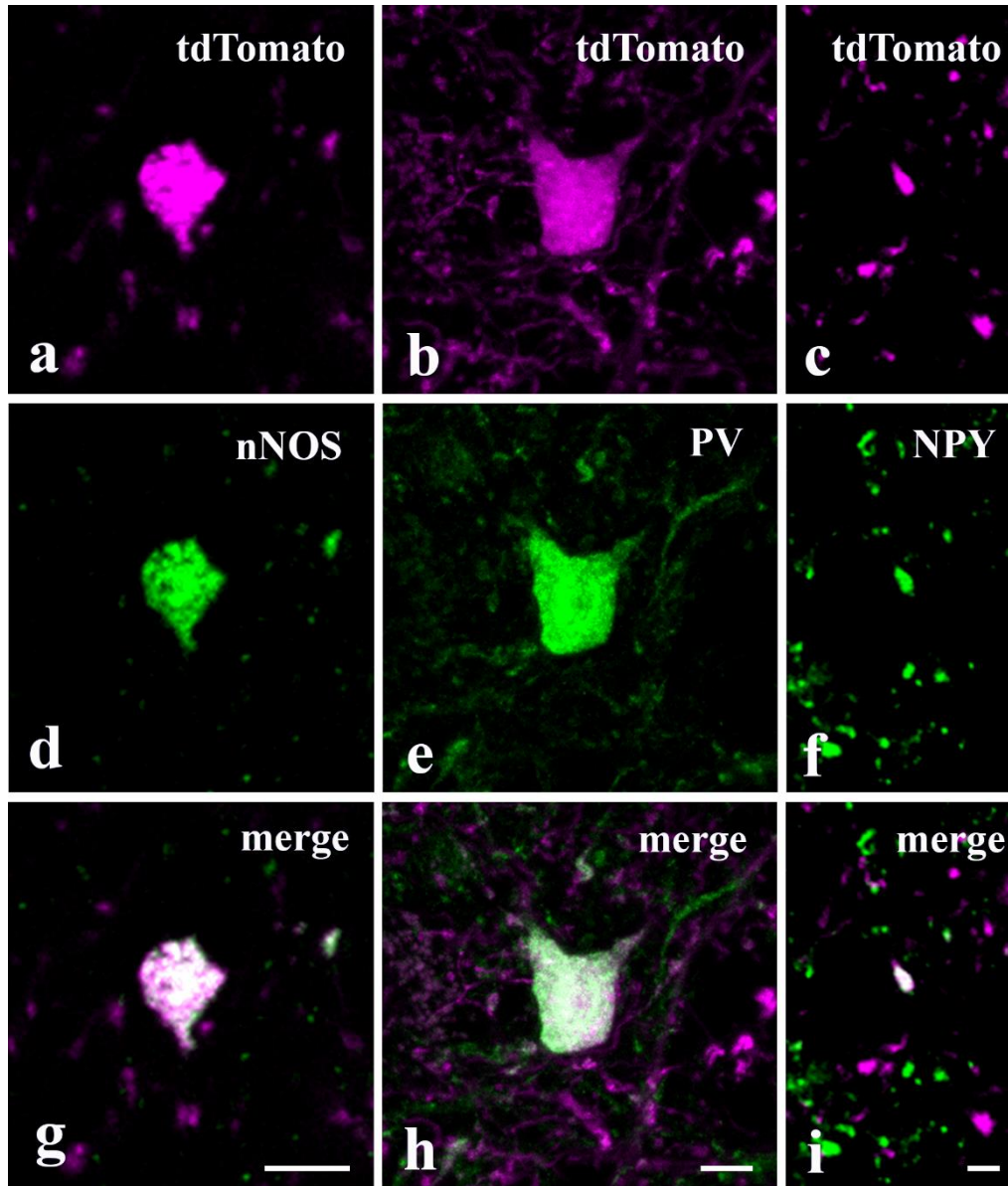


Figure 21: Expression of nNOS, PV, and NPY in GlyT2::CreERT2-tdTomato-labelled cell bodies and axon terminals. Micrographs of a single 1 μ m thick confocal section from a GlyT2::Cre-tdTomato animal that has been immunostained for nNOS (a, d, g), PV (b, e, h), and NPY (c, f, i). The merged pictures (g, h, i) show the colocalization of positive immunostaining for nNOS (d; green), PV (e; green), and NPY (f; green), as well as tdTomato labelling (a, b, and c; magenta). Bar: 5 μ m (g, h) and 2 μ m (i).

5.4.5. Tyrosine kinase RET

We identified many RET-expressing neurons in laminae III–IV but only a small number in laminae I–II, as previously mentioned (Cui *et al.*, 2016). We detected 27 tdTomato-labelled neurons in laminae I–II, of which 15 were also RET positive (55.5%), and 139 neurons in laminae III–IV, from which 79 presented positive hybridization signal for RET (56.8%) (Figure 22d-f).

5.4.6. Nuclear orphan beta receptor ROR β

For ROR β , the hybridization signal was considerable weaker compared to RET. Even though there were significantly fewer ROR β -positive neurons than RET-positive ones, they were distributed similarly. As was previously demonstrated, most of the ROR β -positive neurons were in laminae III–IV whereas they were sporadic in laminae I–II (Koch *et al.*, 2017). In laminae I-II and III-IV we found 21 and 104 tdTomato-positive neurons, of which 5 (23.8%) and 13 (12.5%) also expressed ROR β , respectively (Figure 22a-c).

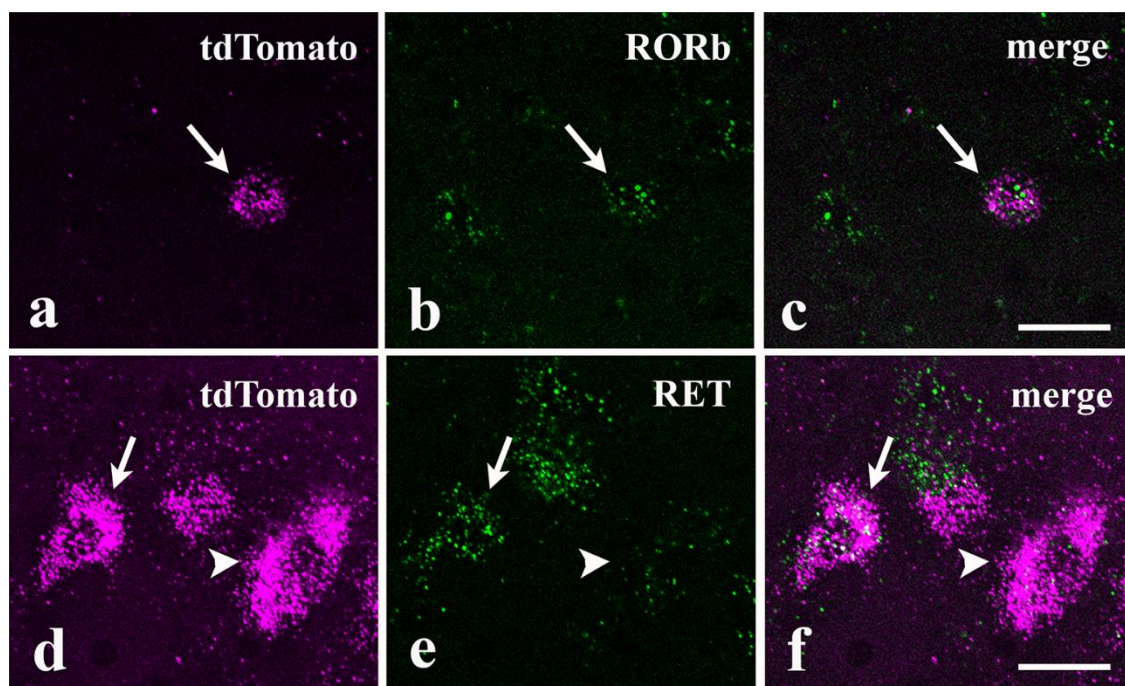


Figure 22: Expression of ROR β and RET mRNAs in GlyT2::CreERT2-tdTomato-labelled neurons. Micrographs of 3 mm thick confocal sections where tdTomato (a, d), ROR β (b), and RET (e) mRNAs were found using multiple fluorescent *in situ* hybridization. The merged images (c, f) show the colocalization of the tdTomato mRNA (a, d; magenta), ROR β mRNA (b; green), and RET mRNA (e; green) with mixed colours. Arrows point to cells in which tdTomato and ROR β mRNAs (a, b, c) and tdTomato and RET mRNAs (d, e, f) colocalize. Arrowheads exhibit a cell in which a strong hybridization signal for tdTomato and a weak one for RET is shown. Bars: 20 μ m.

5.5. Colocalization of GlyT2 and GAD65/67 mRNA in neurons within laminae I-III and IV

The analysis of the neurochemical markers of GlyT2 expressing neurons left the question open, whether the glycinergic neurons are also GABAergic, or some of them can be regarded as glycine-only neurons. Thus next, we raised this question more directly, and investigated the GlyT2 and GAD65/67 mRNA expression with multiple fluorescence *in situ* hybridization in Pax2:Cre-tdTomato transgenic animals in which tdTomato mRNA identifies PAX2 expressing neurons. Since most of the GlyT2-containing neurons were found in lamina IV, we performed this part of the study in a way that neurons in laminae I-III were pooled in one group and neurons in lamina IV were separated in another group.

We used the Advanced Cell Diagnostics pre-treatment and detection techniques and noted that the probes for the target mRNAs were very specific (Figure 23). When we measured the amount of background staining in laminae I–III, we found that in $20\ \mu\text{m} \times 20\ \mu\text{m}$ ($400\ \mu\text{m}^2$) cell free squares, there were 2.4 ± 1.4 , 2.6 ± 1.5 , and 8.2 ± 2.3 dots positive for GlyT2, GAD65/67, and tdTomato mRNAs, respectively. We considered the cellular signals positive if they were at least 3 times greater than the background signal.

We identified 408 neurons in laminae I–III that were positive for tdTomato mRNA, and only 19 (4.6%) of these neurons were negative for both GlyT2 and GAD 65/67 mRNA (Figure 23j, Table 4). Furthermore, we detected 9 neurons that expressed GlyT2 and/or GAD65/67 mRNA but did not express tdTomato mRNA. These findings demonstrated that tdTomato was extremely selectively expressed in inhibitory neurons and expressed in almost all inhibitory neurons in Pax2:Cre-tdTomato transgenic animals. Further investigation was done on the 389 neurons that were positive for tdTomato mRNA and also expressed GlyT2 and/or GAD 65/67 mRNA. We found that 261 (67.1%) of these neurons expressed both GlyT2 and GAD65/67 mRNA, while 128 (32.9%) of them were only positive for GAD65/67 mRNA (Figure 23a, c, d, e, g, Table 4). The intensity of the signals in neurons that expressed both GlyT2 and GAD65/67 mRNA varied greatly from weak to strong along a continuous scale, and the intensity of signals for GlyT2 and GAD65/67 changed independently. Therefore, we identified cells in which GlyT2 mRNA labelling was stronger than GAD 65/67 mRNA labelling (Figure 23d, g), as well as cells with intense GAD65/67 mRNA labelling and weak/moderate GlyT2 mRNA labelling (Figure 23c, d). No cells were found to be GlyT2 mRNA positive while being GAD65/67 mRNA negative.

In lamina IV, the labelling was as specific as in laminae I-III, although the background FISH signal was slightly higher in this lamina, measuring 6.4 ± 2.1 , 5.0 ± 1.9 , and 14.2 ± 2.7 dots positive for GlyT2, GAD 65/67, and tdTomato mRNA, respectively, in cell-free $400\ \mu\text{m}^2$ areas (Figure 23b). Of the 665 tdTomato mRNA labelled cells, only 9 (1.4%) presented negative signal for both GlyT2 and GAD 65/67 mRNAs (Table 4). Even though GlyT2 mRNA labelling predominated in lamina IV neurons (Figure 23b, f, h, i), only 24 (3.7%; 1.6 ± 0.8 in the individual sections) of the 656 cells that presented positive signal for GlyT2 and/or GAD 65/67 mRNAs expressed only GlyT2 mRNA (Figure 23i, Table 4). The percentage of these neurons was lower than that of neurons that expressed only GAD 65/67 mRNA; 43 (6.5%; 2.9 ± 1.2 in the individual sections; Table 4). In the 589 neurons that expressed both GlyT2 and GAD65/67 mRNAs (89.8%; 39.2 ± 3.9 in individual sections; Table 4), the intensity of the signals altered independently for GlyT2 and GAD65/67, and it was very variable from weak to strong along a continuous scale, likewise in laminae I-III. GlyT2 mRNA predominated in most of the neurons in lamina IV (Figure 23b, f, h), in contrast to what was seen in laminae I-III, while GAD65/67 mRNA labelling was, with a few exceptions, typically weak or moderate in these neurons (Figure 23f, h).

Table 4: Numbers of neurons detected in laminae I-III and lamina IV of the spinal dorsal horn that expressed tdTomato, GlyT2, and GAD65/67 mRNAs in various combinations

	1	2	3	4	5	6	7	8
	tdTomato+ GlyT2+ GAD+	tdTomato+ GlyT2+ GAD-	tdTomato+ GlyT2- GAD+	$\Sigma 1-3$	tdTomato+ GlyT2- GAD-	$\Sigma 4-5$	tdTomato+ GlyT2+ and/or GAD+	$\Sigma 6-7$
Laminae I-III	261	0	128	389	19	408	9	417
Lamina IV	589	24	43	656	9	665	2	667

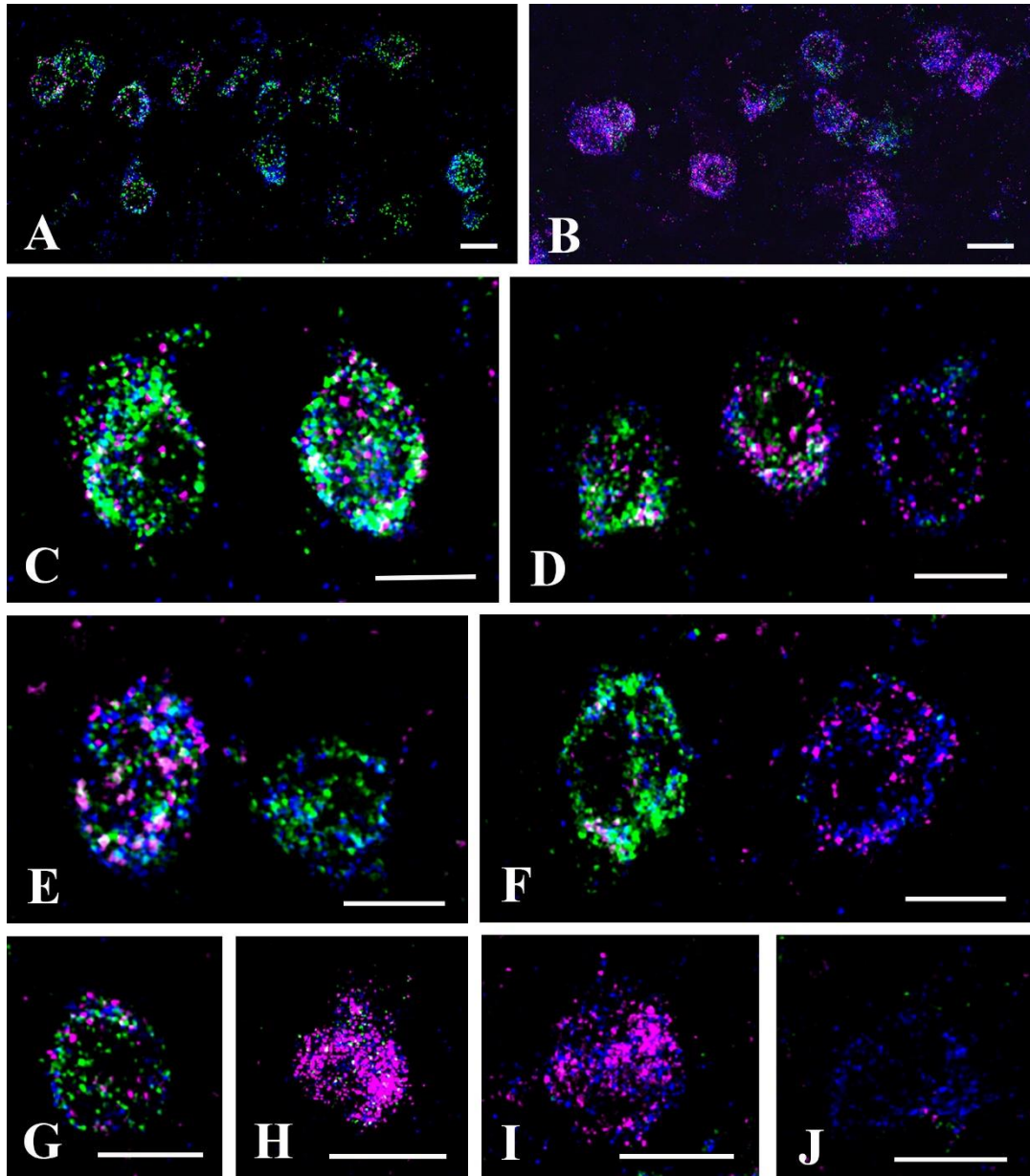


Figure 23: Expression of tdTomato, GlyT2, and GAD65/67 mRNAs in the lumbar spinal dorsal horn of Pax2:Cre-tdTomato mice. Micrograph of 3 μm thick confocal optical sections obtained from the L4-5 spinal dorsal horn of Pax2:Cre-tdTomato animals hybridized for tdTomato (blue), GlyT2 (magenta) and GAD65/67 (green) mRNAs. Within the confines of each individual neuron, the hybridization end products are shown as tiny dots. Low (A, B) and high (C-J) magnifications of the triple labelling images are displayed. Cells from dorsal horn's laminae I-III (A-C-E-G-J) and lamina IV (B-F-H-I) are seen in the illustrations. Most cells were triple-labelled, but some of them do not express GlyT2 (E), GAD 65/67 (F, I), or both GlyT2 and GAD 65/67 (J) mRNAs. Bars: 20 μm .

5.6. Colocalization of GlyT2 and GAD65/67 in axon terminals within laminae I-II

Although we found GlyT2-containing neurons in a very moderate numbers in laminae I-III, especially in laminae I-II (Figure 15), and the GlyT2 mRNA expression was also low in these neurons (Figure 23), the density of dotted, presumably axon terminal labelling was remarkably

high in these laminae. Taking these data into consideration, it seems to be a plausible idea that glycinergic axon terminals in laminae I-III may arise from neurons located out of the confines of laminae I-III, for example from neurons in lamina IV, where GlyT2 mRNA expression has been found to be remarkably strong.

To explore the GlyT2 expression and the colocalization between GlyT2 and GAD65/67 in axon terminals within laminae I-III we performed double immunostaining for GlyT2 and GAD 65/67 in sections obtained from GlyT2::CreERT2-tdTomato animals. Because of the relatively high densities of dendrites that may bias our results in lamina III, we analysed the immunostaining only in laminae I-II.

In the 9 ROIs (see Materials and Methods), 105 tdTomato-labelled puncta were found, of which 68 were also immunostained for GlyT2 ($62.12 \pm 3.94\%$), and 31 of the GlyT2 immunoreactive boutons were also immunostained for GAD65/67 ($45.49 \pm 3.84\%$) (Table 5). GlyT2-negative tdTomato-labelled but GlyT2-negative profiles were also negative for GAD65/67 staining. We found GAD65/67 immunostaining only in 4 (3.8%) of them. Therefore, profiles that are tdTomato positive, but GlyT2 and GAD65/67 negative can be regarded as dendrites or interbouton segments of axons.

To confirm the presence of glycine-only axon terminals in laminae I-II, we also investigated the GAD65/67 immunostaining in GlyT2-positive axon terminals in another way. We counted the GlyT2-positive axon terminals regardless whether they were labelled or not labelled with tdTomato. We found 123 axon terminals immunostained for GlyT2 in our sample, and 56 of them were also immunostained for GAD65/67 ($46.02 \pm 4.22\%$) (Figure 24, Table 5).

These findings indicate that glycine-only inhibition may exist in laminae I-II of the spinal dorsal horn, but glycine only axon terminals may arise primarily, if not exclusively, from glycinergic neurons in lamina IV.

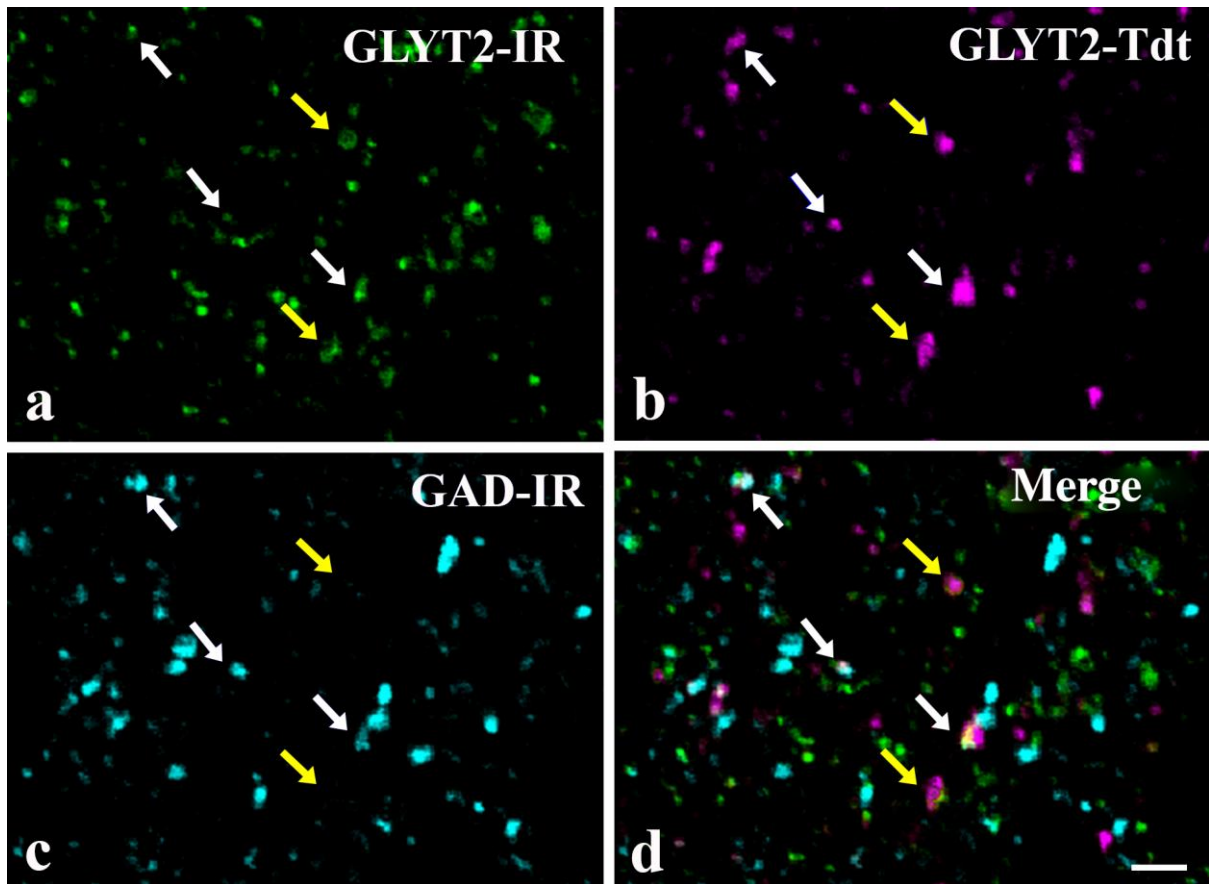


Figure 24: Localization of GlyT2 and GAD65/67 in GlyT2::CreERT2-tdTomato-labelled axon terminals in laminae I–II. Micrograph of a single 1- μ m thick confocal section from a GlyT2::CreERT2-tdTomato animal that was GlyT2 and GAD65/67 double-immunostained. Many of tdTomato-labelled profiles (b, magenta) were also immunostained for GlyT2 (a, green), while some of the tdTomato and GlyT2 double labelled puncta were also immunoreactive for GAD65/67 (c, blue). Yellow arrows indicate profiles that were tdTomato labelled and immunostained for GlyT2, but not for GAD65/67 (a to d). White arrows indicate profiles that are tdTomato labelled and immunostained for both GlyT2 and GAD65/67 (a to d). Bar: 10 μ m.

Table 5: Numbers of transgenically labelled (tdTomato+) and single- (GlyT2+) as well as double-immunostained (GlyT2+ and GAD+) profiles in laminae I–II of the spinal dorsal horn

		1	2	3	4	5	6	7	8
		tdTomato+	tdTomato+ GlyT2+	2/1%	tdTomato+ GlyT2+ GAD+	4/2%	GlyT2+	GlyT2+ GAD+	7/6%
Animal 1	Section1	17	13	76.47	6	46.15	18	10	55.55
	Section2	20	15	75.0	6	40.0	18	7	38.88
	Section3	15	10	66.66	5	50.0	15	6	40.0
Animal 2	Section1	11	6	54.54	4	66.66	13	8	61.53
	Section2	9	6	66.66	2	33.33	10	4	40.0
	Section3	10	5	50.0	2	40.0	18	7	38.88
Animal 3	Section1	9	5	55.55	2	40.0	11	3	27.27
	Section2	7	5	71.42	3	60.0	11	5	45.45
	Section3	7	3	42.85	1	33.33	9	6	66.66
Total		105	68	62.12 \pm 3.94%	31	45.49 \pm 3.84%	123	56	46.02 \pm 4.22%

5.7. Spinal vs supraspinal glycinergic innervation of laminae I-III of the spinal dorsal horn

Besides spinal neurons, glycinergic axons descending from brainstem nuclei (Antal *et al.*, 1996; Hossaini *et al.*, 2012) may also substantially contribute to the glycinergic innervation of the spinal dorsal horn by. Because we intended to identify glycinergic axon terminals of spinal origin, we wanted to eliminate glycinergic terminals of brainstem origin from the dorsal horn. Thus, to remove the descending glycinergic fibres we performed hemisection of the spinal cord at the level of thoracic segments 11 and 12 (Figure 13) and the remaining glycinergic axon terminals in the lumbar spinal cord ipsilateral to the hemisection were considered as terminals of spinal origin.

Then, we counted the numbers of GlyT2 immunostained axon terminals in the L4-L5 spinal segments of hemisected animals ipsilateral to the hemisection and compared these numbers to the numbers of GlyT2 positive axon terminals counted in the same spinal segments of non-operated wild-type B6 animals (Figure 25). The numbers of GlyT2 immunoreactive axon terminals were counted both in laminae I-II and lamina III. In lamina I-II, in total 230 and 156 (15.2 ± 3.3 and 10.4 ± 1.9 in the individual sections; $p < 0.001$) immunostained axon terminals were counted in non-operated mice and mice that underwent hemisection, respectively. In lamina III, in total 715 and 432 (54.0 ± 5.3 and 28.9 ± 3.4 in the individual sections; $p < 0.001$) immunostained axon terminals were counted in non-operated mice and mice that underwent hemisection, respectively. According to these results, we can conclude that at the level of L4-L5 spinal segments roughly 68% and 60% of GlyT2 immunoreactive axon terminals were of spinal origin in laminae I-II and lamina III, respectively, while the rest can be considered as brainstem-origin. These findings also indicate that low thoracic spinal cord hemisection is obligatory for the analysis of glycinergic axon terminals of spinal origin in the superficial lumbar spinal dorsal horn. For this reason, only mice that underwent hemisection were used in the following experiments.

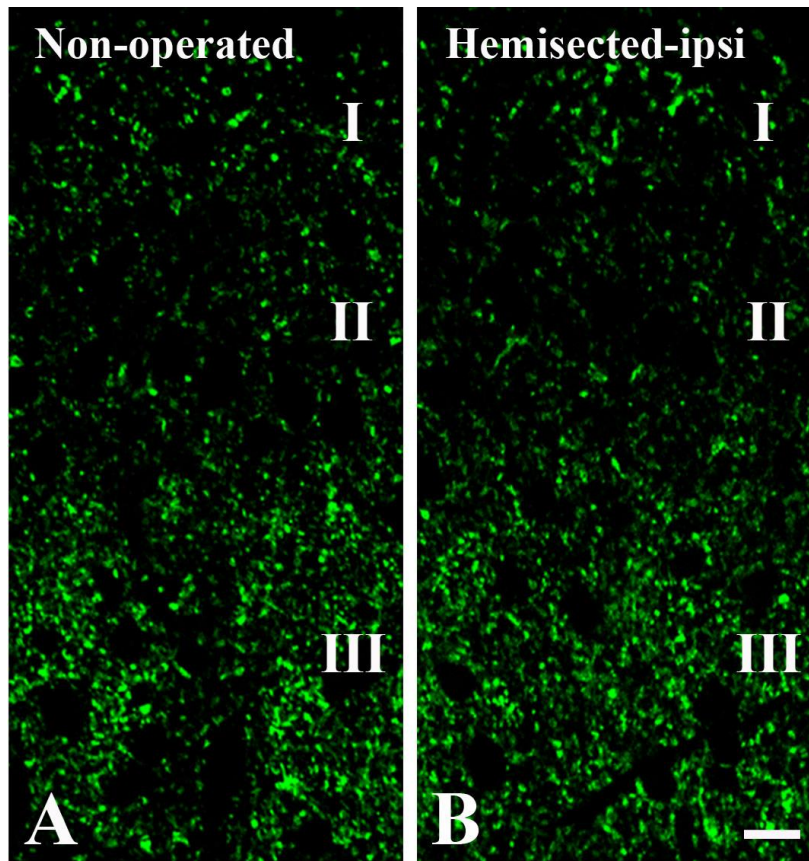


Figure 25: Effect of low thoracic hemisection on GlyT2 immunoreactivity of the lumbar spinal dorsal horn. Micrographs of 1 μm thick optical sections taken from the superficial spinal dorsal horn of non-operated (A) and hemisected (B) mice at the L4 level and immunostained for GlyT2. The superficial spinal dorsal horn's layers (laminae I, II, and III) are denoted by Roman numbers. Bar: 10 μm .

5.8. Synapses made by GlyT2-IR axon terminals in laminae I-III of the spinal dorsal horn

To observe synapses made by GlyT2 axon terminals, NiDAB-silver-gold staining method was used, and it identified the presence of GlyT2-containing axon terminals with great precision and very low background. Figures 26 and 27 show gold particles, the end-products of the staining, labelling GlyT2-immunoreactive boutons. The gold particles were found at the intracellular side of the peri-synaptic cell membrane and over synaptic vesicles, as it was reported earlier (Spike *et al.*, 1997; Núñez *et al.*, 2009). In some cases, we also noticed gold particles above mitochondria (Figure 26b, c), but this presumably nonspecific labelling caused by the diffusion of the NiDAB reaction end product inside the labelled axon terminal. Although the immunoreactive boutons' size and shape varied greatly, most of them varied in the range of 0.5 and 1.0 μm . The labelled boutons made symmetric synaptic contacts. They contained flattened and/or rounded vesicles, but dense-core vesicles were never observed within them.

In total, 138 labelled boutons were collected from which 104 (75.4%) formed axo-dendritic (Figure 26a, b, c, d), 16 (11.6%) axo-somatic (Figure 26e, g), and 18 (13.0%) axo-axonic synaptic contacts (Figures 26f, 27). From the 18 labelled boutons that formed axo-axonic contacts, 7 were found in non-glomerular (Figure 26f) and 11 in glomerular (Figure 27) synaptic arrangements. The size of the GlyT2 immunostained boutons was comparable to that of the postsynaptic dendrites and axons in non-glomerular synaptic configurations. Spherical vesicles and mitochondria were present in the postsynaptic axons of the non-glomerular axo-axonic arrangements, but no dense-core vesicles were present (Figure 26f). The synaptic glomeruli were defined as type II due to the presence of electro lucent cytoplasm, several mitochondria, and clusters of spheroid clear synaptic vesicles within the large central axons (Figure 27) (Ribeiro-da-Silva and Coimbra, 1982; Ribeiro-da-Silva *et al.*, 1989). In addition to the GlyT2 immunoreactive axons, the central axon terminals of the synaptic glomeruli received synapses from other non-immunoreactive axons and made asymmetric synapses with dendrites (Figure 27).

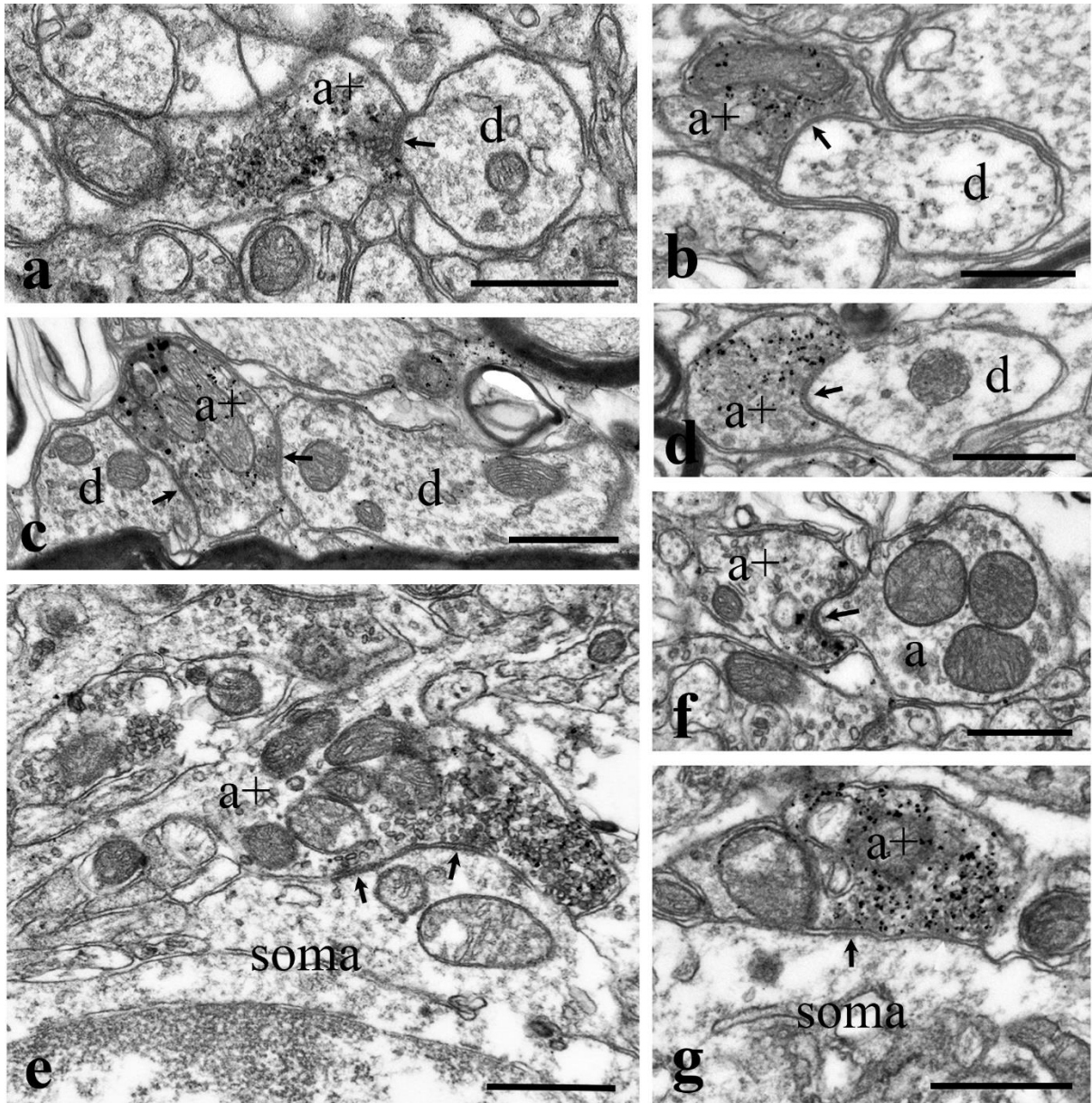


Figure 26: Synapses made by GlyT2 immunostained axon terminals. Electron micrographs showing axo-dendritic (A-D), axo-somatic (E, G) and axo-axonic (F) synaptic contacts made by GlyT2 immunostained axon terminals in laminae I-III of the superficial spinal dorsal horn at the L4-L5 level of the spinal cord. Gold particles accumulate at perisynaptic sites and over synaptic vesicles. a+: axon terminals immunostained for GlyT2, d: postsynaptic dendrites, soma: postsynaptic cell body, a: postsynaptic axon. Arrows point to synaptic contacts. Bars: 0.5 μ m.

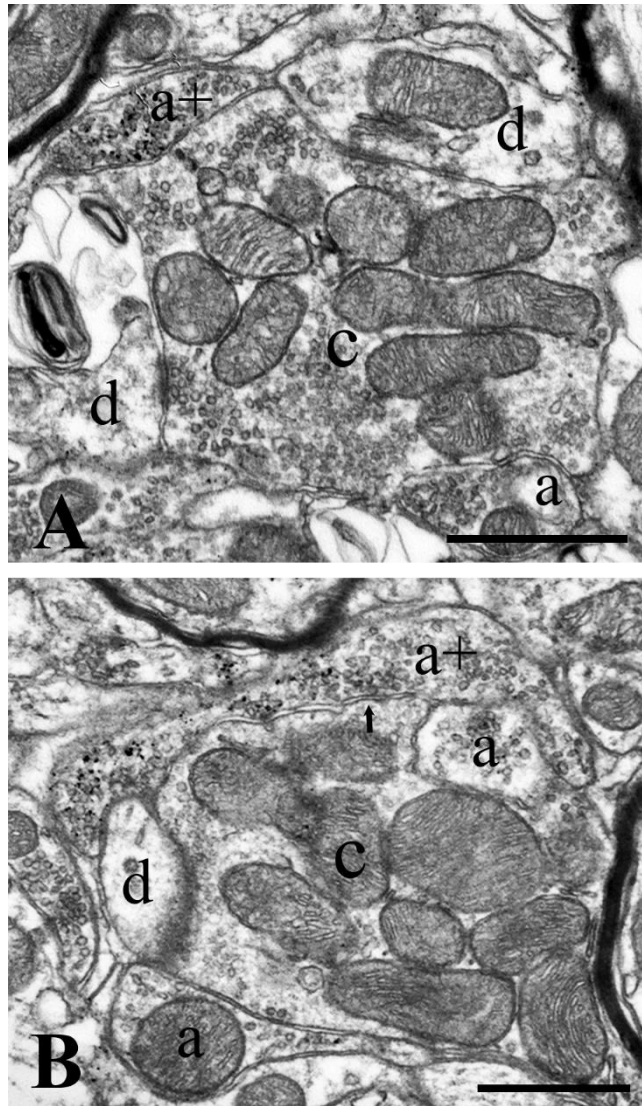


Figure 27: GlyT2 immunostained axon terminals in glomerular synaptic complexes. Electron micrographs presenting glomerular synaptic complexes in laminae II-III of the superficial spinal dorsal horn at the L4-L5 segments of the spinal cord. Note that GlyT2 immunostained axon terminals make synaptic contacts with the central axons of the glomeruli. GlyT2 immunoreactivity appears as accumulated gold particles at perisynaptic locations and distributed over synaptic vesicles. c: central axon terminal of the glomerular synaptic complex, a+: axon terminals immunostained for GlyT2, a: axon terminals negative for GlyT2, d: dendrites postsynaptic to the central axon terminal. Arrows point to synaptic appositions. Bars: 0.5 μ m.

5.9. Neurons receiving axo-somatic inputs from glycinergic axon terminals in laminae I-III

As revealed by electron microscopy, most of the glycinergic inputs, were received by the somato-dendritic compartment of neurons in laminae I-III of the spinal dorsal horn. To identify the types of interneurons that are targets of glycinergic inhibition, we used immunostaining for GlyT2 and several cellular markers, such as CaB, PKC γ , CR, GAL, nNOS, and PV, which

have already been identified as markers of inhibitory and excitatory neurons in laminae I-III of the spinal dorsal horn (Antal *et al.*, 1990; Todd, 2010; Peirs *et al.*, 2015; Abraira *et al.*, 2017; Boyle *et al.*, 2017; Todd, 2017; Smith *et al.*, 2019; Hughes and Todd, 2020). As it was reported earlier, neurons that can be labelled with these markers are heterogeneous in the sense that many of these cellular markers label both excitatory and inhibitory neurons (Smith *et al.*, 2015; Gutierrez-Mecinas *et al.*, 2019; Gradwell *et al.*, 2022). Because we wanted to find out whether glycinergic innervation is received by inhibitory or excitatory neurons, we carried out the immunostaining on sections taken from Pax2:Cre-tdTomato transgenic mice, a strain that we used in our FISH studies and in which the tdTomato labelling proved to be highly specific for inhibitory neurons. Thus, we finally performed a triple immunostaining for GlyT2, the cellular markers and tdTomato as the marker for inhibitory neurons.

Initially, we observed that the CaB and CR immunoreactive neurons significantly outnumbered the other interneuron populations. In total, we found 356 and 346 neurons immunostained for CaB and CR in the investigated sections, respectively (Table 6). PKC γ and PV-containing neurons were also found in large numbers, 242 and 192, respectively (Table 6). On the other hand, however we revealed only 62 and 21 neurons in the same number of sections that were immunostained for nNOS and GAL, respectively (Table 6).

Only 3.1% of the CaB-containing neurons expressed tdTomato. Thus, they can be considered as excitatory neurons with high reliability (Table 6). The PAX2:Cre-tdTomato transgene was absent from the majority of PKC γ (86.8%) and CR (82.1%) immunoreactive neurons, but tdTomato was expressed in the remaining neurons (Table 6). Therefore, even though the majority of PKC γ and CR-expressing neurons are excitatory, these markers are also expressed by a considerable number of inhibitory neurons. On contrary, most of the GAL-expressing neurons can be considered as inhibitory, since 90.5% of them were positive for tdTomato. Most of CaB, PKC γ , and CR positive neurons seems to be excitatory and most of GAL positive neurons inhibitory, however, the inhibitory or excitatory nature of nNOS and PV neurons cannot be identified so easily. Only about half of the nNOS and PV immunostained neurons, 58.1% and 45.3%, respectively, were positively labelled for tdTomato, while the other half was negative for tdTomato. These findings, which essentially correlate with previous investigations, provide strong evidence for the accuracy of our subsequent immunohistochemical data (Simmons *et al.*, 1995; Polgár *et al.*, 1999; Hantman and Perl, 2005; Sardella *et al.*, 2011; Tiong *et al.*, 2011; Duan *et al.*, 2014; Smith *et al.*, 2015, 2016; Gutierrez-Mecinas *et al.*, 2019).

Table 6: Number and percentage of neurons immunostained for CaB, PKC γ , CR, GAL, nNOS, PV, and positive or negative for PAX2:Cre-tdTomato transgene in laminae I-III of the spinal dorsal horn.

Marker	CaB		PKC γ		CR		GAL		nNOS		PV	
	N ^o	%										
Marker+/tdTomato+	11	3.1	32	13.2	62	17.9	19	90.5	36	58.1	87	45.3
Marker+/tdTomato-	345	96.9	210	86.8	284	82.1	2	9.5	26	41.9	105	54.7
Total	356	100	242	100	346	100	21	100	62	100	192	100

Next, we wanted to find out which populations of interneurons make close axo-somatic contacts with GlyT2-positive axonal terminals. Our main finding was that almost all groups of interneurons that we studied formed close axo-somatic appositions with GlyT2 immunostained axon terminals (Figures 28, 29). Several axo-somatic contacts were identified on CaB-, CR-, nNOS-, and PV-positive excitatory (tdTomato negative) neurons (Figure 28). Only few contacts were detected between GlyT2 immunostained axon terminals and the cell bodies of PKC γ -positive excitatory (tdTomato negative) neurons, instead, we found contacts on their proximal dendrites (Figure 28e). Regarding excitatory (tdTomato negative) GAL-containing neurons, we couldn't detect any contacts between their cell bodies and GlyT2-positive axons terminals, but due to the very low sample size for this marker (2 cells), this result is not necessarily reliable. The somata of PKC γ -, CR-, GAL-, nNOS-, and PV-positive inhibitory (tdTomato positive) neurons were likewise in contact with GlyT2 immunostained axon terminals in addition to excitatory neurons (Figure 29). Only CaB positive inhibitory (tdTomato positive) neurons were not found to receive contacts from GlyT2 immunostained boutons. These findings imply that glycinergic postsynaptic inhibition has a significant and variable impact on the activity of almost all populations of excitatory and inhibitory interneurons in laminae I-III of the spinal dorsal horn.

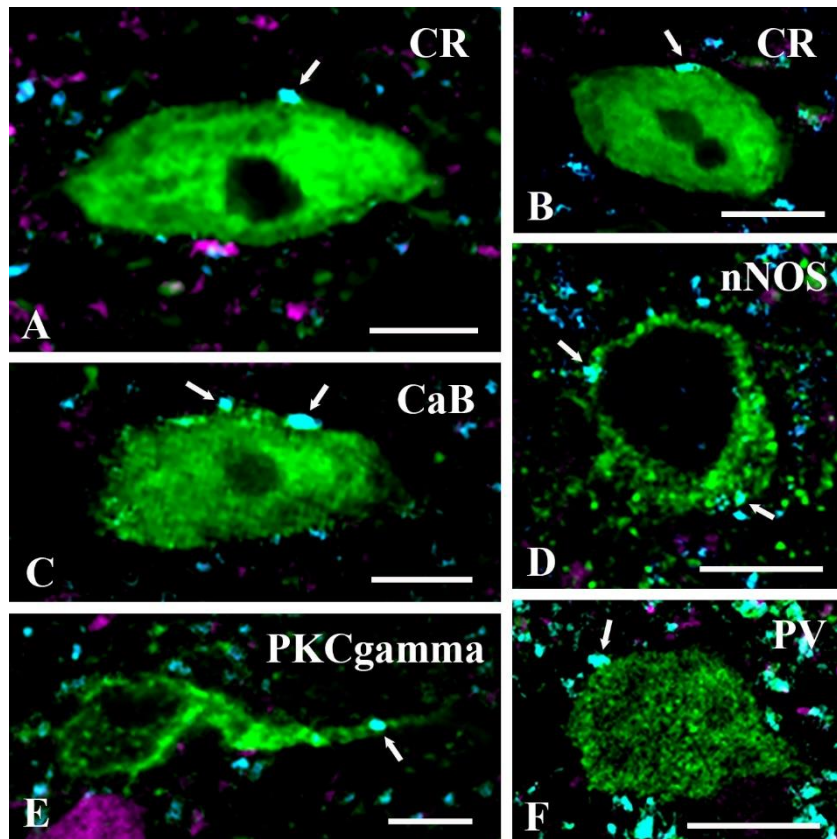


Figure 28: GlyT2 immunostained axon terminals make contacts with excitatory spinal interneurons. Close appositions between GlyT2 immunoreactive axon terminals (cyan) and somata of CR, CaB, nNOS, and PV immunoreactive (green), or proximal dendrites of PKC γ immunoreactive (green) and PAX2Cre-tdTomato (magenta) negative excitatory interneurons. Arrows indicate GlyT2 immunostained axon terminals making close appositions with the labelled neurons. Bars: 10 μ m.

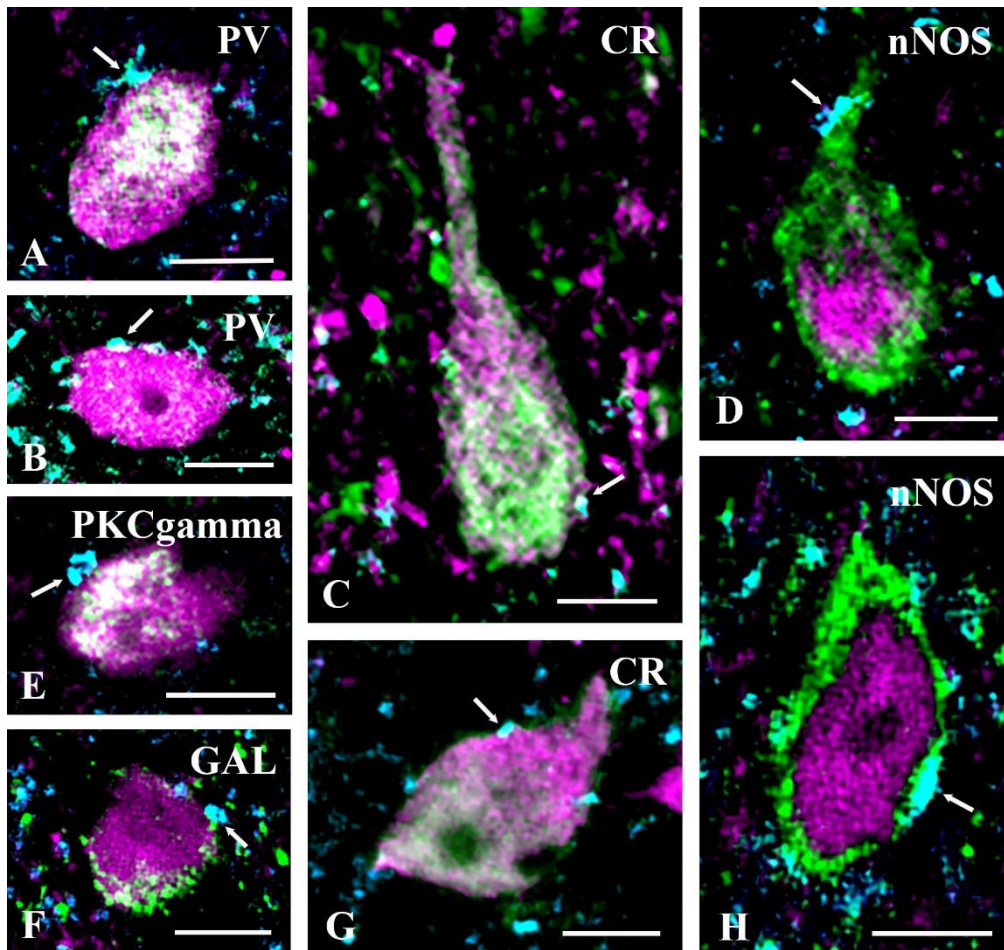


Figure 29: GlyT2 immunostained axon terminals make contacts with inhibitory spinal interneurons. Close appositions between GlyT2 immunoreactive axon terminals (cyan) and the somata or proximal dendrites of PV, CR, nNOS, PKC γ , and GAL (green) immunoreactive and PAX2Cre-tdTomato (magenta) positive inhibitory interneurons. Note the mixed colours of the somata of the illustrated cells. It is interesting to note that unlike in cells positive for the other neuronal markers, in the nNOS positive neurons, nNOS immunostaining is restricted to the peripheral portion of the cytoplasm, whereas tdTomato can be observed in the central part of the cytoplasm. Arrows indicate GlyT2 immunostained axon terminals forming close appositions with the labelled neurons. Bars: 10 μ m.

5.10. Axon terminals receiving axo-axonic inputs from glycinergic axon terminals in laminae I-III

Electron microscopy revealed that 13.0% of GlyT2 immunoreactive axon terminals established axo-axonic synapses. To identify the types of axon terminals that can be the targets of glycinergic presynaptic inhibition in laminae I-III of the spinal dorsal horn, we combined GlyT2 immunostaining with IB4-binding and immunolabelling for CGRP, VGLUT1 and VGLUT2, markers of non-peptidergic nociceptive, peptidergic nociceptive, and non-nociceptive primary afferents, and axon terminals of intrinsic excitatory spinal neurons,

respectively (Li *et al.*, 2003; Oliveira *et al.*, 2003; Todd *et al.*, 2003; Willis and Coggeshall, 2004, Ribeiro-da-Silva and De Korninck, 2009; Todd and Koerber, 2013).

Analysing 1 μm thick confocal sections, we found that GlyT2-positive boutons did not form axo-axonic contacts with CGRP- or VGLUT2-expressing axon terminals. However, we found close appositions between GlyT2 and VGLUT1 immunoreactive as well as IB4-binding axon terminals (Figures 30, 31). All axo-axonic close appositions were found in inner lamina II and lamina III, according to the distribution of the postsynaptic axon terminals. However, GlyT2 immunoreactive axon terminals did not make axo-axonic appositions in lamina I and outer lamina II.

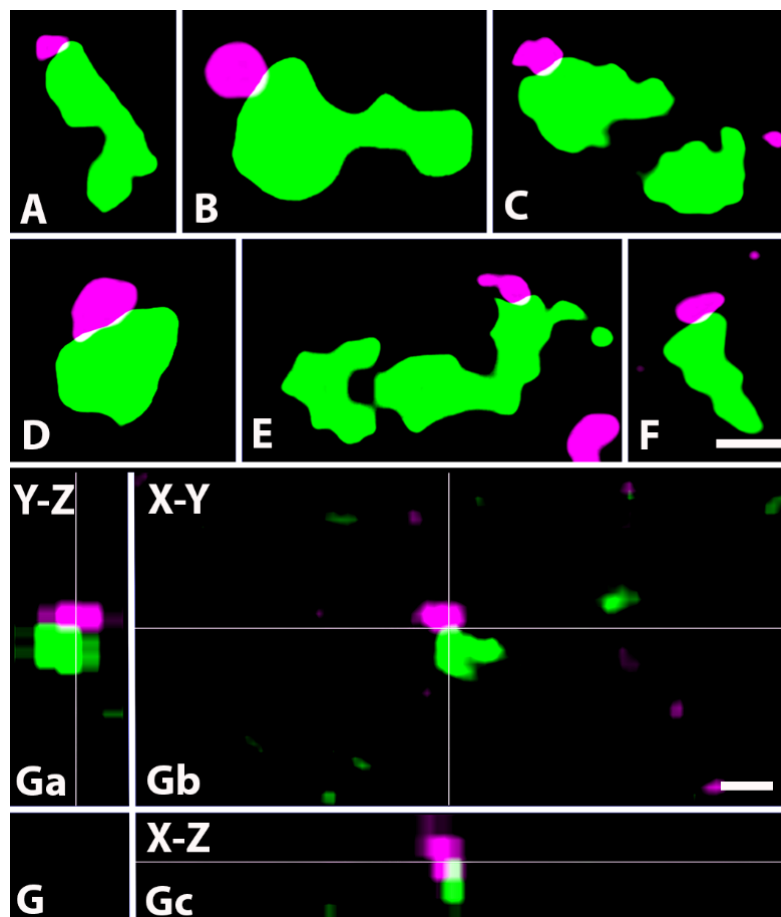


Figure 30: Contacts between axon terminals immunoreactive for GlyT2 and VGLUT1. A-F. Micrographs of 1 μm thick laser scanning confocal optical sections presenting close appositions between axons immunoreactive for GlyT2 (magenta) and VGLUT1 (green), a marker for non-nociceptive primary afferents. The yellow colour labels the contact zones between the two types of axon terminals and may represent axo-axonic synapses observed with electron microscopy. G. Micrographs of a short series of confocal optical sections double immunostained for GlyT2 (magenta) and VGLUT1 (green) presenting contact between GlyT2 (magenta) and VGLUT1 (green)

immunostained axon terminals shown in X-Y (Gb), X-Z (Ga) and Y-Z (Gc) projections. The contact zone between the two labelled axon terminals (yellow) is at the crossing point of two lines indicating the planes through which orthogonal views of the X-Z and Y-Z projections were drawn. Note that the contact zone between the two labelled axon terminals (yellow) can be identified in all three orthogonal images. Scale bars: 0.5 μm (A-F), 1 μm (G).

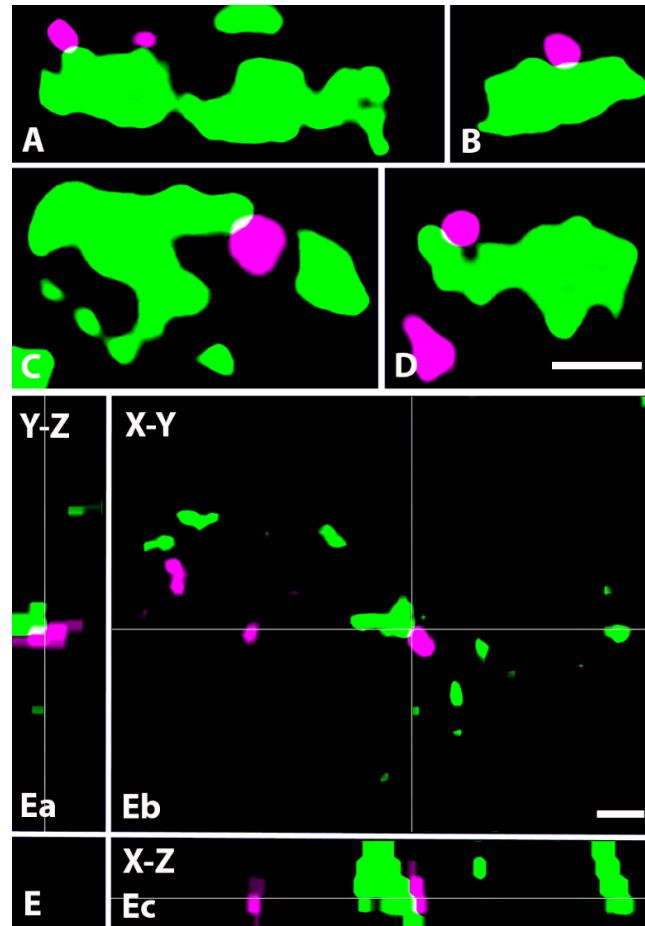


Figure 31: Contacts between axon terminals immunoreactive for GlyT2 and binding IB4. A-D. Micrographs of 1 μm thick laser scanning confocal optical sections showing close appositions between axon terminals immunoreactive for GlyT2 (magenta) and binding IB4 (green), a marker for non-peptidergic nociceptive primary afferents. The yellow colour labels the contact zone between the two types of axon terminals and may represent axo-axonic synapses observed with electron microscopy. E. Micrographs of a short series of confocal optical sections double labelled for GlyT2 (magenta) and IB4-binding (green) presenting contact between GlyT2 immunoreactive (magenta) and IB4 binding (green) axon terminals shown in X-Y (Eb), X-Z (Ea) and Y-Z (Ec) projections. The contact zone between the two labelled axon terminals is at the crossing point of two lines indicating the planes through which orthogonal views of X-Z and Y-Z projections were drawn. Note that the contact zone between the two labelled axon terminals (yellow) can be identified in all three orthogonal images. Scale bars: 0.5 μm (A-D), 1 μm (E).

5.11. Distribution of glycinergic axon terminals in post- and presynaptic positions along the dendrites of PKC γ -containing neurons

We have already identified the types of neurons that receive axo-somatic glycinergic inputs, however, the dendrites of neurons receive the majority of the inhibitory inputs. Therefore, to analyse how axo-dendritic glycinergic synapses are distributed along the dendritic tree, we looked for a population of neurons that could be used as a model. Additionally, we intended to evaluate the dendritic position of synapses made by primary afferent axon terminals, whose function can be modulated by presynaptic glycinergic inhibition. Thus, we chose the PKC γ -containing neurons for this experiment because they are known to receive significant excitatory inputs from primary afferents and are strongly inhibited by pre- and postsynaptic glycinergic neurons (Miraucourt *et al.*, 2007; Neumann *et al.*, 2008; Lu *et al.*, 2013; Peirs *et al.*, 2014, 2015, 2020, 2021; Peirs and Seal, 2016; Artola *et al.*, 2020; El Khoueiry *et al.*, 2022). Furthermore, their dendrites arborize in laminae II and III, where the axo-axonic contacts between GlyT2-positive, IB4-binding, and VGLUT1-positive axon terminals were found (Mori *et al.*, 1990; Malmberg *et al.*, 1997; Polgár *et al.*, 1999; Peirs *et al.*, 2014; Todd, 2017). Considering that 13.2% of PKC γ -positive interneurons were identified as inhibitory (Table 6), and that inhibitory neurons can be under different glycinergic inhibitory control than excitatory neurons, we carried out triple immunostaining of sections from *Prkcg^{tm2/cre}/ERT2-tdTomato* animals for GlyT2, PAX2 and IB4-binding or VGLUT1. After being split into two groups, the sections were stained with the proper combination of antibodies: 1) anti-GlyT2 + IB4-biotin+ anti-PAX2, and 2) anti-GlyT2 + anti-VGLUT1 + anti-PAX2.

We studied 47 and 59 tdTomato-positive PKC γ -containing neurons that received contacts from IB4-binding or VGLUT1 immunoreactive primary afferents, respectively. Nine and 19 of the PKC γ -positive cells contacted by IB4-binding or VGLUT1 immunoreactive axon terminals, respectively, were also positive for PAX2 (Figure 32a, b, c). Most of the reconstructed neurons' cell bodies were in laminae II and III (93 of the 106 cells), while 7 were found in lamina I, and 5 in lamina IV. Surprisingly, neurons that received close appositions from primary afferents that bind IB4 were situated a little bit more dorsally than those that were in touch with VGLUT1 immunoreactive boutons. Regarding the distribution of the neurons' cell bodies making contacts with IB4-binding terminals, 7 of them were found in lamina I, 23 in lamina II, and 17 in lamina III. On the other hand, neurons' cell bodies that received contacts from VGLUT1-positive axon terminals were slightly deeper, 4 of them in lamina II, 50 in lamina III, and 5 in lamina IV. A series of 1 μ m thick confocal sections were used to reconstruct the dendritic trees

of all investigated neurons. Most likely because of the variable degrees of tdTomato expression in the dendritic trees of the labelled neurons, the size of the reconstructed dendritic trees varied greatly as well as its geometries were not uniform. Most of the neurons receiving contacts from IB4-binding terminals presented a vertical/stalked cell morphology (Figure 32d), while the majority of the neurons contacted by VGLUT1-positive axon terminals were classified as islet or central cells (Figure 32e) (Gobel, 1978, Grudt and Perl, 2002).

For the cells stained for GlyT2 and IB4-binding, 1520 and 1306 contacts made by GlyT2 immunoreactive and IB4-binding axon terminals, respectively, were identified on the dendrites. Measuring the total lengths of the dendrites and combining this value with the numbers of counted contacts, we calculated that 4.4 ± 2.9 and 4.8 ± 1.9 contacts were made by IB4-binding and GlyT2 immunoreactive axon terminals in a 100 μm long dendritic segment, respectively. In the case of the cells stained for GlyT2 and VGLUT1, 1763 and 1019 close appositions made by GlyT2 immunoreactive and VGLUT1 immunoreactive axon terminals, respectively, were counted on the dendrites (Figure 32f, g, h, i). Combining the total lengths of the dendrites with the numbers of contacts, it turned out that 2.5 ± 1.3 and 4.5 ± 2.3 contacts were made by VGLUT1 and GlyT2 immunoreactive axon terminals, respectively, in a 100 μm long dendritic segment. Independent of the markers, the contacts were uniformly dispersed along the dendrites and did not exhibit any signs of aggregation. Between PAX positive and PAX negative neurons, there were no appreciable variations in these parameters.

Lastly, we explored the interactions between GlyT2 immunoreactive boutons and IB4-binding or VGLUT1 immunoreactive axon terminals making contacts with tdTomato-containing dendrites (Figure 32j). We were not able to detect any GlyT2 immunoreactive axo-axonic appositions on 22 of the 106 reconstructed cells (6 with IB4-binding and 16 with VGLUT1 immunoreactive axon terminals). For the neurons on which there were GlyT2 terminals making axo-axonic contacts, we found that 101 (9.2%) of the 1095 IB4-binding axon terminals making close appositions with the labelled dendrites were contacted by GlyT2 immunoreactive terminals. On the other hand, 126 (16.4%) of the 765 VGLUT1 immunostained axon terminals making contacts with the labelled dendrites were contacted by GlyT2-positive terminals.

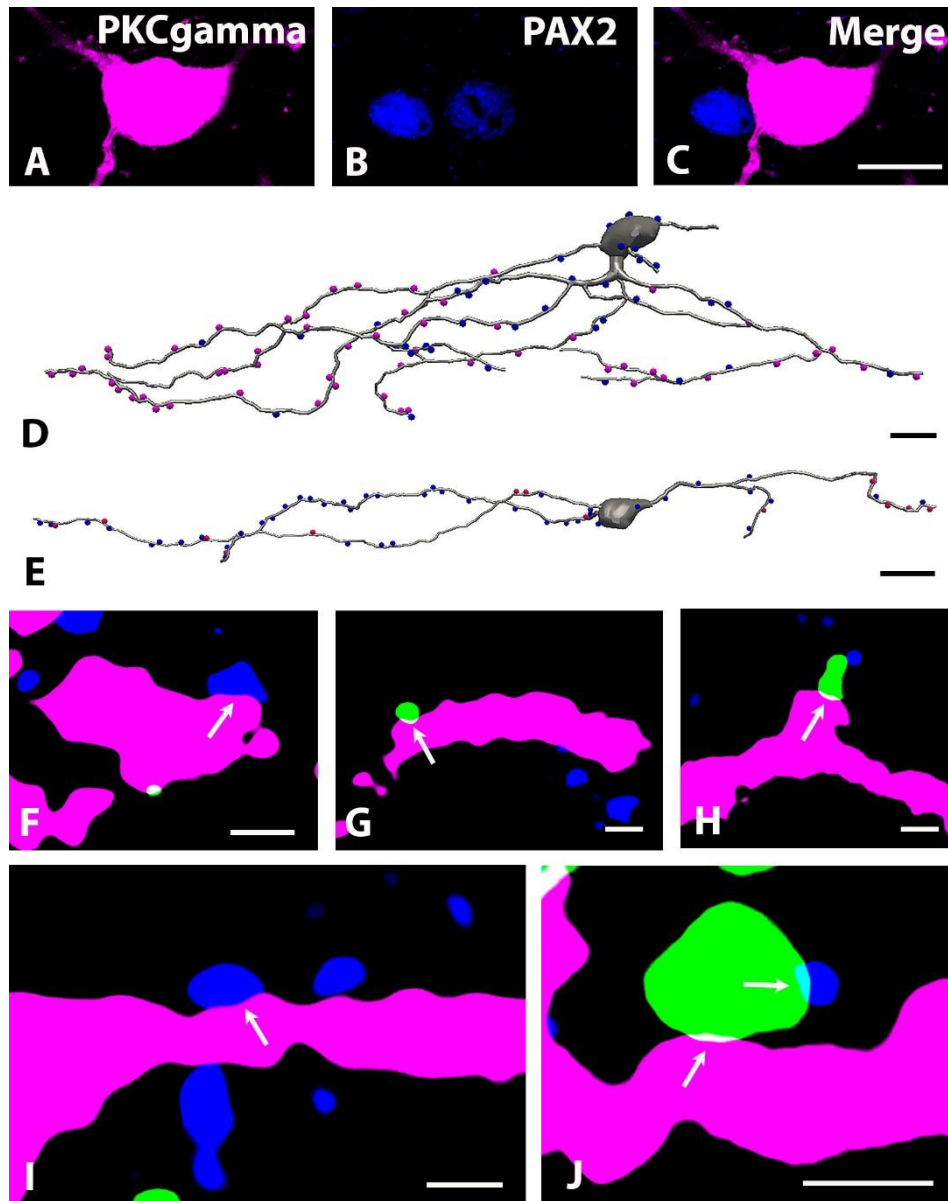


Figure 32: Contacts between unmyelinated (IB4-binding) and myelinated (VGLUT1 immunostained) primary afferents as well as GlyT2 immunoreactive axon terminals on tdTomato-labelled neurons in *Prkcg^{tm2/cre}/ERT2-tdTomato* mice. A-C: Micrographs of a single 1 μm thick laser scanning confocal optical section presenting PAX2 (blue) immunostaining of the nucleus of a tdTomato (magenta) labelled PKC γ -containing neuron. D-E: Neurolucida reconstruction of the dendritic trees of PKC γ (grey)-containing neurons making close appositions with GlyT2 (blue) immunoreactive as well as IB4-binding (D) and VGLUT1 (E) immunostained axon terminals (magenta). F-J: Micrographs of 1 μm thick laser scanning confocal optical sections showing close apposition between tdTomato (magenta) labelled dendrites of PKC γ -containing neurons and VGLUT1 (green; G, H, J) or GlyT2 (blue; F, I) immunoreactive axon terminals. Note that the VGLUT1 immunoreactive axon terminal forming a close apposition with a tdTomato labelled dendrite in inset J contacted by a GlyT2 immunostained axon terminal. Arrows indicate the sites of contacts between the labelled structures. Bars: 10 μm (A-E), 1 μm (J) 0.5 μm (F-I).

6. Discussion

6.1. Specificity of GlyT2::CreERT2-tdTomato construction for the labelling of glycinergic neurons in the spinal dorsal horn

The axonal membrane transporter GlyT2, responsible for glycine reuptake from the extracellular space into axon terminals has been reported as a trustworthy marker for glycinergic neurons in the spinal cord (Poyatos *et al.*, 1997). Immunohistochemistry, *in situ* hybridization, electron microscopy, and autoradiography studies have confirmed that this transporter protein is present in all glycinergic neurons in the spinal dorsal horn (Luque *et al.*, 1995; Poyatos *et al.*, 1997; Spike *et al.*, 1997). In this study, we used the genetic construct of mice expressing CreERT2 recombinase under the control of the GlyT2 gene (GlyT2::CreERT2). The GlyT2::CreERT2 mice were then crossed with tdTomato reporter mice, and the tdTomato expression was induced by intraperitoneal tamoxifen injection in the offsprings.

Using this approach, the tdTomato labelling turned out to be highly specific for glycinergic neurons. Almost all, $97.35 \pm 2.38\%$ of the tdTomato-labelled neurons in laminae I-IV were also immunoreactive for PAX2, and every single one of them expressed GlyT2 mRNA, indicating that the tdTomato-labelled neurons are indeed glycinergic. We must add, however, that the tdTomato expression was highly dependent on the timing of tamoxifen injection. This extremely specific labelling was observed when tamoxifen was administered on the 8 to 10 postnatal days (P8-10). After the tamoxifen injection on P8-10, all injected offspring survived and the tdTomato expression was strong throughout the spinal dorsal horn. Tamoxifen injection at P4-5 resulted in high mortality, while tdTomato expression following injections at P11-P12 was weak and observed in a limited number of neurons. Thus, our tdTomato labelling seems to be close to perfect for qualitative analysis, but it is likely that we did not label all of the glycinergic neurons.

6.2. Morphological characteristics

In laminae I-II, earlier studies of Lima and Coimbra (1986), and Grudt and Perl (2002) provided a detailed morphological description of local interneurons. They described the morphology of these neurons so accurately that their classification proposals, particularly the one of Grudt and Perl (2002) are still valid. Our type 1, and type 2 neurons are very similar to the fusiform neurons of Lima and Coimbra (1986), and islet and/or central neurons of Grudt and Perl (2002). Type 3 neurons observed in our study resemble the multipolar cells of Lima and Coimbra

(1986), and vertical cells of Grudt and Perl (2002). Therefore, our tdTomato labelled glycinergic neurons in laminae I-II appear to belong to the islet, central, and vertical cell populations, as described originally by Grudt and Perl (2002). The findings of Maxwell *et al.* (2007) and Yasaka *et al.* (2010), which indicated that all islet cells and a fraction of central and vertical cells are inhibitory neurons, provide significant support for our results.

In laminae III-IV, the morphological features of the tdTomato labelled neurons were more diverse than in laminae I-II. This finding was in a good agreement, with the results of Abraira *et al.* (2017), who described 11 types of interneurons in the deep dorsal horn. Others (Hughes *et al.*, 2012; Cui *et al.*, 2016; Koch *et al.*, 2017), however, showed that among these cells there are neurons with morphologies that are very similar to those described by Grudt and Perl (2002) in laminae I-II. Our morphological classification of laminae III-IV glycinergic neurons are supported by these earlier findings. Most of our reconstructed tdTomato-labelled neurons were classified as type 1, which resemble islet cells, and our type 2 neurons shows dendritic arbour similar to central cells of Grudt and Perl (2002). Our types 3 and 4 neurons are comparable to Grudt and Perl's (2002) vertical cells, and they are even more like the stalked and inverted stalked neurons as these neurons were classified by Gobel (1978). Our type 5 neurons have pyramidal perikaryon, which haven't been mentioned in recent studies. Nevertheless, in an early Golgi impregnation study, Réthelyi and Szentágothai (1969) identified pyramidal-shaped neurons with cell bodies at the boundary between laminae III and IV and axons projecting into lamina II. In addition to these cell populations, we recovered a number of other tdTomato-labelled neurons whose dendritic arborization did not correspond to any of the previously identified cell types, and they even differed from one another. We put these neurons into one group and identified them as type 6 neurons. The morphological variability of these neurons is consistent with the general idea that the morphology of neurons is quite variable in the deep dorsal horn.

6.3. Neurochemical markers

It is widely accepted that inhibitory neurons in laminae I-II can be assigned to five almost non-overlapping groups that can be distinguished from each other based on their neurochemical markers: GAL, NPY, nNOS, PV, or CR (Boyle *et al.*, 2017). It is also a general assumption that all inhibitory neurons are GABAergic in laminae I-II, and some of the GABAergic neurons may also release glycine as a neurotransmitter (Sardella *et al.*, 2011; Tiong *et al.*, 2011; Polgár *et al.*, 2013; Duan *et al.*, 2014). Our current findings add some refinement to this general idea.

Namely, we found that GlyT2 expressed in some nNOS- and PV-containing neurons. However, we did not find any GlyT2 expression in GAL- and CR-containing neurons, and there was little, if any, colocalization between GlyT2 and NPY. Therefore, GAL, CR, and nearly all NPY-expressing inhibitory neurons are likely to be GABA-only neurons, while glycine may colocalize with GABA in some nNOS- and PV-positive cells. On the other hand, however, we found RET and ROR β expression in some GlyT2 positive neurons, but RET and ROR β have not been reported as markers of GABAergic neurons in laminae I-II. Since in our FISH studies, no glycine only neurons were found in laminae I-II, the GABAergic nature of the RET- and ROR β -containing neurons in laminae I-II should be verified in future studies.

Inhibitory interneurons in laminae III–IV are generally considered to be substantially more diverse compared to the ones in laminae I–II. Laminae III and IV include large populations of inhibitory neurons expressing RET (Cui *et al.*, 2016) and ROR β (Koch *et al.*, 2017), but it is also evident that some inhibitory neurons in these laminae also express PV and nNOS (Tiong *et al.*, 2011; Polgár *et al.*, 2013). In addition to these, there must be more inhibitory neurons in laminae III-IV, which cannot be distinguished by a single neurochemical marker; their identification requires a combination of different markers identified by single-cell transcriptome analysis (Häring *et al.*, 2018; Sathyamurthy *et al.*, 2018; Zeisel *et al.*, 2018). Our principal finding in laminae III–IV is that 56, 40, 12, and 6% of the tdTomato-labelled glycinergic neurons are positive for RET, PV, ROR β , and nNOS, respectively. It is also likely that there might be other smaller populations of glycinergic neurons in laminae III-IV that are still waiting for proper neurochemical characterization.

6.4. GABAergic vs glycinergic inhibition in the spinal dorsal horn

There is general agreement that fast inhibitory neurotransmission is mediated by GABA and glycine. It is, however, under continuous discussion what is the relative contribution of GABAergic and glycinergic inhibition to spinal nociceptive/pain processing. According to the traditional view, GABA is the universal inhibitory transmitter, the effect of which can be modified in some cases by glycinergic events. This view indicates that there are two types of fast inhibitory neurotransmission in laminae I-III of the spinal dorsal horn: mediated only by GABA and mixed GABAergic-glycinergic. In contrast to this, experimental evidence continuously accumulates indicating that in addition to GABA-only and mixed GABA-glycine events glycine-only inhibition also contributes in a substantial extent to inhibitory neurotransmission in laminae I-III. The debate between these two contrasting ideas were

explicitly presented in a recent paper (El Khoueiry *et al.*, 2022), in which GABAergic and glycinergic inputs on PKC γ -containing neurons were investigated in lamina III. They reported that 91.7% of the inhibitory axon terminals contacting PKC γ -immunoreactive interneurons contained GAD, from which 42.2% also expressed GlyT2; therefore, glycinergic axon terminals could be classified as a subgroup of GABAergic boutons. They found only 6.3% of GlyT2-positive boutons that were negative for GAD. In the same study, however, they showed that both GABA_A and glycine receptors were inserted in the postsynaptic membranes of 78.3% of the investigated inhibitory synapses, and only 2.3% of the postsynaptic membranes were positive only for GABA_A receptors. On top of this, 70% of the quantal events were mediated by either glycine-only or GABA-only synaptic transmission by recording sIPSCs and mIPSCs from the same set of synapses. This major disagreement between morphological and physiological findings, which is presented very clearly in this paper makes the interpretation of data regarding the function of GABAergic and glycinergic inhibition in spinal pain processing quite ambiguous.

Some of these previous findings are supported by our FISH data. We found that 32.9% of PAX2 positive inhibitory interneurons in laminae I–III that were positive for GAD65/67 mRNAs and negative for GlyT2 mRNA, indicating that they could only mediate GABAergic synaptic inhibition. The rest of the PAX2 positive neurons (67.1%) in laminae I–III expressed both GlyT2 and GAD65/67 mRNA, with GAD65/67 mRNA clearly dominating. Thus, it is likely that axon terminals arising from laminae I–III inhibitory interneurons can mediate GABA-only or mixed GABA–glycine synaptic events. In contrast to this, however, we demonstrated that less than half of the GlyT2 positive axon terminals show immunostaining for GAD65/67, indicating that there might be glycine-only axon terminals in the superficial spina dorsal horn in abundant number. This observation strongly confirms earlier physiological findings suggesting that in lamina II glycinergic inhibition is as strong, if not stronger, than GABAergic inhibition. Taking our FISH results obtained in laminae I–III into account, the glycine-only axon terminals in lamina I–II can arise from inhibitory neurons located deeper than lamina III. Investigating GlyT2 and GAD65/67 mRNA expression in lamina IV, we found that most of the PAX2 positive inhibitory neurons (89.8%) expressed both GlyT2 and GAD65/67 mRNA and only a small percentage of neurons (3.7%) were positive only for GlyT2 mRNA. However, we also demonstrated that almost all double labelled neurons showed a remarkable GlyT2 mRNA dominance with a weak GAD 65/67 mRNA expression. Thus, it is likely that glycine-only axon terminals in laminae I–II arise from glycinergic neurons in lamina

IV that express exclusively GlyT2 mRNA, or express both GAD65/67 mRNAs with GlyT2 dominance. In neurons with high GlyT2 mRNA and low GAD65/67 mRNA expression, the amount of GAD65/67 transported to the axon terminals and consequently the concentration of GABA in the axoplasm can be so low that GAD65/67 could not be detected in our immunohistochemical experiments, and the concentration of GABA in the axoplasm is probably below the level what is necessary for vesicular GABA transporter (VIAAT) uptake (Gomez *et al.*, 2003; Rousseau *et al.*, 2008). Therefore, due to the lack or limited amount of GABA in synaptic vesicles the postsynaptic action of GABA in these synapses cannot be observed by physiological and pharmacological methods. Most probably the immunocytochemical methodology used by El Khoueiry *et al.* (2022) was so sensitive that they could detect extremely small quantities of peptides, such as GABA_A receptors and GAD, with minimal or no functional significance. This concept obviously requires additional experimental confirmation.

However, the potential contribution of glycine-only and glycine-dominant neurons in lamina IV to spinal pain processing, in addition to that of neurons in laminae I-III, should not be disregarded when pain-related synaptic events are considered in the spinal dorsal horn. Lamina IV glycinergic neurons with their axon terminals in lamina I-III, e.g. pyramidal neurons described first by Réthelyi and Szentágothai (1969), may be crucial in spinal nociceptive/pain processing, e.g. in the onset of allodynia (Lu *et al.*, 2013; Foster *et al.*, 2015; Petitjean *et al.*, 2015; Peirs *et al.*, 2021). That is, these inhibitory lamina IV neurons can be stimulated by A β primary afferents and project their axons to excitatory lamina II neurons, such as PKC γ - and CR-positive neurons, that are components of neural circuits carrying A β primary afferent inputs to nociceptive projection neurons in lamina I (Lu *et al.*, 2013; Peirs *et al.*, 2021).

6.5. Synaptic targets of glycinergic inhibition in laminae I-III

As a number of previous results and our present findings suggest inhibitory axon terminals in laminae I-III of the spinal dorsal horn can release glycine alone or in combination with GABA. In the present synaptological study, however, we examined GlyT2-containing axon terminals, but we did not investigate glycine-only and mixed glycine-GABA terminals separately. Consequently, we are unable to define whether the GlyT2-containing axon terminals that we observed can release glycine only or both glycine and GABA. Therefore, our GlyT2-containing axon terminals can be regarded simply as glycinergic.

Glycinergic axon terminals in the spinal dorsal horn may arise from local spinal neurons or can be terminals of axons that descend from brainstem nuclei (Antal *et al.*, 1996; Hossaini *et al.*, 2012). Our results show that descending fibres of brainstem origin substantially contribute to the glycinergic innervation of lamina I–III. According to our data, in laminae I–III, 32–40% of glycinergic boutons are axon terminals of neurons located above the spinal cord. Therefore, brainstem-derived glycinergic axon terminals must be removed before the examination of glycinergic axon terminals of spinal origin. By performing a low thoracic hemisection, we removed the descending axons, allowing us to conclude that in our synaptological experiments only glycinergic terminals of spinal origin were studied.

6.5.1. Postsynaptic *versus* presynaptic inhibition

We demonstrated that GlyT2 immunoreactive axon terminals formed axo-dendritic, axo-somatic, and axo-axonic synapses, affirming that glycine can mediate both post- and presynaptic inhibition in the spinal dorsal horn (Todd, 1990; Hughes *et al.*, 2012; Petitjean *et al.*, 2015; Abaira *et al.*, 2017; Boyle *et al.*, 2017). Our current findings acquired with the aid of different experimental methods, revealed that 85–90% of GlyT2 immunostained axon terminals made axo-dendritic and axo-somatic synapses as well as close appositions. Therefore, our findings suggests that glycine-mediated postsynaptic inhibition must be significantly more dominant than glycinergic presynaptic inhibition in laminae I–III. Our current findings further show that, in contrast to glycine-mediated presynaptic inhibition, which may only influence special sets of axon terminals, glycinergic postsynaptic inhibition must be a common functional characteristic of neural circuits in laminae I–III of the spinal dorsal horn.

6.5.2. Targets of postsynaptic glycinergic inhibition

Numerous experimental findings have substantiated the significance of postsynaptic glycinergic inhibition in the spinal processing of acute and chronic pain (Miraucourt *et al.*, 2007; Takazawa and MacDermott, 2010; Lu *et al.*, 2013; Duan *et al.*, 2014; Foster *et al.*, 2015; Imlach *et al.*, 2016; Peirs and Seal, 2016; Takazawa *et al.*, 2017; Peirs *et al.*, 2020; El Khoueiry *et al.*, 2022). Most of these investigations have demonstrated that different groups of excitatory interneurons are targeted by glycinergic postsynaptic inhibition, while glycinergic innervation of inhibitory interneurons has been very rarely studied, if studied at all (Takazawa and MacDermott, 2010; Smith *et al.*, 2016; Gradwell *et al.*, 2017; Liu *et al.*, 2021). This is probably the explanation for the lack of representation of glycinergic inhibition of inhibitory interneurons in neural circuit models of spinal pain processing published till today. Despite

this, in this study, we demonstrated that GlyT2 immunoreactive axon terminals formed close somatic appositions with nearly all kinds of inhibitory interneurons in laminae I-III of the spinal dorsal horn, including PV-, CR-, GAL-, nNOS-, and PKC γ - containing inhibitory neurons. Therefore, glycinergic inhibition of inhibitory interneurons may be crucial in spinal pain processing. For example, the glycinergic innervation of PV-containing inhibitory interneurons can be seriously considered when their role in the development of allodynia is discussed (Gradwell *et al.*, 2017).

6.5.3. Targets of presynaptic glycinergic inhibition

Even though postsynaptic inhibition appears to be more frequent in laminae I-III of the spinal dorsal horn, presynaptic glycinergic inhibition may also alter the function of some well definable primary afferents. Our current findings show that glycinergic neurons establish axo-axonic synapses only with IB4-binding and VGLUT1 immunoreactive axon terminals, which correspond to nociceptive nonpeptidergic C and non-nociceptive myelinated A β primary afferents, respectively. It was previously demonstrated that these presynaptic glycinergic axon terminals may arise from PV-containing inhibitory cells (Hughes *et al.*, 2012; Petitjean *et al.*, 2015; Abraira *et al.*, 2017; Boyle *et al.*, 2017;), however, our current findings suggest that glycinergic neurons in lamina IV may also contribute to the presynaptic innervation of IB4-binding and VGLUT1 immunoreactive axon terminals in laminae II-III. It is quite remarkable to notice that the primary afferent and glycinergic innervation of PKC γ -containing neurons, which play a significant role in the development of mechanical allodynia, show very interesting characteristics. In agreement with previous reports, our results show that PKC γ -containing neurons in laminae I-IIo are innervated by IB4-binding non-peptidergic nociceptive C fibres (Todd, 2010), while PKC γ -containing neurons in laminae Iii-III receive innervation from VGLUT1 immunoreactive non-nociceptive myelinated A β fibres (Neumann *et al.*, 2008; Lu *et al.*, 2013; Peirs *et al.*, 2014; Abraira *et al.*, 2017). As we have successfully demonstrated in this study, a fraction of both sets of primary afferent inputs that make synaptic connections with the two different populations of PKC γ -containing neurons can be inhibited presynaptically by glycinergic neurons.

On the contrary, Gradwell *et al.* (2017, 2022) showed that even though PV-containing inhibitory interneurons (iPVINs) make axo-axonic presynaptic inhibitory contacts with non-nociceptive A δ and A β myelinated afferent fibres, iPVINs mediate only postsynaptic glycinergic inhibition, while iPVIN-derived presynaptic inhibition is exclusively mediated by

GABA. Nevertheless, this finding by Gradwell *et al.* (2022) does not rule out the possibility of presynaptic glycinergic inhibition. First, we were unable to identify any presynaptic axo-axonic contacts made by GlyT2 immunoreactive terminals on one-fifth of the studied PKC γ -containing neurons. Therefore, within a population of neurons that can be recognized by a specific neuronal marker, glycinergic presynaptic inhibition may have an impact only on some of these neurons. Second, our results show that the majority (85-90%) of the GlyT2 immunostained axon terminals formed axo-dendritic and axo-somatic appositions, and only the remaining terminals were found to make axo-axonic contacts. This finding clearly indicates that glycinergic postsynaptic inhibition greatly surpasses glycinergic presynaptic inhibition, which may also mean that the majority of glycinergic neurons mediate exclusively postsynaptic inhibition, and only some of them mediate both post- and presynaptic inhibition. Third, we found axo-axonic close appositions established by the GlyT2 immunoreactive terminals on roughly one-tenth of IB4-binding and one-sixth of VGLUT1 immunoreactive axon terminals of primary afferents making contacts with the investigated PKC γ neurons. Therefore, we may say that at cellular level, presynaptic glycinergic inhibition can be difficult to detect because of its weakness. However, it is possible to hypothesize that glycinergic presynaptic inhibition, even though being weak at the cellular level, may be crucial for locally targeting functionally distinct subpopulations of primary afferent inputs.

7. Summary

We studied the morphological and neurochemical properties, as well as the synaptic targets of glycinergic neurons in laminae I-IV of the mouse spinal dorsal horn by using transgenic technologies, immunohistochemistry, *in situ* hybridization, light and electron microscopy.

We showed that although cell bodies of glycinergic neurons were rare in lamina II and only a slightly more numerous in lamina I, axon terminals were densely distributed in these superficial laminae, indicating that glycinergic neurons in the deeper layers of the dorsal horn send their axons into laminae I-II. The number of labelled neurons was higher in lamina III, but the highest density was observed in lamina IV.

We demonstrated that there are at least 3 and 6 subtypes of glycinergic neurons showing distinct morphology in laminae I-II and III-IV, respectively. According to the classification scheme of Grudt and Perl (2002), all the labelled glycinergic neurons in laminae I-II and many of them in laminae III-IV were identified as islet, central and vertical neurons. Cell morphologies in laminae III-IV, however, were more diverse; some labelled neurons in laminae III-IV resembled inverted stalked cells of Gobel (1978) and pyramidal cells of Réthelyi and Szentágothai (1969), while the morphologies of others did not correspond to any of the previously identified cell types.

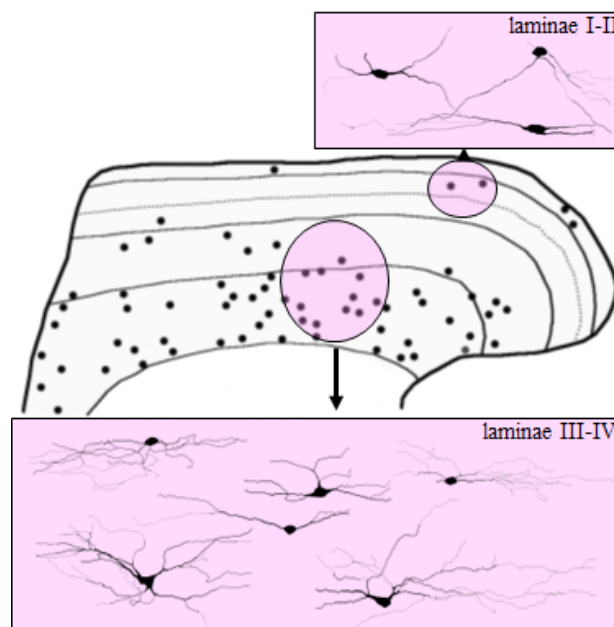


Figure 33: Graphical summary of the distribution and morphologies of glycinergic neurons in laminae I-II and III-IV of the spinal dorsal horn. See detailed description in the text.

We showed that distinct populations of glycinergic neurons in laminae I-IV express neuronal markers like PV, nNOS, RET and ROR β .

First in the literature, we provided experimental evidence that there are glycinergic axon terminals in abundant numbers in laminae I-II that do not express GABA, and these glycine-only axon terminals may arise primarily, if not exclusively, from neurons in lamina IV. Thus, glycinergic neurons with cell bodies in lamina IV may contribute substantially to spinal pain processing.

Our findings suggests that glycine-mediated postsynaptic inhibition must be significantly more dominant than glycinergic presynaptic inhibition in laminae I-III.

Our results indicate that glycinergic postsynaptic inhibition, including glycinergic inhibition of inhibitory interneurons must be a common functional characteristic of neural circuits underlying spinal pain processing. On the other hand, it is possible to hypothesize that glycinergic presynaptic inhibition, even though can be weak at the cellular level, may be crucial for locally targeting functionally distinct subpopulations of primary afferent inputs.

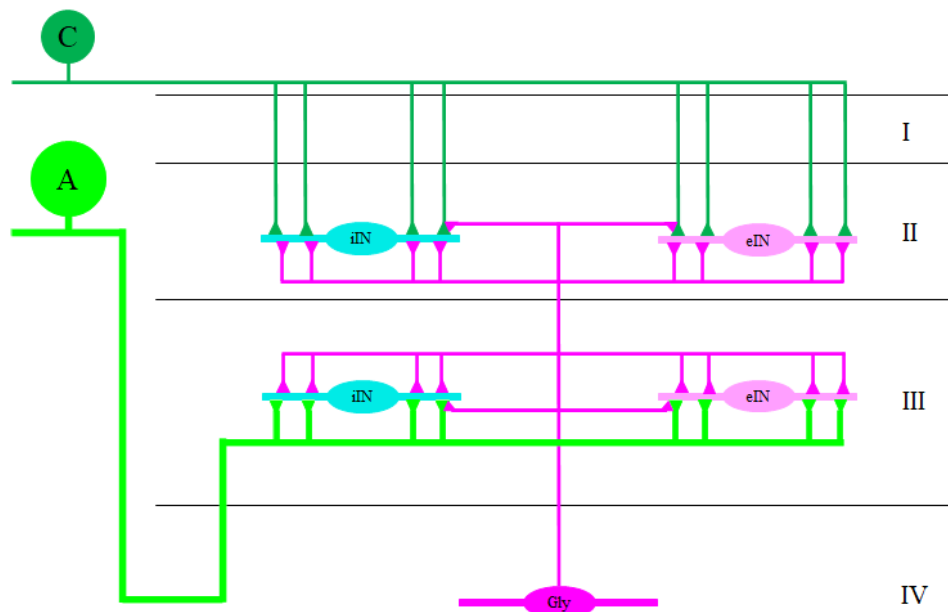


Figure 34: Graphical summary of the pre- and postsynaptic targets of glycinergic inhibition in laminae I-III. Axon terminals of glycinergic neurons in lamina IV (dark magenta) may evoke postsynaptic inhibition on a wide range of inhibitory interneurons (iIN in blue) and excitatory interneurons (eIN in light magenta) in both laminae II and III, while presynaptic inhibition may be crucial for targeting some subpopulations of non-peptidergic nociceptive C (dark green) and non-nociceptive A type (light green) primary afferents.

8. References

- Abraira, V. E.; Ginty, D. D. The sensory neurons of touch. *Neuron* 2013, 79 (4), 618-639. DOI: 10.1016/j.neuron.2013.07.051.
- Abraira, V. E.; Kuehn, E. D.; Chirila, A. M.; Springel, M. W.; Toliver, A. A.; Zimmerman, A. L.; Orefice, L. L.; Boyle, K. A.; Bai, L.; Song, B. J.; et al. The Cellular and Synaptic Architecture of the Mechanosensory Dorsal Horn. *Cell* 2017, 168 (1-2), 295-310.e219. DOI: 10.1016/j.cell.2016.12.010.
- Al-Khater, K. M.; Todd, A. J. Collateral projections of neurons in laminae I, III, and IV of rat spinal cord to thalamus, periaqueductal gray matter, and lateral parabrachial area. *J Comp Neurol* 2009, 515 (6), 629-646. DOI: 10.1002/cne.22081.
- Alaynick, W. A.; Jessell, T. M.; Pfaff, S. L. SnapShot: spinal cord development. *Cell* 2011, 146 (1), 178-178.e171. DOI: 10.1016/j.cell.2011.06.038.
- Alba-Delgado, C.; El Khoueiry, C.; Peirs, C.; Dallel, R.; Artola, A.; Antri, M. Subpopulations of PKC γ interneurons within the medullary dorsal horn revealed by electrophysiologic and morphologic approach. *Pain* 2015, 156 (9), 1714-1728. DOI: 10.1097/j.pain.0000000000000221.
- Alvarez, F. J.; Fyffe, R. E. Nociceptors for the 21st century. *Curr Rev Pain* 2000, 4 (6), 451-458. DOI: 10.1007/s11916-000-0069-4.
- Anderson, W. B.; Graham, B. A.; Beveridge, N. J.; Tooney, P. A.; Brichta, A. M.; Callister, R. J. Different forms of glycine- and GABA(A)-receptor mediated inhibitory synaptic transmission in mouse superficial and deep dorsal horn neurons. *Mol Pain* 2009, 5, 65. DOI: 10.1186/1744-8069-5-65.
- Antal, M.; Freund, T. F.; Polgár, E. Calcium-binding proteins, parvalbumin- and calbindin-D 28k-immunoreactive neurons in the rat spinal cord and dorsal root ganglia: a light and electron microscopic study. *J Comp Neurol* 1990, 295 (3), 467-484. DOI: 10.1002/cne.902950310.
- Antal, M.; Petkó, M.; Polgár, E.; Heizmann, C. W.; Storm-Mathisen, J. Direct evidence of an extensive GABAergic innervation of the spinal dorsal horn by fibres descending from the rostral ventromedial medulla. *Neuroscience* 1996, 73 (2), 509-518. DOI: 10.1016/0306-4522(96)00063-2.
- Artola, A.; Voisin, D.; Dallel, R. PKC γ interneurons, a gateway to pathological pain in the dorsal horn. *J Neural Transm (Vienna)* 2020, 127 (4), 527-540. DOI: 10.1007/s00702-020-02162-6.
- Aubrey, K. R.; Supplisson, S. Heterogeneous Signaling at GABA and Glycine Co-releasing Terminals. *Front Synaptic Neurosci* 2018, 10, 40. DOI: 10.3389/fnsyn.2018.00040.
- Balázs, A.; Mészár, Z.; Hegedűs, K.; Kenyeres, A.; Hegyi, Z.; Dócs, K.; Antal, M. Development of putative inhibitory neurons in the embryonic and postnatal mouse superficial spinal dorsal horn. *Brain Struct Funct* 2017, 222 (5), 2157-2171. DOI: 10.1007/s00429-016-1331-9.

Bardóczi, Z.; Pál, B.; Kőszeghy, Á.; Wilhelm, T.; Watanabe, M.; Záborszky, L.; Liposits, Z.; Kalló, I. Glycinergic Input to the Mouse Basal Forebrain Cholinergic Neurons. *J Neurosci* 2017, 37 (39), 9534-9549. DOI: 10.1523/JNEUROSCI.3348-16.2017.

Basbaum, A. I.; Bautista, D. M.; Scherrer, G.; Julius, D. Cellular and molecular mechanisms of pain. *Cell* 2009, 139 (2), 267-284. DOI: 10.1016/j.cell.2009.09.028.

Basbaum, A. I.; Jessel, T. M. Pain. In *Principles of Neural Science, Fifth Edition* ed.; Eric R. Kandel, J. H. S., Thomas M. Jessel, Steven A. Siegelbaum, A. J. Hudspeth Ed.; The McGraw-Hill Companies, 2013; pp 530 - 555.

Benarroch, E. E. Dorsal horn circuitry: Complexity and implications for mechanisms of neuropathic pain. *Neurology* 2016, 86 (11), 1060-1069. DOI: 10.1212/WNL.0000000000002478.

Boyle, K. A.; Gutierrez-Mecinas, M.; Polgár, E.; Mooney, N.; O'Connor, E.; Furuta, T.; Watanabe, M.; Todd, A. J. A quantitative study of neurochemically defined populations of inhibitory interneurons in the superficial dorsal horn of the mouse spinal cord. *Neuroscience* 2017, 363, 120-133. DOI: 10.1016/j.neuroscience.2017.08.044.

Brooks, J.; Tracey, I. From nociception to pain perception: imaging the spinal and supraspinal pathways. *J Anat* 2005, 207 (1), 19-33. DOI: 10.1111/j.1469-7580.2005.00428.x.

Chandar, K.; Freeman, B. K. Spinal Cord Anatomy. In *Encyclopedia of the Neurological Sciences (Second Edition)*, Aminoff, M. J., Daroff, R. B. Eds.; Academic Press, 2014; pp 254-263.

Chen, J. T.; Guo, D.; Campanelli, D.; Frattini, F.; Mayer, F.; Zhou, L.; Kuner, R.; Heppenstall, P. A.; Knipper, M.; Hu, J. Presynaptic GABAergic inhibition regulated by BDNF contributes to neuropathic pain induction. *Nat Commun* 2014, 5, 5331. DOI: 10.1038/ncomms6331.

Chéry, N.; de Koninck, Y. Junctional versus extrajunctional glycine and GABA(A) receptor-mediated IPSCs in identified lamina I neurons of the adult rat spinal cord. *J Neurosci* 1999, 19 (17), 7342-7355. DOI: 10.1523/JNEUROSCI.19-17-07342.1999.

Colangelo, A. M.; Bianco, M. R.; Vitagliano, L.; Cavaliere, C.; Cirillo, G.; De Gioia, L.; Diana, D.; Colombo, D.; Redaelli, C.; Zaccaro, L.; et al. A new nerve growth factor-mimetic peptide active on neuropathic pain in rats. *J Neurosci* 2008, 28 (11), 2698-2709. DOI: 10.1523/JNEUROSCI.5201-07.2008.

Comitato, A.; Bardoni, R. Presynaptic Inhibition of Pain and Touch in the Spinal Cord: From Receptors to Circuits. *Int J Mol Sci* 2021, 22 (1). DOI: 10.3390/ijms22010414.

Cui, L.; Miao, X.; Liang, L.; Abdus-Saboor, I.; Olson, W.; Fleming, M. S.; Ma, M.; Tao, Y. X.; Luo, W. Identification of Early RET+ Deep Dorsal Spinal Cord Interneurons in Gating Pain. *Neuron* 2016, 91 (6), 1413. DOI: 10.1016/j.neuron.2016.09.010.

Del Barrio, M. G.; Bourane, S.; Grossmann, K.; Schüle, R.; Britsch, S.; O'Leary, D. D.; Goulding, M. A transcription factor code defines nine sensory interneuron subtypes in the mechanosensory area of the spinal cord. *PLoS One* 2013, 8 (11), e77928. DOI: 10.1371/journal.pone.0077928.

Di Lernia, D.; Serino, S.; Riva, G. Pain in the body. Altered interoception in chronic pain conditions: A systematic review. *Neurosci Biobehav Rev* 2016, 71, 328-341. DOI: 10.1016/j.neubiorev.2016.09.015.

Djoughri, L.; Lawson, S. N. Abeta-fiber nociceptive primary afferent neurons: a review of incidence and properties in relation to other afferent A-fiber neurons in mammals. *Brain Res Brain Res Rev* 2004, 46 (2), 131-145. DOI: 10.1016/j.brainresrev.2004.07.015.

Duan, B.; Cheng, L.; Bourane, S.; Britz, O.; Padilla, C.; Garcia-Campmany, L.; Krashes, M.; Knowlton, W.; Velasquez, T.; Ren, X.; et al. Identification of spinal circuits transmitting and gating mechanical pain. *Cell* 2014, 159 (6), 1417-1432. DOI: 10.1016/j.cell.2014.11.003.

El Khoueiry, C.; Alba-Delgado, C.; Antri, M.; Gutierrez-Mecinas, M.; Todd, A. J.; Artola, A.; Dallel, R. GABA. *Cells* 2022, 11 (8). DOI: 10.3390/cells11081356.

Ellis, A.; Bennett, D. L. Neuroinflammation and the generation of neuropathic pain. *Br J Anaesth* 2013, 111 (1), 26-37. DOI: 10.1093/bja/aet128.

Fields, H. State-dependent opioid control of pain. *Nat Rev Neurosci* 2004, 5 (7), 565-575. DOI: 10.1038/nrn1431.

Foster, E.; Wildner, H.; Tudeau, L.; Haueter, S.; Ralvenius, W. T.; Jegen, M.; Johannssen, H.; Hösli, L.; Haenraets, K.; Ghanem, A.; et al. Targeted ablation, silencing, and activation establish glycinergic dorsal horn neurons as key components of a spinal gate for pain and itch. *Neuron* 2015, 85 (6), 1289-1304. DOI: 10.1016/j.neuron.2015.02.028.

Fyffe, R. E. W. Afferent fibers. In *Handbook of the spinal cord, anatomy and physiology*, Davidoff, R. A. Ed.; Vol. vols. 2 and 3; Marcel Dekker, 1984; pp 79-136.

Gardner, E. P.; Johnson, K. O. *The Somatosensory System: Receptors and Central Pathways* In *Principles of Neural Science*, Fifth edition ed.; Kandel, E. R., Schwartz, J. H., Jessell, T. M., Siegelbaum, S. A., Hudspeth, A. J. Eds.; The McGraw-Hill Companies, 2013.

Garland, E. L. Pain processing in the human nervous system: a selective review of nociceptive and biobehavioral pathways. *Prim Care* 2012, 39 (3), 561-571. DOI: 10.1016/j.pop.2012.06.013.

Giesler, G. J.; Nahin, R. L.; Madsen, A. M. Postsynaptic dorsal column pathway of the rat. I. Anatomical studies. *J Neurophysiol* 1984, 51 (2), 260-275. DOI: 10.1152/jn.1984.51.2.260.

Gobel, S. Golgi studies in the substantia gelatinosa neurons in the spinal trigeminal nucleus. *J Comp Neurol* 1975, 162 (3), 397-415. DOI: 10.1002/cne.901620308.

Gobel, S. Golgi studies of the neurons in layer II of the dorsal horn of the medulla (trigeminal nucleus caudalis). *J Comp Neurol* 1978, 180 (2), 395-413. DOI: 10.1002/cne.901800213.

Gomez, J.; Ohno, K.; Hülsmann, S.; Armsen, W.; Eulenburg, V.; Richter, D. W.; Laube, B.; Betz, H. Deletion of the mouse glycine transporter 2 results in a hyperekplexia phenotype and postnatal lethality. *Neuron* 2003, 40 (4), 797-806. DOI: 10.1016/s0896-6273(03)00673-1.

Gradwell, M. A.; Boyle, K. A.; Browne, T. J.; Bell, A. M.; Leonardo, J.; Peralta Reyes, F. S.; Dickie, A. C.; Smith, K. M.; Callister, R. J.; Dayas, C. V.; et al. Diversity of inhibitory and

excitatory parvalbumin interneuron circuits in the dorsal horn. *Pain* 2022, 163 (3), e432-e452. DOI: 10.1097/j.pain.0000000000002422.

Gradwell, M. A.; Boyle, K. A.; Callister, R. J.; Hughes, D. I.; Graham, B. A. Heteromeric α/β glycine receptors regulate excitability in parvalbumin-expressing dorsal horn neurons through phasic and tonic glycinergic inhibition. *J Physiol* 2017, 595 (23), 7185-7202. DOI: 10.1113/JP274926.

Gradwell, M. A.; Callister, R. J.; Graham, B. A. Reviewing the case for compromised spinal inhibition in neuropathic pain. *J Neural Transm (Vienna)* 2020, 127 (4), 481-503. DOI: 10.1007/s00702-019-02090-0.

Grudt, T. J.; Perl, E. R. Correlations between neuronal morphology and electrophysiological features in the rodent superficial dorsal horn. *J Physiol* 2002, 540 (Pt 1), 189-207. DOI: 10.1113/jphysiol.2001.012890.

Gu, Q.; Lee, L. Y. Acid-Sensing Ion Channels and Pain. *Pharmaceuticals (Basel)* 2010, 3 (5), 1411-1425. DOI: 10.3390/ph3051411.

Gutierrez-Mecinas, M.; Bell, A. M.; Shepherd, F.; Polgár, E.; Watanabe, M.; Furuta, T.; Todd, A. J. Expression of cholecystinin by neurons in mouse spinal dorsal horn. *J Comp Neurol* 2019, 527 (11), 1857-1871. DOI: 10.1002/cne.24657.

Gutierrez-Mecinas, M.; Davis, O.; Polgár, E.; Shahzad, M.; Navarro-Batista, K.; Furuta, T.; Watanabe, M.; Hughes, D. I.; Todd, A. J. Expression of Calretinin Among Different Neurochemical Classes of Interneuron in the Superficial Dorsal Horn of the Mouse Spinal Cord. *Neuroscience* 2019, 398, 171-181. DOI: 10.1016/j.neuroscience.2018.12.009.

Hantman, A. W.; Perl, E. R. Molecular and genetic features of a labeled class of spinal substantia gelatinosa neurons in a transgenic mouse. *J Comp Neurol* 2005, 492 (1), 90-100. DOI: 10.1002/cne.20709.

Häring, M.; Zeisel, A.; Hochgerner, H.; Rinwa, P.; Jakobsson, J. E. T.; Lönnerberg, P.; La Manno, G.; Sharma, N.; Borgius, L.; Kiehn, O.; et al. Neuronal atlas of the dorsal horn defines its architecture and links sensory input to transcriptional cell types. *Nat Neurosci* 2018, 21 (6), 869-880. DOI: 10.1038/s41593-018-0141-1.

Hill, R. Z.; Bautista, D. M. Getting in Touch with Mechanical Pain Mechanisms. *Trends Neurosci* 2020, 43 (5), 311-325. DOI: 10.1016/j.tins.2020.03.004.

Hossaini, M.; Goos, J. A.; Kohli, S. K.; Holstege, J. C. Distribution of glycine/GABA neurons in the ventromedial medulla with descending spinal projections and evidence for an ascending glycine/GABA projection. *PLoS One* 2012, 7 (4), e35293. DOI: 10.1371/journal.pone.0035293.

Huang, J.; Polgár, E.; Solinski, H. J.; Mishra, S. K.; Tseng, P. Y.; Iwagaki, N.; Boyle, K. A.; Dickie, A. C.; Kriegbaum, M. C.; Wildner, H.; et al. Circuit dissection of the role of somatostatin in itch and pain. *Nat Neurosci* 2018, 21 (5), 707-716. DOI: 10.1038/s41593-018-0119-z.

Hughes, D. I.; Sikander, S.; Kinnon, C. M.; Boyle, K. A.; Watanabe, M.; Callister, R. J.; Graham, B. A. Morphological, neurochemical and electrophysiological features of

parvalbumin-expressing cells: a likely source of axo-axonic inputs in the mouse spinal dorsal horn. *J Physiol* 2012, 590 (16), 3927-3951. DOI: 10.1113/jphysiol.2012.235655.

Hughes, D. I.; Todd, A. J. Central Nervous System Targets: Inhibitory Interneurons in the Spinal Cord. *Neurotherapeutics* 2020, 17 (3), 874-885. DOI: 10.1007/s13311-020-00936-0.

Hunt, S. P.; Mantyh, P. W. The molecular dynamics of pain control. *Nat Rev Neurosci* 2001, 2 (2), 83-91. DOI: 10.1038/35053509.

Iggo, A.; Steedman, W. M.; Fleetwood-Walker, S. Spinal processing: anatomy and physiology of spinal nociceptive mechanisms. *Philos Trans R Soc Lond B Biol Sci* 1985, 308 (1136), 235-252. DOI: 10.1098/rstb.1985.0024.

Imlach, W. L.; Bhola, R. F.; Mohammadi, S. A.; Christie, M. J. Glycinergic dysfunction in a subpopulation of dorsal horn interneurons in a rat model of neuropathic pain. *Sci Rep* 2016, 6, 37104. DOI: 10.1038/srep37104.

Indra, A. K.; Warot, X.; Brocard, J.; Bornert, J. M.; Xiao, J. H.; Chambon, P.; Metzger, D. Temporally-controlled site-specific mutagenesis in the basal layer of the epidermis: comparison of the recombinase activity of the tamoxifen-inducible Cre-ER(T) and Cre-ER(T2) recombinases. *Nucleic Acids Res* 1999, 27 (22), 4324-4327. DOI: 10.1093/nar/27.22.4324.

Inquimbert, P.; Rodeau, J. L.; Schlichter, R. Differential contribution of GABAergic and glycinergic components to inhibitory synaptic transmission in lamina II and laminae III-IV of the young rat spinal cord. *Eur J Neurosci* 2007, 26 (10), 2940-2949. DOI: 10.1111/j.1460-9568.2007.05919.x.

Iwagaki, N.; Ganley, R. P.; Dickie, A. C.; Polgár, E.; Hughes, D. I.; Del Rio, P.; Revina, Y.; Watanabe, M.; Todd, A. J.; Riddell, J. S. A combined electrophysiological and morphological study of neuropeptide Y-expressing inhibitory interneurons in the spinal dorsal horn of the mouse. *Pain* 2016, 157 (3), 598-612. DOI: 10.1097/j.pain.0000000000000407.

Johnson, K. O. The roles and functions of cutaneous mechanoreceptors. *Curr Opin Neurobiol* 2001, 11 (4), 455-461. DOI: 10.1016/s0959-4388(00)00234-8.

Kalló, I.; Butler, J. A.; Barkovics-Kalló, M.; Goubillon, M. L.; Coen, C. W. Oestrogen receptor beta-immunoreactivity in gonadotropin releasing hormone-expressing neurones: regulation by oestrogen. *J Neuroendocrinol* 2001, 13 (9), 741-748. DOI: 10.1046/j.1365-2826.2001.00708.x.

Keller, A. F.; Coull, J. A.; Chery, N.; Poisbeau, P.; De Koninck, Y. Region-specific developmental specialization of GABA-glycine cosynapses in laminae I-II of the rat spinal dorsal horn. *J Neurosci* 2001, 21 (20), 7871-7880. DOI: 10.1523/JNEUROSCI.21-20-07871.2001.

Koch, S. C.; Del Barrio, M. G.; Dalet, A.; Gatto, G.; Günther, T.; Zhang, J.; Seidler, B.; Saur, D.; Schüle, R.; Goulding, M. ROR β Spinal Interneurons Gate Sensory Transmission during Locomotion to Secure a Fluid Walking Gait. *Neuron* 2017, 96 (6), 1419-1431.e1415. DOI: 10.1016/j.neuron.2017.11.011.

Kopach, O.; Medvediev, V.; Krotov, V.; Borisyyuk, A.; Tsymbaliuk, V.; Voitenko, N. Opposite, bidirectional shifts in excitation and inhibition in specific types of dorsal horn interneurons are

associated with spasticity and pain post-SCI. *Sci Rep* 2017, 7 (1), 5884. DOI: 10.1038/s41598-017-06049-7.

Krames, E. S. The dorsal root ganglion in chronic pain and as a target for neuromodulation: a review. *Neuromodulation* 2015, 18 (1), 24-32; discussion 32. DOI: 10.1111/ner.12247.

Lewin, G. R.; Moshourab, R. Mechanosensation and pain. *J Neurobiol* 2004, 61 (1), 30-44. DOI: 10.1002/neu.20078.

Li, J. L.; Fujiyama, F.; Kaneko, T.; Mizuno, N. Expression of vesicular glutamate transporters, VGluT1 and VGluT2, in axon terminals of nociceptive primary afferent fibers in the superficial layers of the medullary and spinal dorsal horns of the rat. *J Comp Neurol* 2003, 457 (3), 236-249. DOI: 10.1002/cne.10556.

Lima, D.; Coimbra, A. A Golgi study of the neuronal population of the marginal zone (lamina I) of the rat spinal cord. *J Comp Neurol* 1986, 244 (1), 53-71. DOI: 10.1002/cne.902440105.

Lingford-Hughes, A.; Kalk, N. 2 - Clinical neuroanatomy. In *Core Psychiatry (Third Edition)*, Wright, P., Stern, J., Phelan, M. Eds.; W.B. Saunders, 2012; pp 13-34.

Liu, P.; Zhang, X.; He, X.; Jiang, Z.; Wang, Q.; Lu, Y. Spinal GABAergic neurons are under feed-forward inhibitory control driven by A. *Mol Pain* 2021, 17, 1744806921992620. DOI: 10.1177/1744806921992620.

Lu, Y.; Dong, H.; Gao, Y.; Gong, Y.; Ren, Y.; Gu, N.; Zhou, S.; Xia, N.; Sun, Y. Y.; Ji, R. R.; et al. A feed-forward spinal cord glycinergic neural circuit gates mechanical allodynia. *J Clin Invest* 2013, 123 (9), 4050-4062. DOI: 10.1172/JCI70026.

Luque, J. M.; Nelson, N.; Richards, J. G. Cellular expression of glycine transporter 2 messenger RNA exclusively in rat hindbrain and spinal cord. *Neuroscience* 1995, 64 (2), 525-535. DOI: 10.1016/0306-4522(94)00404-s.

Malmberg, A. B.; Chen, C.; Tonegawa, S.; Basbaum, A. I. Preserved acute pain and reduced neuropathic pain in mice lacking PKC γ . *Science* 1997, 278 (5336), 279-283. DOI: 10.1126/science.278.5336.279.

Matthews, M. R.; Cuello, A. C. Substance P-immunoreactive peripheral branches of sensory neurons innervate guinea pig sympathetic neurons. *Proc Natl Acad Sci U S A* 1982, 79 (5), 1668-1672. DOI: 10.1073/pnas.79.5.1668.

Maxwell, D. J.; Belle, M. D.; Cheunsuang, O.; Stewart, A.; Morris, R. Morphology of inhibitory and excitatory interneurons in superficial laminae of the rat dorsal horn. *J Physiol* 2007, 584 (Pt 2), 521-533. DOI: 10.1113/jphysiol.2007.140996.

McClung, J. R. Rexed's laminae as it applies to the rat cervical spinal cord. Castro, A. J., Ed.; *Experimental Neurology*, 1978; pp 145-148.

McHugh, J. M.; McHugh, W. B. Pain: neuroanatomy, chemical mediators, and clinical implications. *AACN Clin Issues* 2000, 11 (2), 168-178. DOI: 10.1097/00044067-200005000-00003.

- McNeill, D. L.; Chung, K.; Hulsebosch, C. E.; Bolender, R. P.; Coggeshall, R. E. Numbers of synapses in laminae I-IV of the rat dorsal horn. *J Comp Neurol* 1988, 278 (3), 453-460. DOI: 10.1002/cne.902780313.
- Melzack, R.; Wall, P. D. Pain mechanisms: a new theory. *Science* 1965, 150 (3699), 971-979. DOI: 10.1126/science.150.3699.971.
- Mirauccourt, L. S.; Dallel, R.; Voisin, D. L. Glycine inhibitory dysfunction turns touch into pain through PKC γ interneurons. *PLoS One* 2007, 2 (11), e1116. DOI: 10.1371/journal.pone.0001116.
- Mirauccourt, L. S.; Moisset, X.; Dallel, R.; Voisin, D. L. Glycine inhibitory dysfunction induces a selectively dynamic, morphine-resistant, and neurokinin 1 receptor-independent mechanical allodynia. *J Neurosci* 2009, 29 (8), 2519-2527. DOI: 10.1523/JNEUROSCI.3923-08.2009.
- Mitchell, E. A.; Gentet, L. J.; Dempster, J.; Belelli, D. GABA and glycine receptor-mediated transmission in rat lamina II neurones: relevance to the analgesic actions of neuroactive steroids. *J Physiol* 2007, 583 (Pt 3), 1021-1040. DOI: 10.1113/jphysiol.2007.134445.
- Mitchell, K.; Spike, R. C.; Todd, A. J. An immunocytochemical study of glycine receptor and GABA in laminae I-III of rat spinal dorsal horn. *J Neurosci* 1993, 13 (6), 2371-2381. DOI: 10.1523/JNEUROSCI.13-06-02371.1993.
- Molander, C.; Xu, Q.; Grant, G. The cytoarchitectonic organization of the spinal cord in the rat. I. The lower thoracic and lumbosacral cord. *J Comp Neurol* 1984, 230 (1), 133-141. DOI: 10.1002/cne.902300112.
- Mori, M.; Kose, A.; Tsujino, T.; Tanaka, C. Immunocytochemical localization of protein kinase C subspecies in the rat spinal cord: light and electron microscopic study. *J Comp Neurol* 1990, 299 (2), 167-177. DOI: 10.1002/cne.902990204.
- Netter, F. H.; Machado, C. A. G. *The Netter collection of medical illustrations*; Elsevier Saunders, 2011.
- Neumann, S.; Braz, J. M.; Skinner, K.; Llewellyn-Smith, I. J.; Basbaum, A. I. Innocuous, not noxious, input activates PKC γ interneurons of the spinal dorsal horn via myelinated afferent fibers. *J Neurosci* 2008, 28 (32), 7936-7944. DOI: 10.1523/JNEUROSCI.1259-08.2008.
- Núñez, E.; Pérez-Siles, G.; Rodenstein, L.; Alonso-Torres, P.; Zafra, F.; Jiménez, E.; Aragón, C.; López-Corcuera, B. Subcellular localization of the neuronal glycine transporter GLYT2 in brainstem. *Traffic* 2009, 10 (7), 829-843. DOI: 10.1111/j.1600-0854.2009.00911.x.
- Oliveira, A. L.; Hydling, F.; Olsson, E.; Shi, T.; Edwards, R. H.; Fujiyama, F.; Kaneko, T.; Hökfelt, T.; Cullheim, S.; Meister, B. Cellular localization of three vesicular glutamate transporter mRNAs and proteins in rat spinal cord and dorsal root ganglia. *Synapse* 2003, 50 (2), 117-129. DOI: 10.1002/syn.10249.
- Peirs, C.; Dallel, R.; Todd, A. J. Recent advances in our understanding of the organization of dorsal horn neuron populations and their contribution to cutaneous mechanical allodynia. *J Neural Transm (Vienna)* 2020, 127 (4), 505-525. DOI: 10.1007/s00702-020-02159-1.

Peirs, C.; Patil, S.; Bouali-Benazzouz, R.; Artola, A.; Landry, M.; Dallel, R. Protein kinase C gamma interneurons in the rat medullary dorsal horn: distribution and synaptic inputs to these neurons, and subcellular localization of the enzyme. *J Comp Neurol* 2014, 522 (2), 393-413. DOI: 10.1002/cne.23407.

Peirs, C.; Seal, R. P. Neural circuits for pain: Recent advances and current views. *Science* 2016, 354 (6312), 578-584. DOI: 10.1126/science.aaf8933.

Peirs, C.; Williams, S. G.; Zhao, X.; Arokiaraj, C. M.; Ferreira, D. W.; Noh, M. C.; Smith, K. M.; Halder, P.; Corrigan, K. A.; Gedeon, J. Y.; et al. Mechanical Allodynia Circuitry in the Dorsal Horn Is Defined by the Nature of the Injury. *Neuron* 2021, 109 (1), 73-90.e77. DOI: 10.1016/j.neuron.2020.10.027.

Peirs, C.; Williams, S. P.; Zhao, X.; Walsh, C. E.; Gedeon, J. Y.; Cagle, N. E.; Goldring, A. C.; Hioki, H.; Liu, Z.; Marell, P. S.; et al. Dorsal Horn Circuits for Persistent Mechanical Pain. *Neuron* 2015, 87 (4), 797-812. DOI: 10.1016/j.neuron.2015.07.029.

Petitjean, H.; Pawlowski, S. A.; Fraine, S. L.; Sharif, B.; Hamad, D.; Fatima, T.; Berg, J.; Brown, C. M.; Jan, L. Y.; Ribeiro-da-Silva, A.; et al. Dorsal Horn Parvalbumin Neurons Are Gate-Keepers of Touch-Evoked Pain after Nerve Injury. *Cell Rep* 2015, 13 (6), 1246-1257. DOI: 10.1016/j.celrep.2015.09.080.

Pleger, B.; Villringer, A. The human somatosensory system: from perception to decision making. *Prog Neurobiol* 2013, 103, 76-97. DOI: 10.1016/j.pneurobio.2012.10.002.

Polgár, E.; Durrieux, C.; Hughes, D. I.; Todd, A. J. A quantitative study of inhibitory interneurons in laminae I-III of the mouse spinal dorsal horn. *PLoS One* 2013, 8 (10), e78309. DOI: 10.1371/journal.pone.0078309.

Polgár, E.; Fowler, J. H.; McGill, M. M.; Todd, A. J. The types of neuron which contain protein kinase C gamma in rat spinal cord. *Brain Res* 1999, 833 (1), 71-80. DOI: 10.1016/s0006-8993(99)01500-0.

Powell, J. J.; Todd, A. J. Light and electron microscope study of GABA-immunoreactive neurones in lamina III of rat spinal cord. *J Comp Neurol* 1992, 315 (2), 125-136. DOI: 10.1002/cne.903150202.

Poyatos, I.; Ponce, J.; Aragón, C.; Giménez, C.; Zafra, F. The glycine transporter GLYT2 is a reliable marker for glycine-immunoreactive neurons. *Brain Res Mol Brain Res* 1997, 49 (1-2), 63-70. DOI: 10.1016/s0169-328x(97)00124-1.

Price, D. D. Psychological and neural mechanisms of the affective dimension of pain. *Science* 2000, 288 (5472), 1769-1772. DOI: 10.1126/science.288.5472.1769.

Punnakkal, P.; von Schoultz, C.; Haenraets, K.; Wildner, H.; Zeilhofer, H. U. Morphological, biophysical and synaptic properties of glutamatergic neurons of the mouse spinal dorsal horn. *J Physiol* 2014, 592 (4), 759-776. DOI: 10.1113/jphysiol.2013.264937.

Ren, K.; Ruda, M. A.; Jacobowitz, D. M. Immunohistochemical localization of calretinin in the dorsal root ganglion and spinal cord of the rat. *Brain Research Bulletin* 1993, 31 (1), 13-22. DOI: [https://doi.org/10.1016/0361-9230\(93\)90004-U](https://doi.org/10.1016/0361-9230(93)90004-U).

- Réthelyi, M.; Szentágothai, J. The large synaptic complexes of the substantia gelatinosa. *Exp Brain Res* 1969, 7 (3), 258-274. DOI: 10.1007/BF00239033.
- Rexed, B. The cytoarchitectonic organization of the spinal cord in the cat. *J Comp Neurol* 1952, 96 (3), 414-495. DOI: 10.1002/cne.900960303.
- Rexed, B. A cytoarchitectonic atlas of the spinal cord in the cat. *J Comp Neurol* 1954, 100 (2), 297-379. DOI: 10.1002/cne.901000205.
- Ribeiro-da-Silva, A.; Coimbra, A. Two types of synaptic glomeruli and their distribution in laminae I-III of the rat spinal cord. *J Comp Neurol* 1982, 209 (2), 176-186. DOI: 10.1002/cne.902090205.
- Ribeiro-da-Silva, A.; Tagari, P.; Cuello, A. C. Morphological characterization of substance P-like immunoreactive glomeruli in the superficial dorsal horn of the rat spinal cord and trigeminal subnucleus caudalis: a quantitative study. *J Comp Neurol* 1989, 281 (4), 497-415. DOI: 10.1002/cne.902810402.
- Ribeiro-da-Silva, A. CHAPTER 6 – Substantia Gelatinosa of the Spinal Cord. 2004.
- Ribeiro-de-Silva, A.; De Korninck, Y. Morphological and neurochemical organization of the spinal dorsal horn. In *Science of Pain* Basbaum, A. I., Bushnell, M. C. Eds.; Elsevier, 2009; pp 279-310.
- Roudaut, Y.; Lonigro, A.; Coste, B.; Hao, J.; Delmas, P.; Crest, M. Touch sense: functional organization and molecular determinants of mechanosensitive receptors. *Channels (Austin)* 2012, 6 (4), 234-245. DOI: 10.4161/chan.22213.
- Rousseau, F.; Aubrey, K. R.; Supplisson, S. The glycine transporter GlyT2 controls the dynamics of synaptic vesicle refilling in inhibitory spinal cord neurons. *J Neurosci* 2008, 28 (39), 9755-9768. DOI: 10.1523/JNEUROSCI.0509-08.2008.
- Rowan, S.; Todd, A. J.; Spike, R. C. Evidence that neuropeptide Y is present in gabaergic neurons in the superficial dorsal horn of the rat spinal cord. *Neuroscience* 1993, 53 (2), 537-545. DOI: [https://doi.org/10.1016/0306-4522\(93\)90218-5](https://doi.org/10.1016/0306-4522(93)90218-5).
- Saito, S.; Kidd, G. J.; Trapp, B. D.; Dawson, T. M.; Bredt, D. S.; Wilson, D. A.; Traystman, R. J.; Snyder, S. H.; Hanley, D. F. Rat spinal cord neurons contain nitric oxide synthase. *Neuroscience* 1994, 59 (2), 447-456. DOI: [https://doi.org/10.1016/0306-4522\(94\)90608-4](https://doi.org/10.1016/0306-4522(94)90608-4).
- Sardella, T. C.; Polgár, E.; Watanabe, M.; Todd, A. J. A quantitative study of neuronal nitric oxide synthase expression in laminae I-III of the rat spinal dorsal horn. *Neuroscience* 2011, 192 (6-2), 708-720. DOI: 10.1016/j.neuroscience.2011.07.011.
- Sasek, C. A.; Elde, R. P. Distribution of neuropeptide Y-like immunoreactivity and its relationship to FMRF-amide-like immunoreactivity in the sixth lumbar and first sacral spinal cord segments of the rat. *J Neurosci* 1985, 5 (7), 1729-1739. DOI: 10.1523/JNEUROSCI.05-07-01729.1985.
- Sathyamurthy, A.; Johnson, K. R.; Matson, K. J. E.; Dobrott, C. I.; Li, L.; Ryba, A. R.; Bergman, T. B.; Kelly, M. C.; Kelley, M. W.; Levine, A. J. Massively Parallel Single Nucleus

Transcriptional Profiling Defines Spinal Cord Neurons and Their Activity during Behavior. *Cell Rep* 2018, 22 (8), 2216-2225. DOI: 10.1016/j.celrep.2018.02.003.

Sengul, G.; Watson, C.; Tanaka, I.; Paxinos, G. Atlas of the spinal cord of the rat, mouse, marmoset, rhesus, and human. Elsevier: 2013.

Shin, J. B.; Martinez-Salgado, C.; Heppenstall, P. A.; Lewin, G. R. A T-type calcium channel required for normal function of a mammalian mechanoreceptor. *Nat Neurosci* 2003, 6 (7), 724-730. DOI: 10.1038/nn1076.

Simmons, D. R.; Spike, R. C.; Todd, A. J. Galanin is contained in GABAergic neurons in the rat spinal dorsal horn. *Neurosci Lett* 1995, 187 (2), 119-122. DOI: 10.1016/0304-3940(95)11358-4.

Smith, K. M.; Boyle, K. A.; Madden, J. F.; Dickinson, S. A.; Jobling, P.; Callister, R. J.; Hughes, D. I.; Graham, B. A. Functional heterogeneity of calretinin-expressing neurons in the mouse superficial dorsal horn: implications for spinal pain processing. *J Physiol* 2015, 593 (19), 4319-4339. DOI: 10.1113/JP270855.

Smith, K. M.; Boyle, K. A.; Mustapa, M.; Jobling, P.; Callister, R. J.; Hughes, D. I.; Graham, B. A. Distinct forms of synaptic inhibition and neuromodulation regulate calretinin-positive neuron excitability in the spinal cord dorsal horn. *Neuroscience* 2016, 326, 10-21. DOI: 10.1016/j.neuroscience.2016.03.058.

Smith, K. M.; Browne, T. J.; Davis, O. C.; Coyle, A.; Boyle, K. A.; Watanabe, M.; Dickinson, S. A.; Iredale, J. A.; Gradwell, M. A.; Jobling, P.; et al. Calretinin positive neurons form an excitatory amplifier network in the spinal cord dorsal horn. *Elife* 2019, 8. DOI: 10.7554/eLife.49190.

Spike, R. C.; Puskár, Z.; Andrew, D.; Todd, A. J. A quantitative and morphological study of projection neurons in lamina I of the rat lumbar spinal cord. *Eur J Neurosci* 2003, 18 (9), 2433-2448. DOI: 10.1046/j.1460-9568.2003.02981.x.

Spike, R. C.; Watt, C.; Zafra, F.; Todd, A. J. An ultrastructural study of the glycine transporter GLYT2 and its association with glycine in the superficial laminae of the rat spinal dorsal horn. *Neuroscience* 1997, 77 (2), 543-551. DOI: 10.1016/s0306-4522(96)00501-5.

Suzuki, R.; Dickenson, A. Spinal and supraspinal contributions to central sensitization in peripheral neuropathy. *Neurosignals* 2005, 14 (4), 175-181. DOI: 10.1159/000087656.

Szentágothai, J.; Réthelyi, M. Funkcionális anatómia. Az ember anatómiája, fejlődéstana, szövettana és tájanatómiája; Medicina, 1989.

Takazawa, T.; Choudhury, P.; Tong, C. K.; Conway, C. M.; Scherrer, G.; Flood, P. D.; Mukai, J.; MacDermott, A. B. Inhibition Mediated by Glycinergic and GABAergic Receptors on Excitatory Neurons in Mouse Superficial Dorsal Horn Is Location-Specific but Modified by Inflammation. *J Neurosci* 2017, 37 (9), 2336-2348. DOI: 10.1523/JNEUROSCI.2354-16.2017.

Takazawa, T.; MacDermott, A. B. Glycinergic and GABAergic tonic inhibition fine tune inhibitory control in regionally distinct subpopulations of dorsal horn neurons. *J Physiol* 2010, 588 (Pt 14), 2571-2587. DOI: 10.1113/jphysiol.2010.188292.

- Tiong, S. Y.; Polgár, E.; van Kralingen, J. C.; Watanabe, M.; Todd, A. J. Galanin-immunoreactivity identifies a distinct population of inhibitory interneurons in laminae I-III of the rat spinal cord. *Mol Pain* 2011, 7, 36. DOI: 10.1186/1744-8069-7-36.
- Todd, A. J. An electron microscope study of glycine-like immunoreactivity in laminae I-III of the spinal dorsal horn of the rat. *Neuroscience* 1990, 39 (2), 387-394. DOI: 10.1016/0306-4522(90)90275-9.
- Todd, A. J. GABA and glycine in synaptic glomeruli of the rat spinal dorsal horn. *Eur J Neurosci* 1996, 8 (12), 2492-2498. DOI: 10.1111/j.1460-9568.1996.tb01543.x.
- Todd, A. J. Neuronal circuitry for pain processing in the dorsal horn. *Nat Rev Neurosci* 2010, 11 (12), 823-836. DOI: 10.1038/nrn2947.
- Todd, A. J. Identifying functional populations among the interneurons in laminae I-III of the spinal dorsal horn. *Mol Pain* 2017, 13, 1744806917693003. DOI: 10.1177/1744806917693003.
- Todd, A. J.; Hughes, D. I.; Polgár, E.; Nagy, G. G.; Mackie, M.; Ottersen, O. P.; Maxwell, D. J. The expression of vesicular glutamate transporters VGLUT1 and VGLUT2 in neurochemically defined axonal populations in the rat spinal cord with emphasis on the dorsal horn. *Eur J Neurosci* 2003, 17 (1), 13-27. DOI: 10.1046/j.1460-9568.2003.02406.x.
- Todd, A. J.; Koerber, H. R. Neuroanatomical Substrates of Spinal Nociception In Wall and Melzack's textbook of pain, Sixth Edition ed.; McMahon, S. B., Koltzenburg, M., Tracey, I., Turk, D. Eds.; Elsevier/Saunders, 2013; pp 77 - 93.
- Todd, A. J.; Spike, R. C.; Chong, D.; Neilson, M. The relationship between glycine and gephyrin in synapses of the rat spinal cord. *Eur J Neurosci* 1995, 7 (1), 1-11. DOI: 10.1111/j.1460-9568.1995.tb01014.x.
- Todd, A. J.; Sullivan, A. C. Light microscope study of the coexistence of GABA-like and glycine-like immunoreactivities in the spinal cord of the rat. *J Comp Neurol* 1990, 296 (3), 496-505. DOI: 10.1002/cne.902960312.
- Todd, A. J.; Watt, C.; Spike, R. C.; Sieghart, W. Colocalization of GABA, glycine, and their receptors at synapses in the rat spinal cord. *J Neurosci* 1996, 16 (3), 974-982. DOI: 10.1523/JNEUROSCI.16-03-00974.1996.
- Torsney, C.; MacDermott, A. B. Disinhibition opens the gate to pathological pain signaling in superficial neurokinin 1 receptor-expressing neurons in rat spinal cord. *J Neurosci* 2006, 26 (6), 1833-1843. DOI: 10.1523/JNEUROSCI.4584-05.2006.
- Tracey, I.; Mantyh, P. W. The cerebral signature for pain perception and its modulation. *Neuron* 2007, 55 (3), 377-391. DOI: 10.1016/j.neuron.2007.07.012.
- Wang, L. H.; Ding, W. Q.; Sun, Y. G. Spinal ascending pathways for somatosensory information processing. *Trends Neurosci* 2022, 45 (8), 594-607. DOI: 10.1016/j.tins.2022.05.005.
- Wemmie, J. A.; Taugher, R. J.; Kreple, C. J. Acid-sensing ion channels in pain and disease. *Nat Rev Neurosci* 2013, 14 (7), 461-471. DOI: 10.1038/nrn3529.

- Wercberger, R.; Basbaum, A. I. Spinal cord projection neurons: a superficial, and also deep, analysis. *Curr Opin Physiol* 2019, 11, 109-115. DOI: 10.1016/j.cophys.2019.10.002.
- West, S. J.; Bannister, K.; Dickenson, A. H.; Bennett, D. L. Circuitry and plasticity of the dorsal horn--toward a better understanding of neuropathic pain. *Neuroscience* 2015, 300, 254-275. DOI: 10.1016/j.neuroscience.2015.05.020.
- Willis, W. D. The somatosensory system, with emphasis on structures important for pain. *Brain Res Rev* 2007, 55 (2), 297-313. DOI: 10.1016/j.brainresrev.2007.05.010.
- Willis, W. D.; Westlund, K. N. Neuroanatomy of the pain system and of the pathways that modulate pain. *J Clin Neurophysiol* 1997, 14 (1), 2-31. DOI: 10.1097/00004691-199701000-00002.
- Willis, W. D.; Coggeshall, R. E. Sensory mechanisms of the spinal cord; Kluwer Academic/Plenum, 2004.
- Xu, Q.; Anderson, S. A. Mapping lineage using BAC-Cre reporter lines. *Curr Protoc Neurosci* 2010, Chapter 1, Unit 1.19. DOI: 10.1002/0471142301.ns0119s50.
- Yasaka, T.; Kato, G.; Furue, H.; Rashid, M. H.; Sonohata, M.; Tamae, A.; Murata, Y.; Masuko, S.; Yoshimura, M. Cell-type-specific excitatory and inhibitory circuits involving primary afferents in the substantia gelatinosa of the rat spinal dorsal horn in vitro. *J Physiol* 2007, 581 (Pt 2), 603-618. DOI: 10.1113/jphysiol.2006.123919.
- Yasaka, T.; Tiong, S. Y. X.; Hughes, D. I.; Riddell, J. S.; Todd, A. J. Populations of inhibitory and excitatory interneurons in lamina II of the adult rat spinal dorsal horn revealed by a combined electrophysiological and anatomical approach. *Pain* 2010, 151 (2), 475-488. DOI: 10.1016/j.pain.2010.08.008.
- Yoshida, S.; Senba, E.; Kubota, Y.; Hagihira, S.; Yoshiya, I.; Emson, P. C.; Tohyama, M. Calcium-binding proteins calbindin and parvalbumin in the superficial dorsal horn of the rat spinal cord. *Neuroscience* 1990, 37 (3), 839-848. DOI: [https://doi.org/10.1016/0306-4522\(90\)90113-I](https://doi.org/10.1016/0306-4522(90)90113-I).
- Zeilhofer, H. U. Synaptic modulation in pain pathways. *Rev Physiol Biochem Pharmacol* 2005, 154, 73-100. DOI: 10.1007/s10254-005-0043-y.
- Zeilhofer, H. U.; Acuña, M. A.; Gingras, J.; Yévenes, G. E. Glycine receptors and glycine transporters: targets for novel analgesics? *Cell Mol Life Sci* 2018, 75 (3), 447-465. DOI: 10.1007/s00018-017-2622-x.
- Zeilhofer, H. U.; Studler, B.; Arabadzisz, D.; Schweizer, C.; Ahmadi, S.; Layh, B.; Bösl, M. R.; Fritschy, J. M. Glycinergic neurons expressing enhanced green fluorescent protein in bacterial artificial chromosome transgenic mice. *J Comp Neurol* 2005, 482 (2), 123-141. DOI: 10.1002/cne.20349.
- Zeilhofer, H. U.; Werynska, K.; Gingras, J.; Yévenes, G. E. Glycine Receptors in Spinal Nociceptive Control-An Update. *Biomolecules* 2021, 11 (6). DOI: 10.3390/biom11060846.

Zeilhofer, H. U.; Wildner, H.; Yévenes, G. E. Fast synaptic inhibition in spinal sensory processing and pain control. *Physiol Rev* 2012, 92 (1), 193-235. DOI: 10.1152/physrev.00043.2010.

Zeisel, A.; Hochgerner, H.; Lönnerberg, P.; Johnsson, A.; Memic, F.; van der Zwan, J.; Häring, M.; Braun, E.; Borm, L. E.; La Manno, G.; et al. Molecular Architecture of the Mouse Nervous System. *Cell* 2018, 174 (4), 999-1014.e1022. DOI: 10.1016/j.cell.2018.06.021.

Zeitz, K. P.; Guy, N.; Malmberg, A. B.; Dirajlal, S.; Martin, W. J.; Sun, L.; Bonhaus, D. W.; Stucky, C. L.; Julius, D.; Basbaum, A. I. The 5-HT₃ subtype of serotonin receptor contributes to nociceptive processing via a novel subset of myelinated and unmyelinated nociceptors. *J Neurosci* 2002, 22 (3), 1010-1019. DOI: 10.1523/JNEUROSCI.22-03-01010.2002.

Zhang, X.; Nicholas, A. P.; Hökfelt, T. Ultrastructural studies on peptides in the dorsal horn of the rat spinal cord—II. Co-existence of galanin with other peptides in local neurons. *Neuroscience* 1995, 64 (4), 875-891. DOI: [https://doi.org/10.1016/0306-4522\(94\)00451-A](https://doi.org/10.1016/0306-4522(94)00451-A).

Zhang, Y.; Liu, S.; Zhang, Y. Q.; Goulding, M.; Wang, Y. Q.; Ma, Q. Timing Mechanisms Underlying Gate Control by Feedforward Inhibition. *Neuron* 2018, 99 (5), 941-955.e944. DOI: 10.1016/j.neuron.2018.07.026.

Zheng, Y.; Liu, P.; Bai, L.; Trimmer, J. S.; Bean, B. P.; Ginty, D. D. Deep Sequencing of Somatosensory Neurons Reveals Molecular Determinants of Intrinsic Physiological Properties. *Neuron* 2019, 103 (4), 598-616.e597. DOI: 10.1016/j.neuron.2019.05.039.

9. Keywords

cell morphology, electron microscopy, glycine, glycine transporter 2, glycinergic neurons, immunohistochemistry, *in situ* hybridization, mouse, pain processing neural circuits, spinal dorsal horn, transgenic mice

10. Acknowledgement

I would like to acknowledge Stipendium Hungaricum Scholarship Program, for my Ph.D. scholarship and for the assistance of moving to Hungary.

To Professor Antal for all the support and supervision during this Ph.D. period, including the teaching and experimental guidance, and welcoming to this research project.

To Krisztina Hegedüs for all the laboratory techniques teaching and collaboration during this entire project, and for being a good company during these years.

To Professor Hanns Ulrich Zeilhofer and Hendrik Wildner for the collaboration in the first published paper for this project.

To Gréta Kis for the collaboration in the second published paper for this project.

To the colleagues of the Anatomy, Histology, and Embryology Department for the welcoming, teaching and collaboration.

To all my former supervisors and colleagues that contributed to my scientific path.

To my family and friends for all the emotional support, especially my husband for all the love and caring during this period.

11. List of publications



**UNIVERSITY of
DEBRECEN**

**UNIVERSITY AND NATIONAL LIBRARY
UNIVERSITY OF DEBRECEN**

H-4002 Egyetem tér 1, Debrecen
Phone: +3652/410-443, email: publikaciok@lib.unideb.hu

Registry number: DEENK/261/2023.PL
Subject: PhD Publication List

Candidate: Camila De Oliveira Miranda
Doctoral School: Doctoral School of Neurosciences

List of publications related to the dissertation

1. **De Oliveira Miranda, C.**, Hegedűs, K., Kis, G., Antal, M.: Synaptic Targets of Glycinergic Neurons in Laminae I-III of the Spinal Dorsal Horn.
Int. J. Mol. Sci. 24 (8), 1-26, 2023.
DOI: <http://dx.doi.org/10.3390/ijms24086943>
IF: 6.208 (2021)
2. **De Oliveira Miranda, C.**, Hegedűs, K., Wildner, H., Zeilhofer, H. U., Antal, M.: Morphological and neurochemical characterization of glycinergic neurons in laminae of the mouse spinal dorsal horn.
J. Comp. Neurol. 530 (3), 607-626, 2022.
DOI: <http://dx.doi.org/10.1002/cne.25232>
IF: 3.028 (2021)





List of other publications

3. Javdani, F., Hegedűs, K., **De Oliveira Miranda, C.**, Hegyi, Z., Holló, K., Antal, M.: Differential expression of Na⁺/K⁺/Cl⁻ cotransporter 1 in neurons and glial cells within the superficial spinal dorsal horn of rodents.
Sci. Rep. 10 (1), 11715-11728, 2020.
DOI: <http://dx.doi.org/10.1038/s41598-020-68638-3>
IF: 4.379
4. Soares Romeiro, L. A., da Costa Nunes, J. L., **De Oliveira Miranda, C.**, Simões Heyn Roth Cardoso, G., de Oliveira, A. S., Gandini, A., Kobrlova, T., Soukup, O., Rossi, M., Senger, J., Jung, M., Gervasoni, S., Vistoli, G., Petralla, S., Massenzio, F., Monti, B., Bolognesi, M. L.: Novel Sustainable-by-Design HDAC Inhibitors for the Treatment of Alzheimer's Disease.
ACS Med. Chem. Lett. 10 (4), 671-676, 2019.
DOI: <http://dx.doi.org/10.1021/acsmchemlett.9b00071>
IF: 3.975

Total IF of journals (all publications): 17,59

Total IF of journals (publications related to the dissertation): 9,236

The Candidate's publication data submitted to the iDEa Tudóstér have been validated by DEENK on the basis of the Journal Citation Report (Impact Factor) database.

21 June, 2023

